The role of Vegfc signaling during cardiac regeneration in zebrafish

Dissertation

zur Erlangung des Doktorgrades

der Naturwissenschaften

vorgelegt beim Fachbereich 15

der Johann Wolfgang Goethe-Universität

in Frankfurt am Main

von

Hadil El Sammak

aus Kairo, Ägypten

Frankfurt 2022

(D30)

vom Fachbereich Biowissenschaften (FB15) der Johann Wolfgang Goethe - Universität als Dissertation angenommen.

Dekan: Prof. Dr. Sven Klimpel

Gutachter: Prof. Didier Y. R. Stainier, Ph.D.

Prof. Amparo Acker-Palmer, Ph.D.

Datum der Disputation:

SUPERVISOR

Prof. Didier Y. R. Stainier, Ph.D.

Department of Developmental Genetics

Max Planck Institute for Heart and Lung Research

Bad Nauheim, Germany

REVIEWERS

Prof. Didier Y. R. Stainier, Ph.D.

Department of Developmental Genetics

Max Planck Institute for Heart and Lung Research

Bad Nauheim, Germany

and

Prof. Amparo Acker-Palmer, PhD

Department of Molecular and Cellular Neurobiology

Institute for Cell Biology and Neuroscience

Johann Wolfgang Goethe University

Frankfurt am Main, Germany

Erklärung

Ich erkläre hiermit, dass ich mich bisher keiner Doktorprüfung im Mathematisch-Naturwissenschaftlichen Bereich unterzogen habe.

Frankfurt am Main, den .....

(Unterschrift)

Versicherung

Ich erkläre hiermit, dass ich die vorgelegte Dissertation über The role of Vegfc signaling during cardiac regeneration in zebrafish selbständig angefertigt und mich anderer Hilfsmittel als der in ihr angegebenen nicht bedient habe, insbesondere, dass alle Entlehnungen aus anderen Schriften mit Angabe der betreffenden Schrift gekennzeichnet sind.

Ich versichere, die Grundsätze der guten wissenschaftlichen Praxis beachtet, und nicht die Hilfe einer kommerziellen Promotionsvermittlung in Anspruch genommen zu haben.

Einen Teil der vorliegende Ergebnisse der Arbeit sind in folgendem Publikationsorgan veröffentlicht:

El-Sammak, H., Yang, B., Guenther, S., Chen, W., Marín-Juez, R., and Stainier, D.Y.R. (2022). A Vegfc-Emilin2a-Cxcl8a Signaling Axis Required for Zebrafish Cardiac Regeneration. *Circ. Res. 130*, 1014–1029.

Frankfurt am Main, den .....

(Unterschrift)

"When the going gets tough, put one foot in front of the other and just keep going. Don't give up."

Roy T. Bennett

TABLE OF CONTENTS

ABSTRACT

Ischemic heart disease caused by occlusion of coronary vessels leads to the death of downstream tissues, resulting in a fibrotic scar that cannot be resolved. In contrast to the adult mammalian heart, the adult zebrafish heart can regenerate following injury, enabling the study of the underlying cellular and molecular mechanisms. One of the earliest responses that take place after cardiac injury in adult zebrafish is coronary revascularization. Previous transcriptomic data from our lab show that *vegfc*, a well-known regulator of lymphatic development, is upregulated early after injury and peaks at 96 hours post cryoinjury, coinciding with the peak of coronary endothelial cell proliferation. To test the hypothesis that *vegfc* is involved in coronary revascularization, I examined its expression pattern and found that it is expressed by coronary endothelial cells after cardiac damage. Using a loss-of-function approach to block Vegfc signaling, I found that it is required for coronary revascularization during cardiac regeneration. Notably, blocking Vegfc signaling resulted in a significant reduction in cardiomyocyte regeneration. Using transcriptomic analysis, I identified the extracellular matrix component gene *emilin2a* and the chemokine gene *cxcl8a* as effectors of Vegfc signaling. During cardiac regeneration, *cxcl8a* is expressed in epicardium-derived cells, while the gene encoding its receptor *cxcr1* is expressed on coronary endothelial cells. I found that overexpressing *emilin2a* increases coronary revascularization, and induces *cxcl8a* expression. Using loss-of-function approaches, I observed that both *cxcl8a* and *cxcr1* are required for coronary revascularization after cardiac injury.

Altogether, my findings indicate that Vegfc acts as an angiocrine factor that plays an important role in regulating cardiac regeneration in zebrafish. Mechanistically, Vegfc promotes the expression of *emilin2a*, which promotes coronary proliferation, at least in part by enhancing Cxcl8a-Cxcr1 signaling. This study helps in understanding the mechanisms underlying coronary revascularization during cardiac regeneration, with promising therapeutic applications for human heart regeneration.

1. INTRODUCTION

1.1. Myocardial Infarction: Causes and Consequences

Recent reports by the world health organization (WHO) showed that ischemic heart diseases represent the leading cause of death worldwide (WHO, 2020). They are caused due to occlusion in the coronary arteries which supply the heart with oxygen and nutrients (Pfeffer and Braunwald, 1990). These occlusions are the result of the accumulation of atherosclerotic plaques which narrow the lumen of coronary arteries and eventually result in their complete blockage (Pfeffer and Braunwald, 1990) (**Figure 1.1 A**). Moreover, these coronary occlusions lead to hypoxia in the downstream tissue and eventually tissue death (Talman and Ruskoaho, 2016). As a compensatory mechanism, the heart undergoes remodeling and replaces the dead tissue with a fibrotic scar (Cleutjens et al., 1995) (**Figure 1.1 B**). The extent and size of the scar dictate the prognostic outcome of this coronary obstruction (Sabia et al., 1992). The scar compromises the contractile efficiency of the heart and eventually leads to myocardial infarction (MI) (Talman and Ruskoaho, 2016).

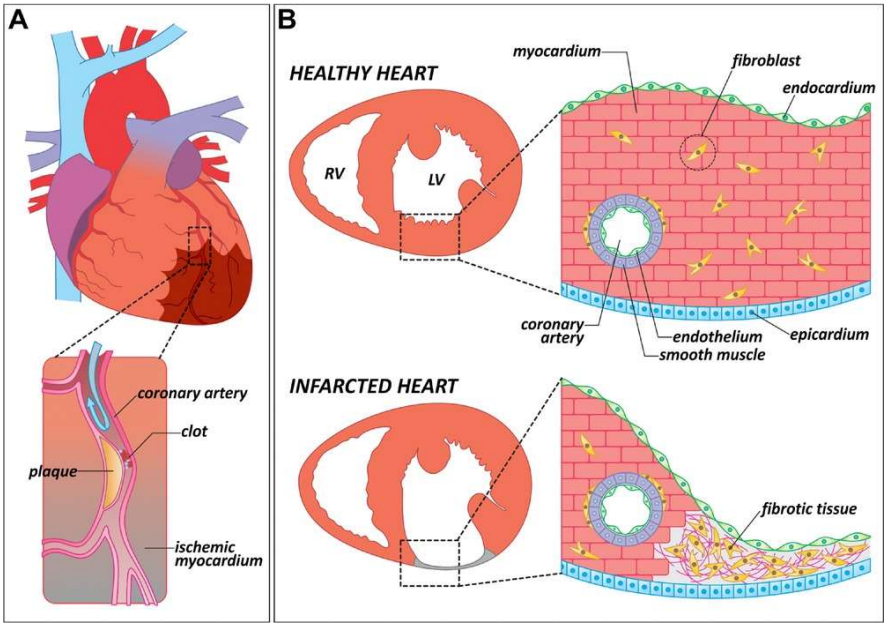

Figure 1.1: Causes and consequences of ischemic heart disease.

A. Schematic representation of an adult mammalian heart with an atherosclerotic plaque causing an occlusion in the coronary artery. **B.** Schematic representation of a section of a healthy heart showing the different cells types and a section of an infarcted heart with the fibrotic tissue. Adapted from (González-Rosa et al., 2017), License: CC BY 4.0

The inability of the adult mammalian heart to regenerate is a result of several factors as outlined below.

1.1.1. Cardiac Fibrosis

Following MI in mammals, extensive extracellular matrix (ECM) remodeling takes places (Talman and Ruskoaho, 2016). It has been well known that these deposits are mainly contributed by epicardium derived fibroblasts, resident cardiac fibroblasts, and more recently, studies have suggested a contribution of endocardial derived fibroblasts (Ali et al., 2014; Norris et al., 2008; Tombor et al., 2021; Zeisberg et al., 2007). The initial fibrotic response in the heart following an injury is important and essential to sustain the physical integrity of the heart and prevent it from collapsing due to the dead tissue (Travers et al., 2016). However, a subset of cardiac fibroblasts become activated and express markers such as smooth muscle actin (αSMA) (Travers et al., 2016). These activated myofibroblasts deposit pro-fibrotic ECM components such as fibrin and different types of collagens, hence resulting in scarring of the heart (Baudino et al., 2006; Cleutjens et al., 1995). Alternatively, ablating these pro-fibrotic myofibroblasts reduces fibrotic remodeling in the heart (Aghajanian et al., 2019; Kaur et al., 2016). Hence studies on how we can limit the number and the activation of these myofibroblasts in the heart could hold great potential in attempts to reducing fibrosis following a cardiac injury.

1.1.2. Reduced proliferative capacity of cardiomyocytes

The incapability of the adult mammalian cardiomyocytes (CMs) to proliferate is due to several factors including polyploidization (Bergmann et al., 2015). It has been previously shown that the number of binucleated CMs in mice rises dramatically at around P7 (Li et al., 1996; Soonpaa et al., 1996), which coincides with the drop of the regenerative potential of the mammalian heart (Porrello et al., 2011). Polyploidization of CMs is mainly the result of failed cytokinesis. However, a recent report has also shown that another possible hypothesis is the fusion of mononucleated CMs (Ali et al., 2020). In contrast to the adult mammalian heart, regenerating zebrafish hearts as well as neonatal mammalian hearts have majority of CMs as mononucleated, with a very minor population that is polyploid (González-Rosa et al., 2018; Li et al., 1996). Interestingly, inducing polyploidization of CMs in zebrafish, results in fibrotic scarring, similar to what is observed in mice (González-Rosa et al., 2018). Hence identifying

the factors that affect cytokinesis and manipulating them could have great therapeutic potential to induce the adult mammalian CM to proliferate (Wu et al., 2020).

Another important factor affecting the proliferative capacity of CMs is metabolism (Puente et al., 2014). CMs largely depend on fatty acid metabolism as their main source of energy. The increased oxygenation state of the heart produces high levels of oxygen reactive species which result in its reduced proliferative potential (Puente et al., 2014). A more glycolytic metabolism is indeed required for CM proliferation as observed in the zebrafish hearts which shifts from oxidative phosphorylation to glucose metabolism (Fukuda et al., 2020; Honkoop et al., 2019) during regeneration. Blocking this process impairs CM proliferation in models with an endogenous regenerative capacity (Fukuda et al., 2020) .

1.1.3. Poor revascularization potential in the adult mammalian heart

One of the very important factors contributing to the heart‘s poor ability to regenerate is its poor revascularization potential (Kocijan et al., 2021; Sabia et al., 1992). Indeed, if one compares the revascularization response of the cardiac muscle and that of skeletal muscle following injury, we will observe that vessels are able to vascularize the injured skeletal muscle which is able to regenerate, however in the adult mammalian heart, coronaries do not revascularize the injured tissue to a great extent (Kocijan et al., 2021). The main sources of new coronaries are majorly from pre-existing coronary endothelial cells (cECs) and minimal contribution from endocardial cells (Habib et al., 1991; Tian and Zhou, 2022). The mammalian heart has a unique mechanism to reestablish blood flow to the injured area by forming collateral arteries through different mechanisms (Seiler et al., 2013). The three main mechanisms of collateral artery formation have been reported from mouse studies include arterialization, in which capillaries existing before the injury form new collateral connections to restore the blood flow to the infarct region (Gabhann and Peirce, 2010) (**Figure 1.2**). The second mechanism is arteriogenesis, in which preexisting arterioles enlarge and widen to increase blood flow in the infarct region (He et al., 2016) (**Figure 1.2**). The last mechanism is artery reassembly, which involves endothelial cells (ECs) migration and expansion to form a network of collaterals around the infarct area (Das et al., 2019) (**Figure 1.2**).

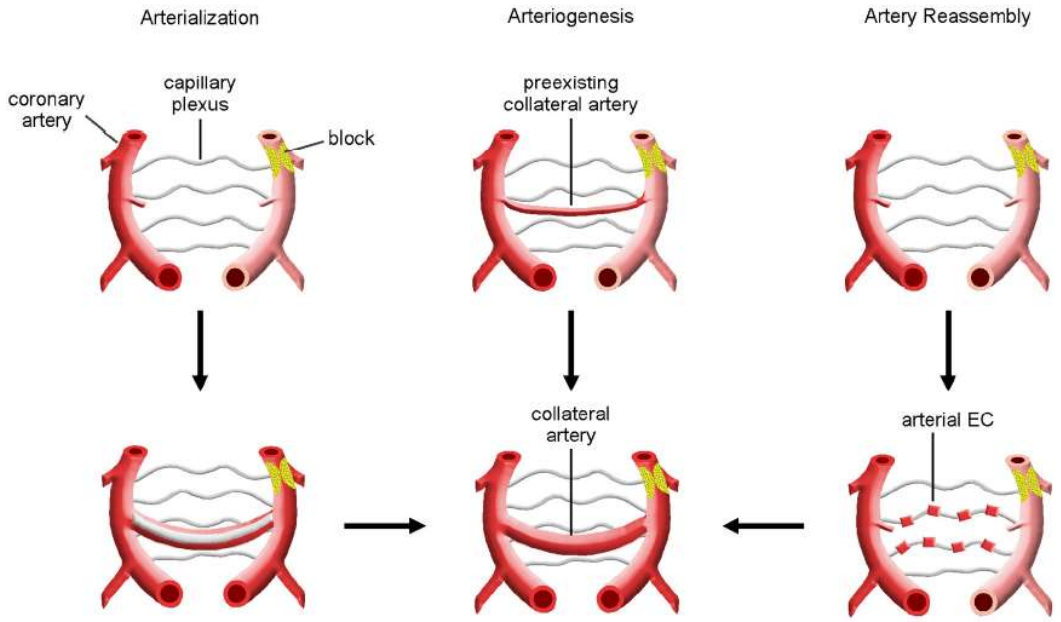

Figure 1.2: Collateral formation in the mammalian heart

Schematic representation illustrating the different mechanisms of collateral artery formation following myocardial infarction either by arterialization, arteriogenesis or artery reassembly. Adapted from (Tian and Zhou, 2022), License: 5302010121047.

The extent to which these collaterals form dictates the prognostic outcome following MI (Habib et al., 1991). Indeed a recent study by Das and colleagues revealed that CXCR4 is a main player promoting the formation of these collaterals in the regenerating neonatal mouse heart, and that inducing collateral formation in the adult mouse heart resulted in a significant functional improvement following MI (Das et al., 2019). Moreover, it has been recently shown that improving coronary revascularization in the adult mouse heart, stimulates CM proliferation (Debenedittis et al., 2021). All of these data suggest that coronaries are a vital factor that contributes to the regenerative outcome following injury. An increasing number of studies are emerging with the aim of identifying the cellular and molecular mechanisms that regulate coronary revascularization as well as identifying the factors released by ECs and investigating how they aid in CM proliferation. These studies hold great potential for devising effective therapeutics that would in aid in promoting the adult mammalian heart to regenerate.

1.2. Therapeutic approaches to promote cardiac regeneration in mammals

Given that ischemic cardiac disease is the leading cause of death, in addition to the high health and economic burden that it imposes, a lot of research has focused on trying to promote cardiac regeneration and limit the pathological fibrosis following MI. In this section, I will review some of these attempts and the challenges that the field is still facing.

1.2.1. Stem cell therapy

One of the most debated topics in the cardiac regeneration field is the presence of stem cells in the heart (MAURO, 1961). The current consensus is that the heart contains no stems cells, or to a very low extent that they do not contribute to new CMs to replace the lost tissue following MI (Alkass et al., 2015). However, the concept of using the highly dividing and programmable stem cells was and still remains of high interest. Researchers have tried to utilize embryonic stem cells or induced pluripotent stem cells, differentiate them in culture to CMs and inject them after MI (Martin-Puig et al., 2008) (**Figure 1.3**). Results were promising when experiments were conducted on guinea pigs, as well as macaque monkeys, showing long-term survival. However, cardiac arrhythmias were observed as a side effect of this treatment (Chong et al., 2014). Another approach that continues to be under investigation, is the use of tissue scaffolds alone or with materials including collagen, fibrin, hyaluronic acid, along with growth factors, CMs and ECs (Ogle et al., 2016) (**Figure 1.3**). Although cardiac arrhythmias persisted as a side effect, however this approach better recapitulates and improves cellular interactions with the surrounding environment, and with regular improvements and advances in the scaffold recipes, this approach might be promising in improving cardiac function following MI (Ogle et al., 2016).

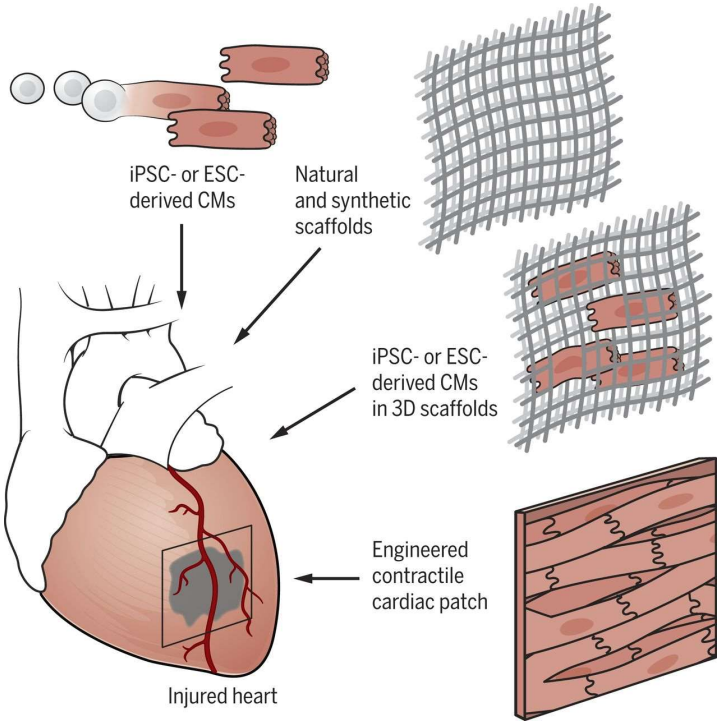

Figure 1.3: Strategies to promote cardiac regeneration.
Schematic representation on the use of stem cells, tissue scaffolds as well as cardiac patches to promote cardiac regeneration in mammals. Adapted from (Tzahor and Poss, 2017), reused with permission from AAAS.

1.2.2. Cardiomyocyte reprogramming

Since myofibroblasts are one of the predominant cell types in the heart following injury, an attractive concept was to transdifferentiate these fibroblasts to contractile CMs. Indeed, scientists were able to reprogram mouse fibroblasts to CMs by transfecting these fibroblasts with several factors including Gata4, Mef2c and Tbx5 (Srivastava and DeWitt, 2016). However, only a minor proportion of CMs were traced back to transfected fibroblasts, indicating low effectiveness of this approach.

1.2.3. Model organisms with endogenous cardiac regeneration capacity

Given the current challenges in the cardiac regeneration field, a lot of studies have started focusing on analyzing and understanding the mechanisms that govern cardiac regeneration in organisms with an innate capacity to regenerate the heart after injury (Tzahor and Poss, 2017). One of the most widely used models to study cardiac regeneration are the neonatal mice. Mice from P0 to P7, retain the capacity to regenerate the cardiac tissue following injury, which makes them a great model to

study cardiac regeneration (Porrello et al., 2011). However, one caveat of using them is that these neonatal mice are still developing, and hence their biology is mainly governed by developmental programs (Tzahor and Poss, 2017). Ideally, one would want to study cardiac regeneration in an adult model with this innate ability. Luckily, the adult zebrafish have this remarkable ability to regenerate the cardiac tissue following different types of injury (Poss et al., 2002). Interestingly, in 2021, research led the group of Kerstin Bartscherer revealed that the adult spiny mouse is able to tolerate cardiac injury and displays an ability to repair and regenerate (Koopmans et al., 2021). Studies using all of these organisms with their endogenous ability to regenerate the heart will help identify unique cellular and molecular mechanisms that promote cardiac regeneration, and will help in designing more effective approaches to promote cardiac regeneration in humans following MI.

1.3. Zebrafish as a regenerative model

Model organisms are indispensable in biological research to study various processes. In the regenerative biology field, several model organisms are used due to their remarkable ability to regenerate following the injury or amputation of a part of their body (Mehta and Singh, 2019). Models as planaria, hydra as well annelids are only some of the models showing a high regenerative capacity. Regeneration is also observed in several vertebrate models including axolotls and newts which are able to regenerate their limbs following amputation (Mehta and Singh, 2019). Amongst these models, the zebrafish has been and continues to be a great model of choice to study tissue regeneration due to ease of breeding and maintaining and the high accessibility of a wide variety of genetic tools and manipulations (Marques et al., 2019).

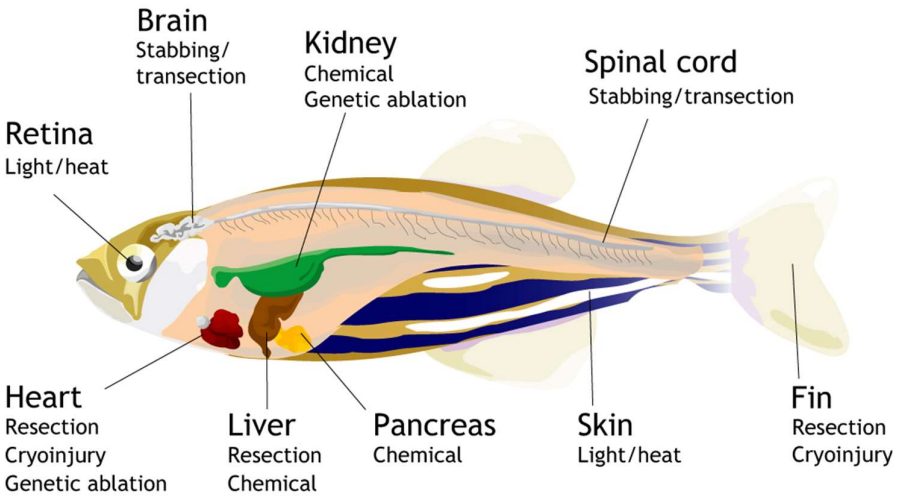

Figure 1.4: The zebrafish can regenerate multiple organs.
Schematic representation of an adult zebrafish illustrating the different organs that the adult zebrafish can regenerate and their modes of injury. Adapted from (Marques et al., 2019), License by CC CB 4.0.

The zebrafish was introduced as a model organism back in the 1970s at the University of Oregon. Due to its relatively easy genetic manipulations, external fertilization and transparent embryos, the zebrafish became a very powerful model to study various developmental processes in a real-time manner (Meyers, 2018). Besides its potent application in developmental biology and modelling human diseases, the adult zebrafish became a favorable model in the regeneration field due to its ability regenerate various organs including the retina, spinal cord, brain, fin, kidney, as well as the heart following injury (Marques et al., 2019) (**Figure 1.4**).

1.4. Cardiac regeneration in zebrafish

In this section, I will review the methods used to study cardiac regeneration in zebrafish, and the cellular and molecular pathways that are involved in this process.

1.4.1. The adult zebrafish heart

The heart is the first organ that develops and starts functioning in vertebrates. Unlike the four-chambered mammalian heart, the zebrafish heart consists of two chambers, one atrium and one ventricle. Deoxygenated blood passes from the atrium to the ventricle, where it is pumped into the gills for oxygenation (**Figure 1.5 A**). The bulbus arteriosus dampens the high pressure of the blood pumped from the ventricle. The unidirectional blood flow is maintained by the atrioventricular valve as well as the bulbo-ventricular valve (Gunawan et al., 2020; Hu et al., 2000).

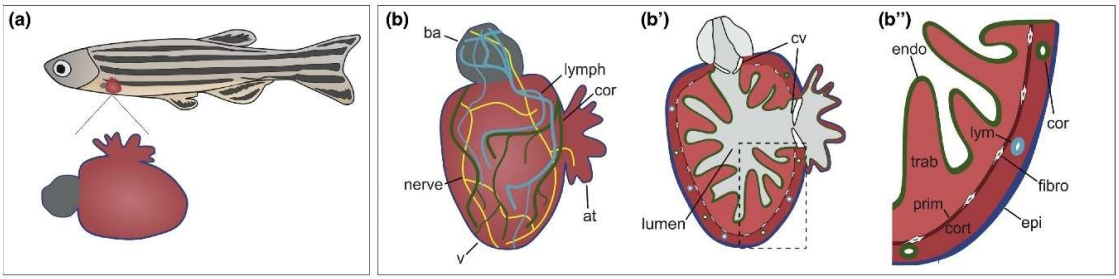

Figure 1.5: Anatomy of the zebrafish heart.
A. Schematic representation of an adult zebrafish with the location and orientation of the heart.
B. Schematic representation of a wholemount adult zebrafish heart showing the superficial

arrangement of the nerves, coronaries and lymphatics. **B'.** Schematic representation of a section of a healthy adult zebrafish heart showing the arrangement of the different cells types of the cardiac tissue. Adapted from (Sanz-Morejón and Mercader, 2020), License: CC BY 4.0.

The zebrafish ventricle consists of various cell types which are essential for maintaining the heart's physiology and also aid in its regeneration (**Figure 1.5 B**).
The main cell types that make up the zebrafish ventricle are CMs, which are the contractile cells in the heart. CMs can be subdivided into three, the outer compact layer, which is a multilayer of CMs in which coronaries are embedded. The second layer is the primordial layer of CMs, which is a single layer of immature CMs. And lastly trabecular CMs, which are the most abundant and from spongy-like structure within the heart (Gupta and Poss, 2012). The second cell type is epicardial cells which form the outermost epithelial layer of the heart. Epicardial cells are also a source of different cell types including fibroblasts and perivascular cells, as well as resident fibroblasts (Cao and Poss, 2018). The endothelial compartment in the heart can be subdivided into three, the endocardium which are ECs that form a lining over CMs, the cECs, which line the blood vessels that supply the ventricle with oxygen and nutrients, and lastly the lymphatic ECs, which form the lymphatic vasculature in the ventricle (Fernandez et al., 2018). The heart is also a well innervated organ, with sympathetic and parasympathetic nerves covering the surface of the ventricle (Stoyek et al., 2015). Moreover, recent reports have indicated the presence of resident immune cells, particularly macrophages in the heart under physiological conditions (Bohaud et al., 2021).
All of these different cell types (**Figure 1.5 B**) play vital roles in regulating the heart's development, and are essential in maintaining its function, as well as promote regeneration after cardiac injury.

1.4.2. Models of cardiac injury in zebrafish

There are several models of injury that are used to study cardiac regeneration in zebrafish, each with their own advantages.

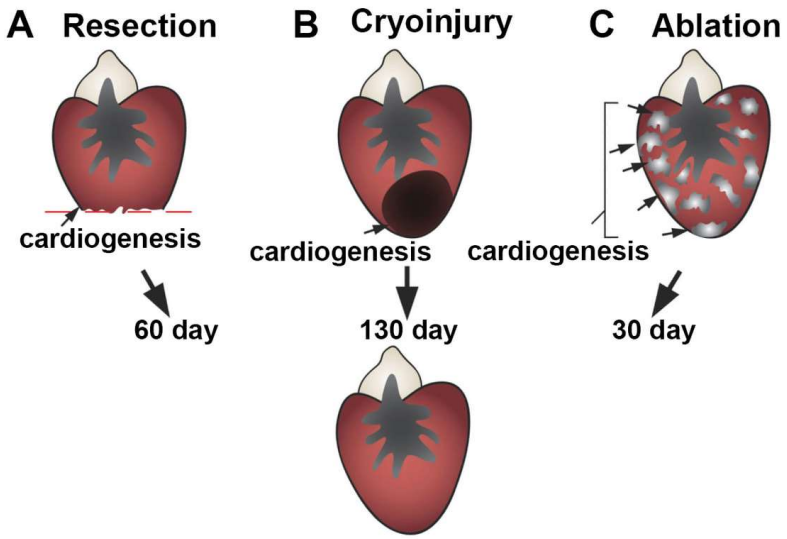

Figure 1.6: Models of cardiac injury in zebrafish.

A. Illustration of the apical resection model. B. Illustration of the cryoinjury model. C. Illustration of the genetic ablation model. Adapted from (Choi and Poss, 2012), License: 5302010996245.

Apical resection was the first method of cardiac injury introduced to the field in 2002, in which around 20% of the ventricle (the apical part) is cut off using spring scissors. This method allows the study of the cellular and molecular mechanisms that govern epimorphic regeneration of the heart (Poss et al., 2002) (**Figure 1.6 A**). In 2011, the cryoinjury model was introduced, which is widely used nowadays in the field. A metallic probe is precooled in liquid nitrogen, and is used to injure the apex of the heart (**Figure 1.6 B**). This method induces tissue death, and the deposition of a transient scar, which is similar to an extent to the tissue death that occurs following MI in the mammalian heart (Chablais et al., 2011; González-Rosa et al., 2011; Schnabel et al., 2011). The third cardiac injury model used in the field is Nitroreductase-mediated genetic ablation (**Figure 1.6 C**), which was introduced in 2008 (Curado et al., 2008). Basically, Nitroreductase enzyme (NTR) is expressed downstream of a specific promoter. NTR converts the prodrug Mitronidazole (MTZ) to a toxic compound which will kill the cells that express this enzyme. This and other genetic ablation methods are very beneficial to study the role of specific cells and their contribution to various processes (Wang et al., 2011). Another advantage of this method, is that it can be used in adults as well as in larval stages which helps analyze the roles of specific cell

types during various processes at different developmental stages as well as in regeneration.

1.4.3. Cellular and molecular responses to cardiac injury in zebrafish

Cardiac regeneration in zebrafish is a complex process that involves various signaling pathways, ECM remodeling and an interaction between the different cellular compartments in the ventricle to promote the proliferation and restoration of the damaged tissue by 60-90 days post cryoinjury (dpci) (**Figure 1.7**) (Bise et al., 2020; González-Rosa et al., 2017). As the field started back in 2002, a lot of attention was drawn to identifying mitogens that stimulate CM proliferation. However, more recently, various research groups have shed the light on the importance of the various cell types in the heart and how their timely activation and intercellular communication is essential in promoting CM proliferation during cardiac regeneration.

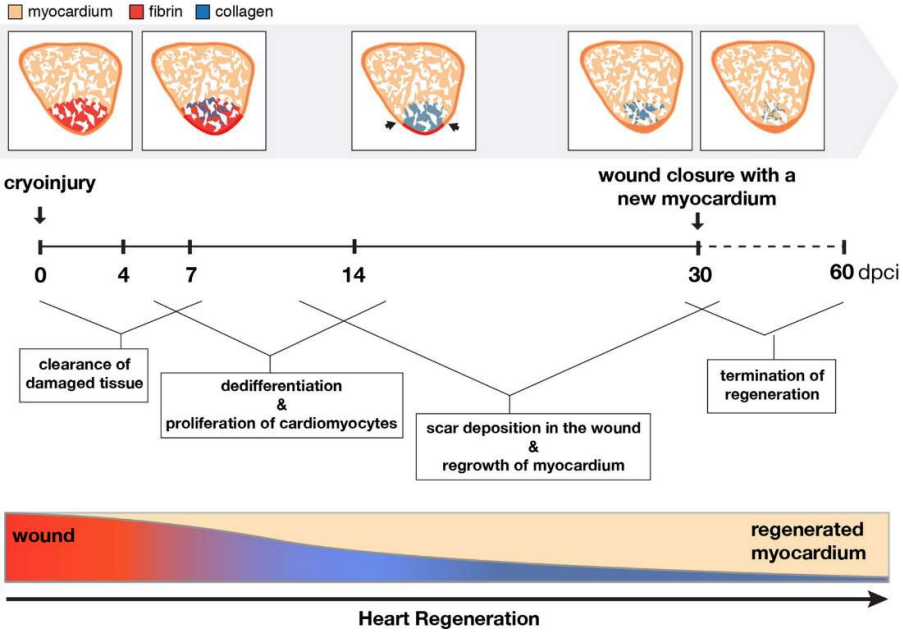

Figure 1.7: Cardiac regeneration in zebrafish.

A.F.O.G staining of heart sections at the different time points after cryoinjury. Illustration of the progress of cardiac regeneration process at different stages after cryoinjury. Adapted from (Bise et al., 2020), License: CC BY 4.0.

In the following sub-sections, I will review the roles of different cell types in the heart during the process of cardiac regeneration and highlight some of the important pathways needed for this process.

1.4.3.1. Immune cell response

One of the first responses that take place following cardiac injury is inflammation. Within hours after cardiac injury, pro-inflammatory genes are significantly upregulated and neutrophils start to infiltrate the injured tissue. Neutrophils peak in their numbers at 24 hours post cryoinjury (hpci). They play an essential role in clearing out the dead tissue debris, as well as signaling to other cells. At 48 hpci, the number of neutrophils decrease gradually, while more macrophages start infiltrating the injury (Lai et al., 2017) (**Figure 1.8**). The injured tissue is first infiltrated by pro-inflammatory M1 macrophages which phagocytose and clear the neutrophils. The anti-inflammatory M2 macrophages then infiltrate the injury and are believe to secrete paracrine factors which are necessary for repair and regeneration (Bevan et al., 2020; Ferraro et al., 2019). However, more research is required to identify the different molecular pathways which govern the effect of macrophages on other cells in the heart during regeneration. The timely recruitment of macrophages is very important for cardiac regeneration (**Figure 1.8**). Indeed, Lai and colleagues have previously shown that one of the main differences between the regenerating zebrafish heart and the non-regenerating medaka heart is the immune response (Lai et al., 2017, 2019). Along the same line of observations, injecting the toll-like receptor agonist Poly I:C enhanced macrophage recruitment in the non-regenerating medaka heart resulting in the formation of vessel-like structures from the endocardium and reduced scarring (Lai et al., 2017; Marín-Juez et al., 2019) (**Figure 1.8**). On the other hand, ablating macrophage using clodronate liposome injections resulted in a reduction of neutrophil clearance and coronary revascularization, and eventually resulted in increased scarring in zebrafish (Lai et al., 2017) (**Figure 1.8**).

Most work to date on the role of immune cells in cardiac regeneration revolves around the innate immune response. However, more recently, attention has been drawn to the role of the adaptive immune response. It has been shown that regulatory T-cells (Treg) play an important role in maintaining a pro-regenerative program after injury of several organs in zebrafish including the heart (Hui et al., 2017). However, more work is needed for a deeper understanding on the role of the adaptive immune response during cardiac regeneration in zebrafish.

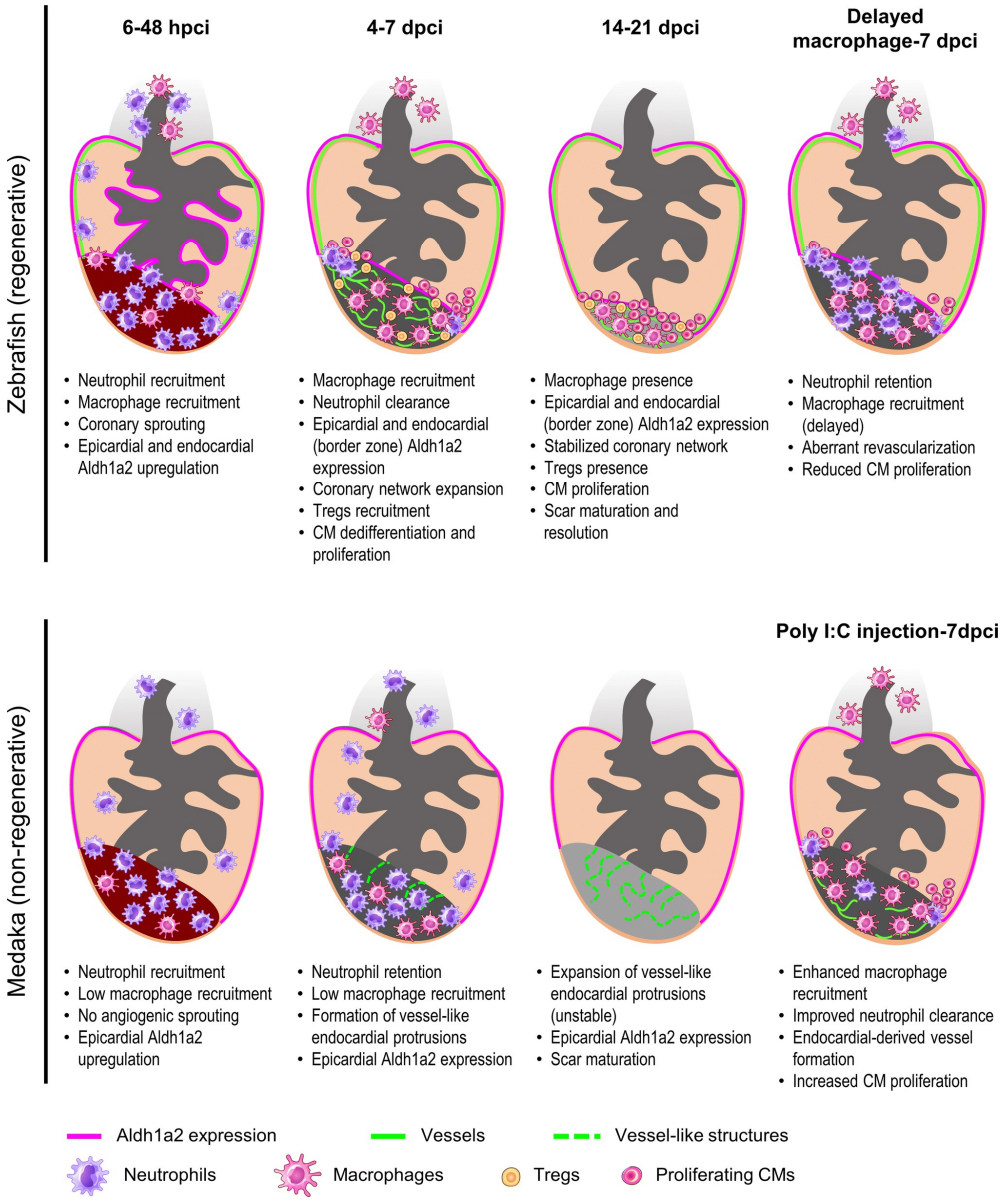

Figure 1.8: The immune response following cardiac injury in zebrafish and medaka. Schematic representation of the immune response along with other cellular processes in the regenerating zebrafish heart and the non-regenerating medaka heart, following cardiac injury. Adapted from (Lai et al., 2019), License: CC BY 4.0.

1.4.3.2. Endothelial response

ECs comprise three main compartments in the heart, namely, the endocardium, coronaries and lymphatics. Each of these endothelial compartments play a role in regulating cardiac regeneration via distinct molecular pathways in cellular interactions.

The endocardium

The endothelial lining of the heart is one of the first responders to cardiac injury (Lepilina et al., 2006). Within only few hours after injury, there is an upregulation of the endocardial expression of the enzyme retinaldehyde dehydrogenase (*aldh1a2*) that synthesized retinoic acid (RA) (Kikuchi et al., 2011a; Lepilina et al., 2006). The current hypothesis is that *aldh1a2* upregulation is caused due to increased inflammation following injury (Kikuchi et al., 2011a). This upregulation to date is considered as a hallmark of endocardial activation. The increased expression of *aldh1a2* is also observed in the epicardium following cardiac injury. After 24 hpci, the expression of *aldh1a2* becomes more confined to the border of the injured tissue. RA signaling is one of the important signaling pathways promoting cardiac regeneration. Blocking it results in a significant reduction in CM proliferation (Kikuchi et al., 2011a). A study by Kikuchi and colleagues suggested that endocardial RA signaling is observed in regenerating models such as the zebrafish heart but not in the non-regenerating adult mammalian heart, inferring a possible pro-regenerative role of endocardial RA signaling (Kikuchi et al., 2011a). However, the exact role of endocardial specific RA signaling is not yet known.

Following their activation after cardiac injury, endocardial cells change their morphology and become more rounded (Münch et al., 2017). They divide to replace the lost endocardial cells and peak in their proliferation at 72 hpci. They then extend their filipodia in order to invade the injured tissue (**Figure 1.9**). It has been reported by Münch and colleagues that infiltrating immune cells are in direct association and contact with the activated endocardium, suggesting that the endocardium might have an important role in immune cell recruitment (Koth et al., 2020; Münch et al., 2017). However, future studies addressing endocardial-immune interactions are needed to further understand the importance of the intercellular communication between these cell types during cardiac regeneration. It has also been shown that endocardial Notch signaling is essential for limiting endocardial inflammation and promoting its proliferation and invasion into the injured tissue, as well as the proliferation of CMs (Münch et al., 2017) (**Figure 1.9**).

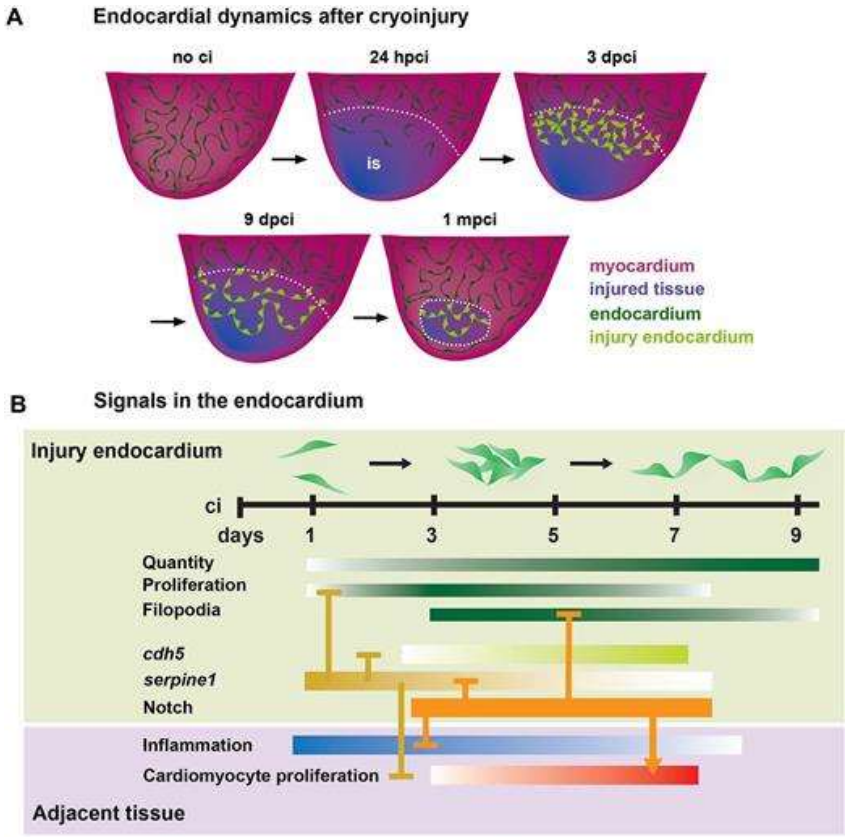

Figure 1.9: Endocardial response in the regenerating zebrafish heart.

A. Schematic representation of the endocardial dynamics after cardiac cryoinjury. **B.** Illustration of the endocardial response and endocardial signaling pathways after cardiac injury in zebrafish. Adapted from (Münch et al., 2017), reused with permission from The Company of Biologists.

Besides its role in signaling to CMs, recent studies have addressed a potential role of endocardial cell giving rise to fibroblasts by undergoing an Endo-MT (endothelial to mesenchymal transition) like process in the mammalian heart (Moore-Morris et al., 2014; Tombor et al., 2021). This phenomenon is also observed in zebrafish (Allanki et al., 2021). However, Allanki and colleagues have shown that this process is limited by Il-11 signaling and thereby limiting fibrosis in the zebrafish heart (Allanki et al., 2021).

Another important role of endocardial cells is revascularization. In the mammalian heart, endocardial cells are a source of coronary revascularization as reported previously in various studies (Räsänen et al., 2021; Tian and Zhou, 2022; Wu et al., 2012). However, in zebrafish, endocardial cells do not seem to give rise to coronaries,

but rather signal to them to aid in the process of coronary revascularization via Vegfaa signaling (Marín-Juez et al., 2019).

Coronaries

In the mouse heart, coronaries develop in embryonic stages E10.5 and are derived from the endocardium, the pro-epicardium as well as the sinus-venosus (Chen et al., 2014a; Lupu et al., 2020; Tian and Zhou, 2022; Wu et al., 2012). In contrast, coronaries in the zebrafish heart start to develop later at juvenile stages, around 30 days post fertilization (dpf) (Harrison et al., 2015). To date, our knowledge about coronary development in zebrafish is that they develop from endocardial cells around the atrio-ventricular canal and that Cxcr4a signaling plays an important role in this process (Harrison et al., 2015). In the adult heart and within 15 hours after cardiac cryoinjury, sprouts of cECs are observed to develop from pre-existing ones, reach their peak in proliferation at 96 hpci (Marín-Juez et al., 2016, 2019) (**Figure 1.10 A**). Coronary revascularization is majorly regulated by Cxcl12/Cxcr4 signaling where the regenerating cECs express the receptor *cxcr4a*, while the ligand *cxcl12b* is expressed by the epicardium and epicardium-derived cells (EPDCs) (Marín-Juez et al., 2019). These observations highlight the importance of intercellular communication between cECs and EPDCs in regulating coronary revascularization and cardiac regeneration (Lowe et al., 2019; Zhou et al., 2011). Coronaries revascularize the injured tissue in two modes: by sprouting superficially, as well as by sprouting intraventricularly into the lumen of the ventricle (**Figure 1.10 B**). Superficial revascularization is guided by Apelin signaling, whereas intraventricular sprouting is guided by endocardial Vegfaa signaling (Marín-Juez et al., 2019) (**Figure 1.10 B**).

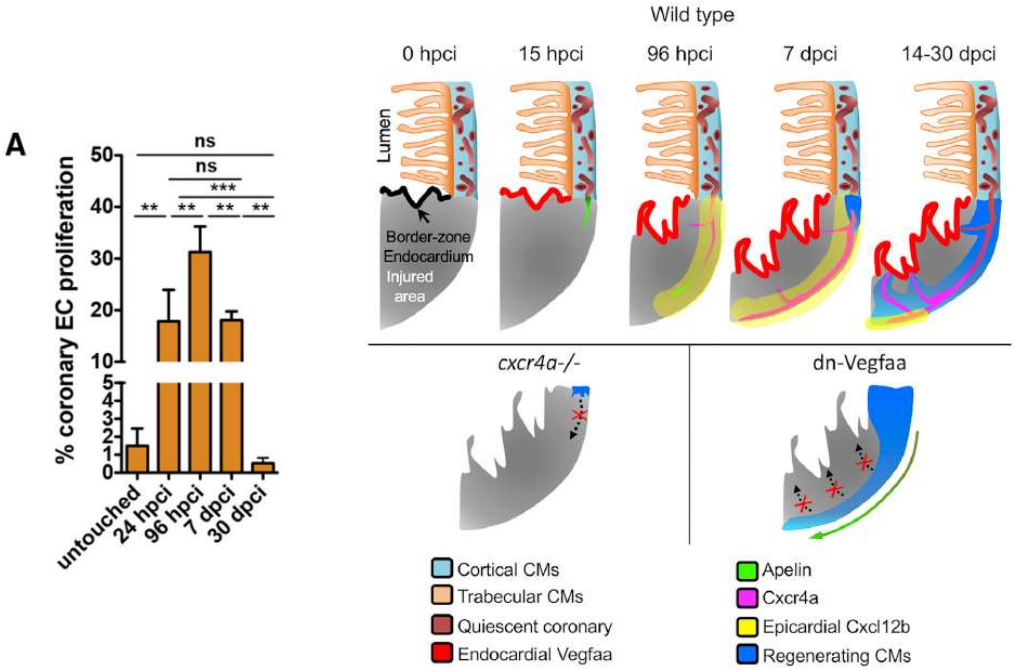

Figure 1.10: Coronary revascularization in the regenerating zebrafish heart.
A. Quantification of the coronary endothelial cell proliferation at various time points after cardiac cryoinjury. **B.** Schematic representation illustrating superficial and intraventricular revascularization guided by Apelin and Vegfaa signaling respectively. Adapted from (Marín-Juez et al., 2019), License: 5302020021515.

Marin-Juez and colleagues showed that coronary revascularization of the injured area is a crucial process during cardiac regeneration and that blocking it results in permanent fibrotic scarring (Marín-Juez et al., 2016). Along the same line of observations, stabilizing vessel-like structures in the non-regenerating medaka hearts after cardiac injury, significantly reduced scarring (Lai et al., 2017; Marín-Juez et al., 2019). Similarly, enhancing collateral formation in adult mouse hearts after MI results in a significant improvement in cardiac function (Das et al., 2019; Debenedittis et al., 2021). All of these data and observations emphasize the important role of coronary revascularization in promoting cardiac regeneration after cardiac injury.

Lymphatics

The last endothelial compartment that has been shown to be of great importance in enhancing cardiac regeneration is lymphatics. The lymphatic network develops much later than coronaries in the zebrafish heart, starting at around 3-month-old fish (Harrison et al., 2019). Lymphatics cover the bulbus artersiosus and then sprout into

the ventricle at around 4 months post fertilization (Gancz et al., 2019; Harrison et al., 2019). Recently, more attention has been drawn to the role that lymphatics play during cardiac regeneration in both mice as well as in zebrafish. In 2015, work from Paul Riley's group have shown that injecting recombinant VEGFC enhanced lymphangiogenesis which resulted in improved cardiac function of the heart following MI (Klotz et al., 2015). More recently, two studies in zebrafish have shown that lymphangiogenesis following injury is important for cardiac regeneration, and that blocking lymphangiogenesis delays neutrophil clearance from the injured ventricle, resulting in an increased inflammatory state and hence perturbed cardiac regeneration response (Gancz et al., 2019; Harrison et al., 2019). However, more work is needed for a more profound understanding on the molecular mechanisms governing lymphatics in the heart and to understand if the role of lymphatic ECs extends beyond clearance of immune cells during cardiac regeneration.

1.4.3.3. Epicardial response

Epicardial cells are amongst the early responders to cardiac injury. Within hours after cardiac injury, the epicardium becomes activated and upregulates the expression of the RA synthesizing enzyme (*aldh1a2*) (Kikuchi et al., 2011a; Lepilina et al., 2006). The epicardium represents one of most important cell types indispensable for cardiac development and regeneration. Indeed, epicardial ablation results in a significant reduction in CM proliferation following apical resection (Wang et al., 2015). In addition, hearts in which epicardial cells have been ablated retain a larger scar in comparison to their unablated controls, further highlighting the essential role that the epicardium plays during cardiac regeneration (Wang et al., 2015). Following injury, the epicardium upregulates the expression of several markers including *wt1a*, *tbx18* and *aldh1a2* (Lepilina et al., 2006). The epicardium also gives rise to various cell types including fibroblasts and perivascular cells, which play important role during cardiac regeneration (Cao and Poss, 2018; González-Rosa et al., 2012; Hu et al., 2021; Quijada et al., 2020) (**Figure 1.11 A**). Cells arising from the epicardium are collectively known as epicardium-derived cell (EPDCs). Some fibroblasts arising from the epicardium upregulate the expression of *postnb*, and are believed to be activated fibroblasts which are responsible of changing the ECM composition to aid in cardiac regeneration (Sánchez-Iranzo et al., 2018). Although the epicardium is a source of several cell types, it does not contribute to the CM lineage during cardiac regeneration.

Lineage tracing experiments using the epicardial specific *Tg(tcf21:CreERT2)* line revealed that the epicardium does not give rise to regenerating CMs (Kikuchi et al., 2011b). And hence, it is believed that the epicardium is a source of paracrine signals needed to support various cells types including during cardiac regeneration (Cao and Poss, 2018; Lepilina et al., 2006) (**Figure 1.11 B**).

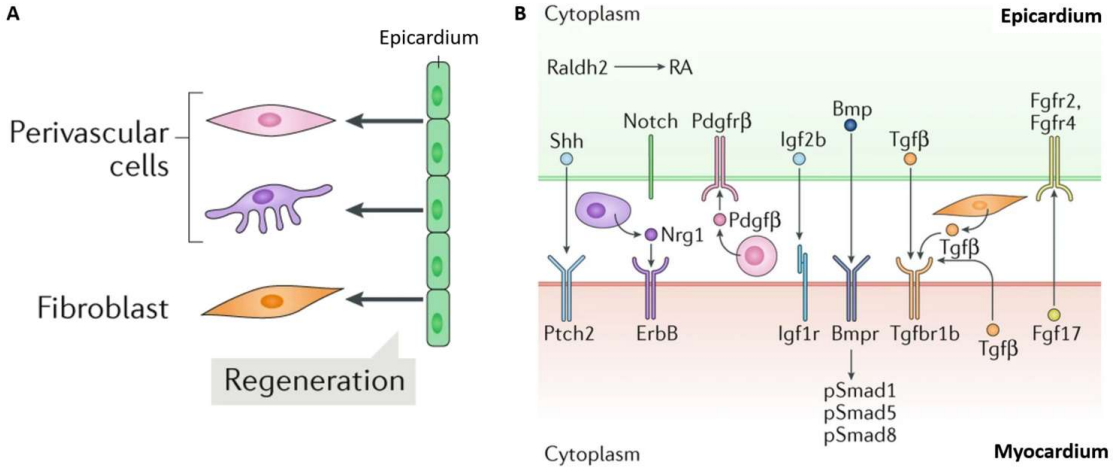

Figure 1.11: The epicardium during zebrafish cardiac regeneration.
A. Schematic representation of the cellular contribution of epicardial cells after cardiac injury in zebrafish. **B.** Schematic representation of the molecular contribution of epicardial cells during cardiac regeneration in zebrafish. Adapted from (Cao and Poss, 2018), License: 5302020193681.

For instance, the epicardium is a source of RA, which is essential for CM proliferation (Kikuchi et al., 2011a). Moreover, the epicardium produces several molecules such as Fn1, Prrx1b, and Nrg1a, all of which are required for CM proliferation (de Bakker et al., 2021; Gemberling et al., 2015; Wang et al., 2013). Paracrine signals from the epicardium do not only have an effect on CM, but on coronary revascularization as well. Marin-Juez and colleagues have shown that epicardial Cxcl12b regulates an important crosstalk to cECs through the receptor Cxcr4a to mediate coronary revascularization (Marín-Juez et al., 2019). Moreover, it has been shown that epicardial Nrp1 is quite important for coronary revascularization (Lowe et al., 2019), further highlighting the critical role of the epicardium in communicating with different cells in the heart to regulate cardiac regeneration.

1.4.3.4 Cardiomyocyte response

CMs have been the center of research in the cardiac regeneration field in both mice and zebrafish. For CMs to successfully replace the lost tissue after an injury, they need to proliferate and migrate into the injured area. It has been previously shown that newly regenerated CMs arise from pre-existing ones (Gupta and Poss, 2012; Kikuchi et al., 2010). Within the first 3 days following injury, CMs at the border of the injury first dedifferentiate into a less differentiated state which is characterized by their disorganized sarcomeres and the upregulation of immature or embryonic-like markers such as embryonic cardiac myosin heavy chain (embCMHC), *gata4* and *tnnc2* (Kikuchi et al., 2010; Tsedeke et al., 2021). This dedifferentiation state is then followed by their proliferation to replace the lost tissue. CM proliferation starts at around 3 days post cryoinjury (dpci), peaks at 7 dpci and levels off between 14 and 21 dpci (Bise et al., 2020; Chablais et al., 2011; González-Rosa et al., 2011) (**Figure 1.12**).

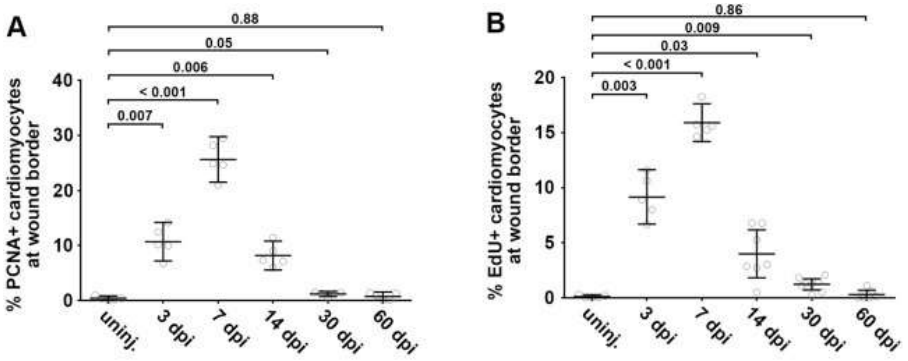

Figure 1.12: Cardiomyocytes proliferation profile after cardiac cryoinjury.
Quantification of cardiomyocyte proliferation at different time points after cardiac cryoinjury using PCNA immunostaining **(A)** and EdU incorporation **(B)**. Adapted from (Bertozzi et al., 2021), License: 5302020354482.

The proliferation of CMs is highly regulated by metabolism, whereby a shift from an oxidative phosphorylation dependent metabolic state to a more glycolytic state of CMs stimulates their proliferation (Fukuda et al., 2020; Honkoop et al., 2019). This shift in metabolism is also observed in the regenerating neonatal mouse heart (Puente et al., 2014). Besides their proliferation, CMs extend protrusions and migrate into the injured area, which is partly regulated by AP-1 transcription factors. Blocking these CM protrusions blunts the regeneration response (Beisaw et al., 2020). It is believed that the muscle is regenerated by 30 dpci, which is followed by changes in the ECM

composition and degradation of the fibrotic scar for a successful and complete regeneration of the heart which is achieved around 90 dpci (Bise et al., 2020).

1.4.3.5. Scar resolution

As previously outlined, almost most of the different cells in the heart become activated following an injury and they all respond to different signaling cues to proliferate and replace the damaged tissue. However, cardiac regeneration is not complete without resolving the transient scar that is formed as a result of the injury (Bertozzi et al., 2021; Bise et al., 2020; Chablais et al., 2011; González-Rosa et al., 2011). As previously outlined, the transient scar is formed following cardiac injury in zebrafish, consists of fibrin and collagen, which are deposited by several cells types such as fibroblasts as well as macrophages (González-Rosa et al., 2012; Sánchez-Iranzo et al., 2018; Simões et al., 2020). Following the activation and proliferation of the several cell types, the scar starts to degrade, mainly due to the increased expression of several metalloproteinases including *mmp2* and *mmp14a*, observed at 14 and 30 dpci (Gamba et al., 2017). These and other factors adjust the ECM composition and degrade the transient scar for the completion of the regenerative response. However, more work is needed for a deeper characterization on the ECM changes that take place to resolve the scar, and which factors contribute to this process. It would also interesting to identify which cells are actively involved in degrading the fibrin and collagen deposits and promoting cardiac regeneration. These findings could hold great potential applications in attempts to resolve the fibrotic scar resulting from MI in the adult mammalian heart.

1.5. VEGF signaling

As previously outlined, one of the important causes contributing to the mammalian's heart reduced capacity to regenerate is its poor revascularization potential, and that promoting coronary revascularization can promote cardiac regeneration and functional improvement in non-regenerative models (Debenedittis et al., 2021; Habib et al., 1991; Kocijan et al., 2021). These observations motivated many researchers to explore and identify factors that can promote this process. One of the very well-known factors that regulate endothelial sprouting and development are the vascular endothelial growth factor (VEGF) family members. The VEGF family comprises several ligands and receptors that regulate ECs (Olsson et al., 2006) (**Figure 1.13**). The main ligands

belonging to this family are VEGFA, VEGFB, VEGFC, VEGFD and placental growth factor (PlGF) (**Figure 1.13**). All of these growth factors are ligands to a family of tyrosine kinase receptors, namely, VEGFR1 (FLT1), VEGFR2 (KDR) and VEGFR3 (FLT4), as well as the co-receptors NRP1 and NRP2 (**Figure 1.13**). All of the VEGFRs typically form homo- and heterodimers. The different ligands bind preferentially to different VEGF receptors to regulate several aspects of EC biology (Koch and Claesson-Welsh, 2012).

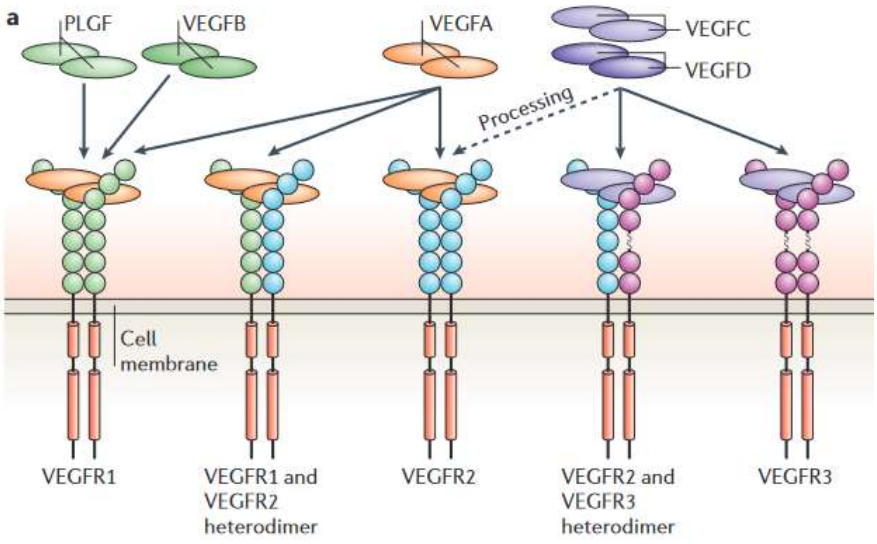

Figure 1.13: Overview of VEGF family.

Schematic representation of the different VEGF ligands and their associated receptors. Adapted from (Olsson et al., 2006), License: 5302020672176.

For instance, VEGFA and VEGFB can bind and activate VEGFR1 and VEGFR2 homo- and heterodimer whereas VEGFC can bind to VEGFR2 and VEGFR3 homo-and heterodimers, while VEGFD mainly binds to VEGFR3 homodimers (**Figure 1.13**). All of the different VEGF ligand have been studies for their role in promoting angiogenesis or lymphangiogenesis in different settings (Koch et al., 2011). Due to their highly potent role in promoting angiogenesis, VEGF family members were the center of investigations in attempts to promote coronary revascularization. Recent work has shown that overexpressing *Vegfa* in adult mouse hearts increased coronary revascularization and CM proliferation following MI (Debenedittis et al., 2021). Furthermore, it has been shown that in zebrafish, Vegfaa plays a vital role in promoting intraventricular revascularization to promote cardiac regeneration (Marín-Juez et al., 2016, 2019). Studies have also addressed the roles of other VEGF ligands in the

heart. For instance, a recent study has shown that endocardial VEGFB improves cardiac function following MI in mice (Räsänen et al., 2021). On the other hand, the role of VEGFD seems to be confined to regulating lymphangiogenesis during development in mice and zebrafish. Although it promotes lymphangiogenesis during development, however VEGFD is dispensable in this process (Astin et al., 2014; Baldwin et al., 2005; Haiko et al., 2008). Moreover, recent studies revealed that the absence of *vegfd* has no effect on cardiac regeneration in zebrafish (Gancz et al., 2019; Vivien et al., 2019). In the following section, I provide a more detailed review on the role of VEGFC signaling.

1.5.1. VEGFC signaling

As outlined above, VEGFC in particular binds to VEGFR2 and VEGFR3 (Oh et al., 1997). VEGFC is usually produced in an inactive form. It is then cleaved by collagen and calcium binding EGF domains 1 (CCBE1), a disintegrin and metalloproteinase with thrombospondin motifs 3 (ADAMTS3), Cathepsin D and kallikrein-related peptidase 3 (KLK3) at both the N- and C-termini, to be secreted in its mature and active form ΔNΔC-VEGFC (Jha et al., 2019) (Jeltsch et al., 2014; Joukov et al., 1997; Künnapuu et al., 2021) (**Figure 1.14**).

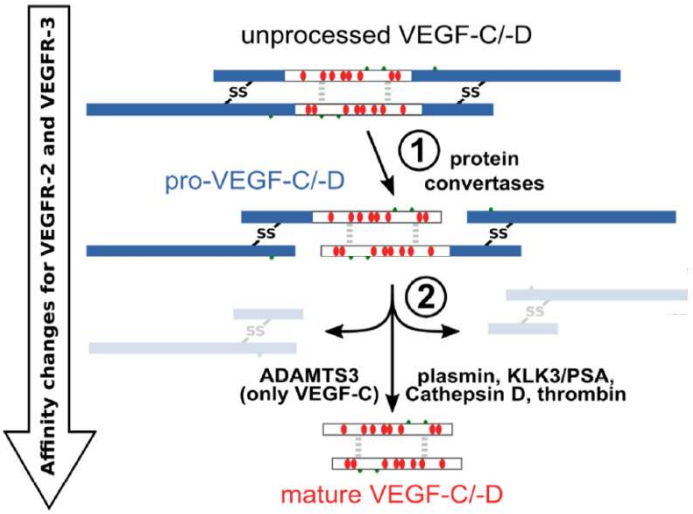

Figure 1.14: VEGFC processing and maturation.

Schematic representation of the stepwise mechanism of cleavage and activation of VEGFC. Adapted from (Künnapuu et al., 2021), License: CC BY 4.0.

The processed and mature form of VEGFC has a high binding affinity to both VEGFR2 and VEGFR3 (Künnapuu et al., 2021) (**Figure 1.14**). Upon binding to VEGFR2 and/or VEGFR3, VEGFC activates these receptors and induces the phosphorylation of different tyrosine residues in the intracellular tyrosine kinase domain. Depending on the different tyrosine residues' phosphorylation patterns, different intracellular pathways are activated. Activation of VEGFR2 by VEGFC or other VEGF ligands would lead to different phosphorylation patterns resulting in the activation of PI3K-AKT pathway or MEK-ERK pathway, as well as MAPK pathway (Olsson et al., 2006). These different pathways would regulate several aspects of ECs, including permeability, proliferation, migration and survival to promote vasculogenesis and angiogenesis. In VEGFR3, phosphorylation of the tyrosine kinase domain would activate PI3K-AKT pathway as well as MAPK pathway to induce lymphangiogenesis (Koch and Claesson-Welsh, 2012).

Extensive studies have shown that VEGFC acts as a master regulator of lymphatics in various contexts, including development and regeneration.

VEGFC was first identified in 1997 for its essential role in regulating lymphatic development in mice through VEGFR3 signaling (Oh et al., 1997). It has been shown that *Vegfr3* knock out mice start dying at around E10.5 due to edema and severe vascular defects (Dumont et al., 1998). Similarly, *Vegfc* knock out mice also die at E16.5 due to lack of lymphatics, highlighting the importance of VEGFC signaling promoting lymphangiogenesis during development (Karkkainen et al., 2004). Along the same line of observations, Vegfc is also a master regulator of lymphatic development in the zebrafish embryo (Küchler et al., 2006). *vegfc* as well as *vegfr3* mutants both display a significant reduction in lymphatic sprouting in the trunk, indicating a conserved role of Vegfc-Vegfr3 signaling in regulating lymphatic development across different species (Le Guen et al., 2014; Hogan et al., 2009a). The role of VEGFC in regulating lymphangiogenesis extends beyond developmental phases, and is also observed during regeneration. A study by Klotz and colleagues showed that injecting recombinant VEGFC results in increased lymphangiogenesis in the ventricle following MI, and lead to improved cardiac function (Klotz et al., 2015). A follow-up study by the same group revealed lymphangiogenesis is important for neutrophil clearance from the infarct tissue after MI (Vieira et al., 2018). In 2019, several studies have shown similar observations in the regenerating zebrafish heart.

They showed that Vegfc signaling is important is regulating lymphangiogenesis in the zebrafish ventricle following cryoinjury, and that blocking this process results in increased scarring (Gancz et al., 2019; Harrison et al., 2019; Vivien et al., 2019).

Although the role of VEGFC in regulating lymphangiogenesis has been extensively studies, a lot of groups have also investigated a possible role of VEGFC in regulating blood vessels. Indeed, Coa and colleagues have shown that VEGFC regulates angiogenic sprouting in several context including chick embryos as well as in mouse corneas (Cao et al., 1998). More recently in 2014, two studies have highlighted an important role of VEGFC signaling in promoting the development of coronaries arising from the sinus venosus (Chen et al., 2014a, 2014b). The role of VEGFC in regulating angiogenic sprouting is also conserved in zebrafish. Knock-down experiments using morpholinos result in a significant reduction in intersegmental vessel sprouting in the zebrafish embryo (Villefranc et al., 2013). On the other hand, overexpressing the constitutive active form of VEGFC in zebrafish embryos led to hypersprouting of intersegmental vessels (Le Guen et al., 2014). It has been suggested that in zebrafish, Vegfc acts in an autocrine manner via Vegfr2 to induce angiogenic sprouting, and in a paracrine manner via Vegfr3 to induce lymphatic spouting (Villefranc et al., 2013).

The role of VEGFC in regulating angiogenic sprouting in developmental settings across different species has motivated researches to look into a possible role of VEGFC in inducing collateral formation following MI. Notably, intramyocardial administration of adenovirus encoding VEGFC increased collateral formation following MI in porcine hearts, highlighting a high therapeutic potential of VEGFC signaling in inducing collateral formation (Pätilä et al., 2006). However, the mechanisms how VEGFC regulates collateral formation or coronary revascularization remain to be explored.

2. AIMS OF THE PROJECT

Coronary revascularization is critical for cardiac regeneration following injury in zebrafish (Marín-Juez et al., 2016). Hence, it is important to identify key angiogenic factors and understand the mechanism by which they promote cardiac regeneration in zebrafish. Previous transcriptomic data on the regenerating zebrafish heart, revealed an upregulation in the expression of the angiogenic factor *vegfc* (Lai et al., 2017; Lien et al., 2006)

A number of studies have shown that VEGFC signaling is a key regulator of lymphatic development in mice (Klaourakis et al., 2021). Moreover, studies have highlighted the role of VEGFC in stimulating lymphangiogenesis following myocardial infarction which lead to improved ejection fraction (Klotz et al., 2015). In addition to its role in regulating lymphangiogenesis, recent studies have shown that VEGFC is also required for coronary development in mice (Chen et al., 2014a, 2014c). Similarly, studies in zebrafish have emphasized the role of Vegfc signaling in promoting lymphangiogenesis during development, as well as during cardiac regeneration (Gancz et al., 2019; Harrison et al., 2019; Hogan et al., 2009b; Küchler et al., 2006). However, no studies to date have investigated the role of Vegfc signaling in regulating coronary revascularization during cardiac regeneration.

Taking advantage of the high regenerative capability of the zebrafish heart, the main goal of this project is to understand the role of Vegfc signaling during cardiac regeneration.

The project is subdivided into three aims:

Aim 1: Determine the expression dynamics of *vegfc* during cardiac regeneration in zebrafish

Aim 2: Investigate the role of Vegfc signaling during cardiac regeneration

Aim 3: Understand the mechanism how Vegfc regulates cardiac regeneration

3. MATERIALS AND METHODS

3.1 Materials

3.1.1. Antibiotics

Table 3.1. List of antibiotics used with their respective working concentrations.

Antibody	Working concentration
Ampicillin	100 µg/ml

3.1.2. Antibodies

Table 3.2. List of antibodies used with their respective sources, references, suppliers and working concentrations.

Antibody	Source	Reference	Supplier	Working Concentration
MEF2	Rabbit	sc-313	Santa Cruz	1:200
PCNA	Mouse	sc-56	Santa Cruz	1:500
FLI1a	Rabbit	ab133485	abcam	1:100
N2.261 (embMHC)	Mouse	N2.261	DSHB	1:20
GFP	Chicken	GFP-1010	Aves Labs	1:500
DsRed	Rabbit	632496	Takara Living Colors	1:100
RFP	Rabbit	600-401-379	Rockland	1:200
Goat anti-Rabbit IgG (H+L) Alexa Fluor 647	Goat	A-21244	Invitrogen	1:500
Goat anti-Chicken IgG (H+L) Alexa Fluor 488	Goat	A-11039	Invitrogen	1:500
Goat anti-Mouse IgG (H+L) Alexa Fluor 488	Goat	A-11029	Invitrogen	1:500

Goat anti-Mouse IgG (H+L) Alexa Fluor 568	Goat	A-11004	Invitrogen	1:500
Anti-DIG-AP, Fab fragments	Sheep	11093274910	Roche	1:1000

3.1.2. Bacterial strains

Table 3.3. Bacterial strain used and its application

Bacterial strain	Application
DH5α	Competent cells for transformation

3.1.3. Buffers and solutions

Table 3.3. List of buffers and solutions used and their compositions

Buffer/Solution	Composition
Alkaline Tris Buffer	100 mM Tris HCl pH 9.5, 100 mM NaCl, 50mM MgCl2
DEPC Water	0.01% DEPC dissolved in distilled water and autoclaved
E3 embryo medium	3g Instant Ocean, 0.75g Calcium sulphate dissolved in 10 L of distilled water
PBS	8g NaCl 0.2g KCl 1.44g Na2HPO4 0.24g KH2PO4 dissolved in 900 ml of distilled water, pH was adjusted to 7.4, volume was made up to 1000 ml with distilled water
PBST	0.1% Triton-X in PBS

20x SSC	175.3g NaCl, 88.2g Sodium Citrate dissolved in 800 ml distilled water and pH was adjusted to 7, volume was made up to 1000 ml with distilled water
DEPC-PBS	1 L PBS was filtered and 1 ml DEPC was added, followed by stirring for 1 hour and autoclaving.
1M (10x) Triethanolamine, pH 8.0	66.5 mL Triethanolamine and 20 mL concentrated HCl were added to 413.5ml DEPC-water
Hybridization Solution for Day1 (ISH)	50% Formamide 5X SSC 0.3 mg/mL Yeast tRNA 0.1 mg/mL Heparin 0.1% Tween 20 Adjust to pH 6.0 with 1M Citric acid
Hybridization Solution for Day2 (ISH)	50% Formamide 5X SSC 0.1% Tween 20 Adjust to pH 6.0 with 1M Citric acid
Blocking buffer (ISH)	TBST with 0.5% BSA
TBS	50 mM Tris-HCl pH 7.4 150 mM NaCl
Blocking buffer (IHC)	1X PBS 1% DMSO 2% Sheep Serum 0.2% Triton-X
TBST	TBS with 0.05% Tween-20

3.1.4. Centrifuges

Table 3.4. List of centrifuges used with their respective suppliers

Centrifuge	Supplier

Centrifuge (slow speed, 1.5-2ml tubes)	VWR Ministar
Centrifuge 5415 D (1.5-2 ml tubes)	Eppendorf
Centrifuge 5418 (1.5-2 ml tubes)	Eppendorf
Centrifuge 5418 (1.5-2 ml tubes)	Eppendorf
Centrifuge 5810 R (15-50 ml tubes and 96-well plates)	Eppendorf

3.1.5. Chemicals and reagents

Table 3.5. List of all the chemical and reagents used with their suppliers.

Chemical/reagent	Supplier	Catalogue no.
Mineral oil	Sigma-Aldrich	M8410
LB agar	Roth	X969
DIG RNA labelling mix	Roche	11277073910
Bovine serum albumin (BSA)	Sigma-Aldrich	A2153
Chloroform	Merck	102445
Citric acid	Sigma-Aldrich	27487
DNA ladder (100 bp)	Thermo Fisher Scientific	SM0241
DNA ladder (1 kbp)	Thermo Fisher Scientific	SM0311
Ethanol (molecular grade)	Roth	5054.4
Ethanol (denatured)	Roth	K928.3
Methanol	Roth	4627.5
16% Paraformaldehyde (PFA)	Alfa Aesar	43368
1X HBSS	Gibco	14175
Gel loading dye	Thermo Fisher Scientific	R0611

Heparin	Sigma-Aldrich	H5515
20X SSC	Ambion	AM9763
Methylene blue	Sigma-Aldrich	M9140
BM Purple	Roche	11442074001
Tricaine	Pharmaq	NA
Phosphate-buffered saline (PBS) tablets	Sigma-Aldrich	P4417
Dimethylsulfoxide (DMSO)	Sigma-Aldrich	D4540
Sheep serum	Sigma-Aldrich	S3772
Tris	Roth	5429.2
Triton X-100	Sigma-Aldrich	RES3103T-A101X
tRNA	Sigma-Aldrich	R7876
CutSmart buffer	NEB	B7204S
Agarose, low gelling temperature	Sigma-Aldrich	A9414
Agarose	Peqlab	35-1020
LB medium	Roth	X968
Nuclease-free water	Ambion	AM9938
TRIzol	Ambion	15596018
Glycerol	Millipore	356350
Pronase	Roche	10165921001
SYBR safe	Invitrogen	S33102
NaCl	Sigma-Aldrich	S3014
KCl	Sigma-Aldrich	P9541
MgSO4	Sigma-Aldrich	M2643

H_2O_2	Sigma-Aldrich	31642
KOH	Sigma-Aldrich	P1767
Proteinase K	Roche	1092766
Formamide (deionized)	Ambion	AM9342
Sucrose	Sigma-Aldrich	S0389
Phenol red	Sigma-Aldrich	P0290
$MgCl_2$	Sigma-Aldrich	63068
HCl	Sigma-Aldrich	H1758
HEPES	Sigma-Aldrich	H3375
NaHCO3	Roth	965.1
MgSO4.7H2O	VWR	437044K
Qtracker 705	Invitrogen	Q21061MP
4-hydroxytamoxifen	Sigma-Aldrich	H7904
DAPI	Thermo Scientific	D1306
O.C.T.	Sakura	4583
Fluorescence Mounting Medium	Dako (Agilent)	s3023

3.1.6. Microscopes

Table 3.6. List of microscopes used and their respective suppliers.

Microscope	**Supplier**
Confocal microscope LSM 700	Zeiss
Lightsheet microscope Z.1	Zeiss
SMZ25 stereo microscope	Nikon
Stemi 2000 stereomicroscope	Zeiss

3.1.7. Enzymes

Table 3.7. List of enzymes used and their respective suppliers.

Enzymes	Supplier
AgeI-HF, XhoI, MsI1, BamHI, NotI, ISce-HF and other restriction enzymes	NEB
Pronase	Roche
Proteinase K	Roche
Rnasein	Promega
RQ1 RNase free DNase	Promega
SP6 RNA Polymerase	Promega
T4 DNA ligase	NEB
T3 RNA Polymerase	Promega
T7 RNA Polymerase	Promega
RNase-free DNase set	Qiagen
SYBR green PCR mastermix	Thermo Fisher Scientific
Primestar Max DNA polymerase	Takara
2x Dynamo Color Flash	Thermo Fisher Scientific

3.1.8. Growth media

Table 3.8. List of all the growth media used and their respective suppliers.

Growth media	Supplier
LB medium	Roth
LB agar	Roth
Endothelial growth medium (EGM-2)	Lonza

3.1.9. Cell lines

Table 3.9. List of the cell lines used and their respective suppliers.

Cell lines	Supplier
HUVECs (primary cell line)	Lonza

3.1.10. Kits

Table 3.10. List of all the kits used and their respective suppliers.

Kits	Supplier
Cold Fusion Cloning Kit	System Biosciences
Gel extraction kit	Thermo Fisher Scientific
Mini Prep Plasmid isolation kit	Thermo Fisher Scientific
Maxima cDNA synthesis kit	Thermo Fisher Scientific
miRNAeasy micro kit	Qiagen
mMessage mMachine kits (SP6, T7, T3)	Ambion
MEGA shortscript (SP6, T7, T3)	Invitrogen
PCR product Cleanup	Jena Bioscience
PCR purification kit	Thermo Fisher Scientific
pGEM-T easy cloning kit	Promega
RNA cleanup and concentrator kit	Zymo research
Pierce Cardiomyocyte dissociation kit	Thermo Fisher Scientific
Lipofectamine RNAiMAX kit	Invitrogen

3.1.11. Lab equipment

Table 3.11. List of the all the lab equipment used and their respective suppliers.

Equipment	Supplier
PCR Mastercycler pro	Eppendorf
PTC-100 thermalcycler	MJ Research
NanoDrop 2000c	Thermo Fisher Scientific
Injection micromanipulator	World precision instruments
Picospritzer III	Parker
CFX connect Real Time PCR	BioRad
Eco Real-time PCR system	Illumina
Gel Doc EZ	BioRad
Electrophoresis power supply	BioRad
Microscale	Novex
Weighing balance	Sartorius
Micropipette puller P-1000	Sutter Instrument
Bacterial shaker	Infors HAT
Bacterial incubator	Heraeus
Bacterial incubator shaker	Infors HAT
Heating block	VWR
Microwave oven	Bosch
Zebrafish breeding tanks	Tecniplast
Zebrafish aquaculture system	Tecniplast

Zebrafish incubator	VWR Incu-Line
Zebrafish incubator	Binder
CM1950 cryostat	Leica
Bullet Blender	Next Advance

3.1.12. Lab supplies

Table 3.12. List of all the lab supplies and their respective suppliers.

Supplies	**Supplier**
Bacterial culture tubes	Sarstedt
Latex gloves	Roth
Nitrile gloves	VWR
Beakers	VWR
Eppendorf tubes	Sarstedt
Falcon tubes	Greiner bio-one
Glass bottom dish	MatTek
Microloader pipette tips	Eppendorf
PCR tubes	Sarstedt
Scalpel	Braun
Pipettes	Gilson
Petri dishes	Greiner bio-one
Forceps	Dumont
Glass bottles	Duran
Laboratory film	Parafilm
Pipetboy	Integra

Pipette tips	Greiner bio-one
Filtered pipette tips	Greiner bio-one
Conical flasks	VWR
Serum pipette	Greiner bio-one
Spring scissors	Dumont
0.5 mm Cryoprobe	Custom-made
DNA and RNA Oligos	Sigma
CELLSTAR cell culture multi-well plates (6 well plates)	Greiner bio-one

3.1.13. Plasmids

Table 3.13. List of the plasmids used and their details.

Plasmids	Antibiotic resistance	Source
pGEM-T	Ampicillin	Promega
pCS2+	Ampicillin	Addgene
pT3TS-nlsCas9nls	Ampicillin	Addgene
pT7-gRNA	Ampicillin	Addgene
HOTCRE plasmid (modified)	Ampicillin	(Hesselson et al., 2009)
hsp70l plasmid (modified)	Ampicillin	(Matsuoka et al., 2016)

3.1.14. Peptides and inhibitors

Table 3.14. List of the peptides and chemical inhibitors used and their suppliers.

Inhibitor	Supplier	Catalogue no.
SB225002 (Cxcr1 inhibitor)	Sigma-Aldrich	182498-32-4

3.1.15. Oligonucleotides

Table 3.15. List of all the DNA and RNA oligonucleotides used and their application.

Target Gene	Primer sequence
RT-qPCR	
rpl13a	**Fwd:** TCTGGAGGACTGTAAGAGGTATG **Rev:** AGACGCACAATCTTGAGAGCAG
vegfc	**Fwd:** TCGAGTCAAGTCACGACTACTATG **Rev:** ATCCACACTACCCGCTGAAC
sflt4	**Fwd:** CGCCAGCTCCTACGTGTTCGTGAGAG **Rev:** CGTCTGGCCACAGCACCGAGC
apln	**Fwd:**GCTGTGTTCAGCCAGTGCT **Rev:** TTCTGCCGCAAAGGAGTC
cxcr4a	**Fwd:** AGAGTGAGCACAAACAGAAGG **Rev:** GGCTTATTACGAACACATCGTC
vegfr1	**Fwd:** GCTCATTCAGGTGAAGTGGACAG **Rev:** AGAAGATCGCCTTCATAATGTGG
vegfr2	**Fwd:** ACCTCAGTCAAAGCCTTCTTCAC **Rev:** AGCAGTTGTGGATCAGGCAGAC
vegfr3	**Fwd:** GACCCAGAGCATCCATTCAT **Rev:** AGGCTCTGGATACGGCACTA
vmhcl	**Fwd:** GCGATGCTGAAATGTCTGTT **Rev:** CAGTCACAGTCTTGCCTCCT
tnnt2a	**Fwd:** CAACGAAGAAGTGGAAGAGTACGAG **Rev:** TTCTCCATCGTGTTCCTGAGTG
nppa	**Fwd:** GATGTACAAGCGCACACGTT **Rev:** TCTGATGCCTCTTCTGTTGC
myl7	**Fwd:** GGCTCTTCCAATGTCTTCTCC **Rev:** GGACTCCAGCTCTTCATCAC
emilin2a	**Fwd:** CCTCCTGTCAACCCTGTCTCATATGATACC **Rev:** GGCAATGATGCCGAAGTCCCCAGAG

ccl25b	**Fwd:** GGCTTTGCTCCTGCTGTTGGCTTGC **Rev:** ACAGCGGGAATGTTGCATCCTCCGT
mhc2dab	**Fwd:** GTCCTGGCTGAGAGATGGTAAAGAGGTG **Rev:** GGTTGAGTTAAGCTGGCGTGCTCC
adrb2b	**Fwd:** GCGCTGGTCATCAGTGCCATTGTACGATTCC **Rev:** GCCGAAGGGCACCACCATAAGACCC
fn1b	**Fwd:** CTCTTCCAAATGGTGTCACG **Rev:** CACACTTGAACTCTCCTTTGC
cebpd	**Fwd:** CCAAAGGGATTCATTCACAA **Rev:** CTGTTGTTGTTGTTGTTCTC
htra3a	**Fwd:** TGACAAGAAATCAGACATCG **Rev:** AGAGCGACCTAATGATAAGA
c6	**Fwd:** GTCACTTAAGATTCAACAAGCGTC **Rev:** GTTTCTCCCATGTACCATCCTG
agmo	**Fwd:** CTCTCCGTTGGCGCTGCTGATTCCTCCT **Rev:** TTCGCCCGTGGTGAACTCTGTGGTGGC
bnip4	**Fwd:** GCTGTCTTCAACACACATAC **Rev:** TATAAATGCTGTGGGTGGTA
cxcl8a	**Fwd:** TGTGTTATTGTTTTCCTGGCATTTC **Rev:** GCGACAGCGTGGATCTACAG
cxcr1	**Fwd:** GTGATCGTACGCGCTATGGA **Rev:** ATTCGGGTTGCTAATCGCCA
cxcr2	**Fwd:** GTCACTGGCCGTTCGGCACCATCATG **Rev:** CCCAATCAGATGGAGCTTTCGGTTGAGG
GAPDH	**Fwd:** TGTTGCCATCAATGACCCCTT **Rev:** CTCCACGACGTACTCAGCG
VEGFC	**Fwd:** CACACTTCCTGCCGATGC **Rev:** GTTCGCTGCCTGACACTG
EMILIN2	**Fwd:** AAAGCCACAGATAATGAACC **Rev:** CCTCTAGCACCTGTATCTTC
	***in situ* hybridisation**
vegfc	**Fwd:** ATGCACTTATTTGGATTTTCTGTC **Rev:** TTAGTCCAGTCTTCCCCAGTATGTGGG

emilin2a	**Fwd:** TTGAGGAATTGCGGGGAACAGTG **Rev:** AATCTGGTTGTGGCTTGGTCTGC
cxcl8a	**Fwd:** ATGACCAGCAAAATCATTTCAGTG **Rev:** TCATGGTTTTCTGTTGACAATG
cxcr1	**Fwd:** GCAACTTCACGTTTGTTCCCGACGAG **Rev:** CTGTAGCAGCTCAACATGACCACTAGG
Primers used for cloning/generation of transgenic lines	
***hsp70l:emilin2a* line**	**Fwd:** CCTGATCGATACCGTCGGCGCGCCATGAATTACCATACACGATTG **Rev:** GTTAGTAGCTCCGCTTCCCTCGAGTCTCTTCGCTTGAGGCG
***HOTCRE-emilin2a* line**	**Fwd:** TACATTATACGAAGTTATACCGGTCGCCACCATG AATTACCATACACGATTGTTTGG **Rev:** AGTTCGTGGCTCCGGACCCTCTCTTCGCTTGAGGCGAG
Genotyping	
HRMA	
***emilin2a* (exon 1)**	**Fwd:** CATCATAAGCTTTTCTCTCACTCATG **Rev:** GTGAACGGCTCCTGAATACGCG
***emilin2a* (exon 9)**	**Fwd:** GGTCAGCGTCTTTCAGCCTCA **Rev:** GGCGAGTAGAGGAATATAGCGCTGAA
PCR	
emilin2a	**Out-Out primers to detect the deletion** **Fwd:** CCATACACGATTGTTTGGAGCAAAGTTAT **Rev:** GGCGAGTAGAGGAATATAGCGCTGAA **In-In primers to detect the gene** **Fwd:** CTGGAGTAGCTGAGGGTGTCTCT **Rev:** GTTATTCATTTGTGCCACCTTCCTCTCC
cxcl8a	**Fwd:** GCTTTCAGGAATGAGCTTGAGAG **Rev:** TCTTAACCCATGGAGCAGAGG
RNA oligo sequences	
***emilin2a* (exon 1)**	AGCAGTGCGGACCAAGGCCA

***emilin2a* (exon 9)**	TACCCGTCAAGTCTGTTCCA
cxcl8a	TAATACGACTCACTATAGGCCTTGATGACAAC TGGACGTTTTAGAGCTAGAAATAGCAAG
Universal oligo	TTTTGCACCGACTCGGTGCCACTTTTTCAAGTTGATAACG GACTAGCCTTATTTTAACTTGCTATTTCTAGCTCTAAAA

3.1.16. Software and databases

Table 3.16. List of software and databases used in this thesis and their purposes.

Software	Purpose
Adobe Illustrator	Image formatting
Fiji (ImageJ)	Image processing and data analysis
Zen (Zeiss, Blue and Black)	Image acquisition, processing and data analysis
GraphPad Prism	Data analysis
Microsoft Office (Word, Excel, PowerPoint)	Writing, data analysis, and presentation
R Studio	Data analysis and visualization
Ensembl.org	Genome browsing and analysis
ZFIN	Zebrafish gene expression and nomenclature
IGV	NGS analysis
Primer BLAST	Primer generation
Snapgene	Plasmid editor
CHOPCHOP	gRNA design
Nikon (NIS elements)	Image acquisition, processing and analysis
zfregeneration.org	Zebrafish regeneration data repository

3.1.17. Zebrafish lines

Table 3.17. List of zebrafish lines used in this thesis and their details.

Line	Description	Source
Tg(hsp70l:slft4)^{bns82}	*sflt4* overexpression line	(Matsuoka et al., 2016)
Tg(hsp70l:vegfaa121-F17A)^{bns100}	*dn-vegfaa* overexpression line	(Rossi et al., 2016)
Tg(-0.8flt1:RFP)^{hu5333}	Reporter line labels lymphatic endothelial cells	(Bussmann et al., 2010)
Tg(myl7:DsRed)^{s879}	Reporter line labels cardiomyocytes	(Chi et al., 2008)
TgBAC(tcf21:NTR-mCherry)^{pd108}	Reporter and ablation of epicardium-derived cells	(Wang et al., 2015)
TgBAC(tcf21:CreERT2)^{pd42}	Recombination in epicardium-derived cells	(Kikuchi et al., 2011b)
Tg(-5.2lyve1b:DsRed)^{nz101}	Reporter line labels lymphatic endothelial cells	(Okuda et al., 2012)
Tg(flt1:Mmu.Fos-GFP)^{wz2}	Reporter line labels coronary endothelial cells	(Nicenboim et al., 2015)
vegfc^{hu5055}	*vegfc* mutant	(Le Guen et al., 2014)
vegfd^{bns257}	*vegfd* mutant	(Gancz et al., 2019)
cxcr1^{sa14414}	*cxcr1* mutant	(Kettleborough et al., 2013)
Tg(hsp70l:emilin2a, cryaa:CFP)^{bns504}	Global *emilin2a* overexpression	This study (El-Sammak et al., 2022)
Tg(hsp70l:loxP-CFP-loxP-emilin2a-p2A-mCherry)^{bns510}	HOTCRE *emilin2a* overexpression	This study (El-Sammak et al., 2022)
emilin2a^{bns556}	*emilin2a* mutant	This study (El-Sammak et al., 2022)
cxcl8a^{vu660}	*cxcl8a* mutant	This study (El-Sammak et al., 2022)

3.1.18. Zebrafish food

Table 3.18. List of zebrafish food used and the feeding regime.

Food	Regime
SDS100	5 dpf - 12 dpf
Brine Shrimp	> 1 month
SDS200	1 - 2 months
SDS300	2 - 3 months
SDS400	> 3 months

3.2. Methods

Note: Parts of this section are used *verbatim* from the following article published in *Circulation Research*.

[**El-Sammak, H.**, Yang, B., Guenther, S., Chen, W., Marín-Juez, R., and Stainier, D.Y.R. (2022). A Vegfc-Emilin2a-Cxcl8a Signaling Axis Required for Zebrafish Cardiac Regeneration. Circ. Res. *130*, 1014–1029.]

3.2.1. Zebrafish maintenance and treatments

3.2.1.1. Zebrafish husbandry and maintenance

All zebrafish (*Danio rerio*, strain: AB/Tü) were handled according to institutional (Max-Planck Gesellschaft) and national animal welfare guidelines approved by the animal experiments committee at the Regierungspräsidium Darmstadt in Germany.

All zebrafish were maintained in Tecniplast fish culture system at 27-28.5°C water temperature. For breeding, male and female zebrafish were placed in a breeding tank with a divider between them the evening before. The dividers were then removed the next morning, and the fish lay eggs within 20-30 minutes. The eggs were collected from the bottom of the mating tanks into 10 cm Petri dishes. Zebrafish larvae until 5 days post fertilization (dpf) were kept in egg water and maintained in a BOD incubator at 28°C, and later moved to the fish culture system.

3.2.1.2. Zebrafish heat shock treatments

Adult zebrafish were housed in 39ºC in a VWR Incu-Line incubator for one hour every 12 hours and then transferred back to their fish culture system.

3.2.1.3. Zebrafish adult intra-peritoneal (IP) injections

For 4-hydroxy tamoxifen (4-OHT) injections, 25 mM stock was heated at 60°C for 10 minutes and then diluted in 1x PBS. Adult zebrafish were first anesthetized in 0.025% (v/v) Tricaine in E3 water. Fish were then laid on their dorsal side and injected with 10 µl of 1.25 mM 4-OHT or ethanol as control, using a BD Micro-Fine U-100 Insulin needle. Following IP-injections, fish were placed in fresh water to recover.

For SB225002 injections, SB225002 was dissolved in DMSO to prepare the stock solution and then diluted in egg water. Adult zebrafish were first anesthetized in

0.025% (v/v) Tricaine in E3 water. Fish were then laid on their dorsal side and injected with 20 µl of 0.01 mM SB225002 or DMSO as a vehicle control, using a BD Micro-Fine U-100 Insulin needle. Following IP-injections, fish were placed in fresh water to recover.

3.2.1.4. Zebrafish adult intra-myocardial injections

Micro-needles were made ready from glass capillaries using the needle puller instrument as per the manufacturer's instructions (Sutter instruments). 5 µl of Qdots were loaded into a pre-cut microneedle, which was then fixed into a micromanipulator. Injection pressure was calibrated to get a consistent droplet size. Adult zebrafish were anesthetized in 0.025% (v/v) Tricaine in E3 water. Fish were then laid on their dorsal side and a small cut was made in the thoracic region to expose the ventricle. Once exposed, the ventricle was gently penetrated with the microneedle for injecting the Qdots. Injected fish were then placed in fresh water to recover (Harrison et al., 2019).

3.2.1.5. Zebrafish adult heart cryoinjury

Adult zebrafish were first anesthetized in 0.025% (v/v) Tricaine in water. Fish were then laid on their dorsal side and a small incision is made in the thoracic region to expose the ventricle. Once exposed, the apex of the ventricle is injured using a metallic probe pre-cooled in liquid nitrogen. The probe is removed from the tissue after it thaws out. Cryoinjured zebrafish are then transferred to fresh water for recovery (Chablais et al., 2011; González-Rosa et al., 2011; Schnabel et al., 2011).

3.2.1.6. Zebrafish sham operations

Adult zebrafish were first anesthetized in 0.025% (v/v) Tricaine in water. Fish were then laid on their dorsal side and a small cut is made in the thoracic region to expose the ventricle. Once, exposed, a metallic probe at RT was used to gently touch the apex of the ventricle. Sham-operated zebrafish are then transferred to fresh water for recovery.

3.2.2. Zebrafish embryo micro-injections

3.2.2.1. Preparing microinjection plates

2% agarose solution made in egg water in petri dishes to prepare injection plate. A plastic mould with lanes was placed on the agarose solution and left to solidify at RT. After solidification, the mould is removed and the injection plate is stored at 4°C.

3.2.2.2. Preparing microinjection needles

Micro-needles were made from glass capillaries using the needle puller instrument as per the manufacturer's instructions (Sutter instruments).

3.2.2.3. Microinjections

5 µl of the injection mix (DNA/RNA) along with 0.5 µl phenol red for visual confirmation were loaded into the microneedle. The loaded needle was then fixed into a micromanipulator. Injection pressure was calibrated to get a consistent droplet size as measured by a microscale. One-cell stage embryos were placed in the injection plate lanes and were injected. For DNA mixes, injections were performed into the cell, and into the yolk for RNA mixes.

3.2.3. Molecular techniques

3.2.3.1. RT-qPCR

RNA isolation

RNA was extracted using either the Zymo research kit or the Qiagen miRNeasy micro kit. The tissue was collected into 700 µl TRIzol, and stored in -80°C for later processing. For RNA isolation, samples were brought to room temperature and the tissue was homogenized using a bullet blender (Next Advance) following the manufacturer's protocol. 140 µl of Chloroform was added and vortexed. Samples were then left at room temperature for 5 minutes, followed by centrifugation at 12,000 g for 15 minutes at 4°C. The upper aqueous phase was collected into a different tube and processed following the manufacturer protocol of the Zymo and Qiagen kits. The RNA was stored at -80°C until further usage.

cDNA synthesis

cDNA was synthesized using the Maxima first strand cDNA synthesis kit for RT-qPCR (Thermo Fisher Scientific) following the manufacturer's protocol. The reaction was set up as follows:

Table 3.19. Components of the cDNA synthesis reaction mixture.

Components	Reaction volume
Template RNA	100 ng – 1 µg
5x reaction mix	4 µl
Maxima enzyme mix	2 µl
Nuclease-free water	Up to 20 µl

Using a thermocycler, the reaction was kept at 25°C for 10 minutes followed by 30 minutes at 50°C. The reaction was stopped at 85°C for 5 minutes. The 20 µl of cDNA was stored at -20°C for further usage.

For whole ventricles, 250 ng of RNA were reverse transcribed. For sorted cells, 100 ng of RNA were reverse transcribed. For HUVECs, 500 ng of total RNA were reverse transcribed.

RT-qPCR reaction

RT-qPCR was used to analyse gene expression levels. SYBR green reagent-based enzyme mix (DyNAmo color flash, Thermo Fisher Scientific) was used. mRNA levels of the different genes were normalized to mRNA levels of the housekeeping genes: *rpl13a* (zebrafish) and *GAPDH* (HUVECs) and fold changes were calculated using the log2 ΔΔ Ct (Livak and Schmittgen, 2001). At least four biological replicates, each in three technical replicates were performed for all reactions, using the SYBR Green PCR Master Mix (Thermo Fisher Scientific) on CFX Connect Real-Time System (Bio-Rad). Nuclease-free water was used to dilute all cDNA samples in a 1:10 ratio. The qPCR reaction mix and thermo-cycling conditions were as the following:

Table 3.20. Components of the RT-qPCR reaction mix.

Components	Reaction volume
2x Maxima SYBR mastermix	5 µl
Forward and reverse primer mix	4 µl
cDNA	5 µl
Nuclease-free water	6 µl

Table 3.21. Reaction conditions for RT-qPCR.

Step	Temperature	Duration	No. of cycles
Polymerase activation	95°C	2 mins	1
PCR cycling	95°C	5 secs	44
	60°C	30 secs	
HRMA	95°C	5 secs	1
	65°C	5 secs	
	95°C	5 secs	

3.2.3.2. PCR amplifying genes from cDNA

Primers amplifying specific genes were designed using DNA sequences acquired from Ensembl.org and validated for specificity using the NCBI Primer BLAST database. PCR was carried out using the Eppendorf Mastercycler Pro machines and 2x Takara PrimeSTAR Max polymerase mastermix. The reaction mix and conditions used were as follows:

Table 3.22. Components of the PCR reaction mix.

Components	Reaction volume
2x PrimeSTAR Max mix	12.5 µl

Forward and reverse primer mix	5 µl
cDNA template	1 – 2 µl (100 pg)
Nuclease-free water	Up to 25 µl

Table 3.23. Reaction conditions- PCR.

Step	Temperature	Duration	No. of cycles
Polymerase activation	95°C	3 mins	1
PCR cycling	95°C	10 secs	40
	60°C	5 secs	
	72°C	10 sec/kb	
Final extension	72°C	5 mins	1
Storage	4°C	∞	

3.2.3.3. Agarose gel electrophoresis

Following PCR, samples were resolved on an agarose gel containing SYBR safe to visualize the DNA bands and to verify the size of the amplicons. Large DNA fragments (>5 kb) were loaded on a 1% agarose gel and smaller fragments were resolved on a 3% agarose gel, using appropriate DNA ladders (1 kb and 100 bp). The time of electrophoresis ranged between 40-60 minutes at a voltage range 120-150 V. DNA fragments were then observed under UV light using a gel doc imager.

3.2.3.4. PCR product purification

Gel slices containing the desired PCR band were cut out using a scalpel and processed further using the GeneJet Gel Extraction kit (Thermo Fisher Scientific). The gel slice was transferred to a 2 ml Eppendorf tube. 1:1 (weight to volume) binding buffer was added, and incubated at 55°C until the gel was entirely dissolved. 700 µl of this solution was loaded on a gel purification column and centrifuged for 1 min at 13000 rpm. The flow-through was discarded and the column was washed with 700 µl of wash buffer by centrifugation. After discarding the flow-through, the empty column

was centrifuged at full speed for 2 minutes to remove any remaining solutions on the membrane. 15 µl of nuclease-free water was added to the column and centrifuged to elute the DNA. The concentration was then measured and DNA stored at -20°C.

3.2.3.5. DNA restriction digestion

NEB enzymes and buffers were used to digest DNA fragments and/or plasmids. Specific temperatures, incubation timings and inactivation conditions were performed as specified on the NEB manuals.

3.2.3.6. Preparation of competent cells

Day 1

3 ml liquid LB medium were added to two 15 ml falcon tubes. E.coli competent cells from the stock were inoculated in one of the falcons, while the other falcon served as a sterile control. The cells were then cultured at 37°C overnight.

Day 2

After confirmation of no contamination in the sterile control tube, 200 ml of liquid medium with 1 ml of the overnight culture were added to 500 ml flasks. The flasks were incubated at 37°C for 4 hours. Meanwhile, the centrifuge was pre-cooled to 4°C. After 4 hours, the 200 ml culture was cooled on ice and aliquoted into pre-cooled 50 ml falcon tubes. The bacterial pellet was formed by centrifugation at 4000 rpm for 10 minutes at 4°C. The supernatant was discarded and the pellet was air dried on clean tissues by inverting the tubes. 5 ml ice-cold 0.1 M CaCl2 was added to the pellet and homogenized by pipetting. The homogenate was cooled on ice for a few minutes and spun at 4000 rpm for 5 minutes at 4°C. All the above steps were repeated till the pellet was obtained once more. The pellet was dried again after discarding the supernatant. 1 ml cold 0.1 M CaCl2 and 15% glycerol were added to the dried pellet and the tubes were left on ice. The pellet was then homogenized and the solution was aliquoted in 1.5 ml Eppendorf tubes and snap-frozen in liquid nitrogen. The Eppendorf tubes were then stored at -80°C until later use.

3.2.3.7. Transformation of competent cells

Competent cells were thawed on ice. A 2 µl mix of vector-insert mix was then added to the competent cells and the mixture is incubated for 20 minutes on ice. This step is followed by a brief heat shock at 42°C for 45 seconds and then the solution was left

on ice for 3 minutes. Next, the transformed cells were plated into LB-agar plates with specific antibiotics and incubated overnight at 37°C.

3.2.3.8. Molecular cloning

TA cloning

pGEM-T Easy Vector kit was used for TA cloning to insert PCR products into the pGEM-T vector for synthesizing for sequencing purposes. The ligation reaction was set and carried out following manufacturer's instructions. The reaction mix was then incubated for 1 hour at RT. The ligation mix was then transformed into competent cells.

In-Fusion cloning

This strategy was used to clone HOTCRE *emilin2a* overexpression plasmid and *hsp70l:emilin2a* overexpression plasmid. In general, the vectors were linearized using specific restriction enzymes and the inserts were amplified from cDNA. The primers used for amplifying the insert were designed in Snapgene software. The primers contained at least 18 bp overhangs that are homologous to the digested vector. The digested vector and purified insert were then mixed with the 5x In-Fusion mastermix. The reaction was mixed via pipetting gently, and incubated at 50°C for 15 minutes followed by 5 minutes on ice. The mix was then transformed into competent cells.

3.2.3.9. Plasmid DNA isolation

Plasmid extraction was done using a GeneJET Plasmid Miniprep Kit (Thermo Fisher Scientific). The bacterial culture tubes were centrifuged at 4°C at 4000 rpm for 10 minutes to pellet down the bacteria. The supernatant was discarded. To the pellet, 250 µl of resuspension buffer was added. The suspension was then was transferred to an Eppendorf tube followed by addition of 250 µl of lysis buffer and the solution was mixed by inverting the tube. 350 µl of neutralization buffer was added and the tube was inverted for 6-8 times. The mix was then centrifuged for 5 minutes at room temperature. 700 µl of the supernatant was added in the spin column and was centrifuged for 1 minute. After discarding the flow-through, the column was washed twice with 500 µl of wash buffer and centrifuged for 1 minute. The flow-through was removed and the column was centrifuged empty for 2 minutes at full speed. 20 µl of elution buffer was added to the column and centrifuged at full speed for 1 min. The elute was collected into 1.5 ml Eppendorf tubes and the plasmid was stored at -20°C.

3.2.3.10. Genotyping by High Resolution Melt Analysis (HRMA)

Genomic DNA was isolated and PCR was done using primers adjacent to the mutation using SYBR green reagents similar to RT-qPCR analysis described earlier using a HRMA-specific RT-qPCR machine (Illumina Eco) was used in this case.

3.2.4. Generation of zebrafish transgenic and mutant lines

3.2.4.1. Generating transgenic zebrafish

To establish the *Tg(hsp70l:emilin2a, cryaa:CFP)bns504* line, WT zebrafish embryos were injected at the one-cell stage with 25 pg/nl of *hsp70l:emilin2a, cryaa:cerulean* plasmid DNA along with I-Sce enzyme. Injected embryos were screened for the eye marker and the positive ones were raised to adulthood and founders were screened by examining for CFP expression in larval eyes. To establish the *Tg(hsp70l:loxP-CFP-loxP-emilin2a-p2A-mCherry)bns510* line, (hereafter *Tg(hsp70l:LCL-emilin2a-p2A-mCherry))*, WT zebrafish embryos were injected at the one-cell stage with 30 pg/nl of *hsp70l:loxP-CFP-loxP-emilin2a-p2A-mCherry* plasmid DNA, along with 50 ng/µl Tol2 transposase mRNA. Injected embryos were raised and founders were screened by outcrossing and examining for CFP expression in embryos after performing two heat shocks at 39°C for one hour each.

3.2.4.2. CRISPR-Cas9 mutagenesis

Cas9 mRNA synthesis

pT3TS-nlsCas9nls plasmid was linearized using XbaI, run on a gel and purified as previously described. Cas9 mRNA was then transcribed using a T3 mMessage mMachine kit. mRNA was then purified using the Zymo resreach kit.

gRNA design

gRNAs were designed using the CHOPCHOP (http://chopchop.cbu.uib.no/) software. The gRNAs which were predicted to be highly efficient (low non-specificity) were chosen.

Generation of zebrafish *cxcl8a* mutant lines

The *cxcl8a*^{vu660} allele was generated using a gRNA with the sequence CCTTGATGACAACTGGAC resulting in a 28 base pair deletion and an insertion of 12 bases in exon 3. For gRNA synthesis, 2.5 µl of 2x NEB buffer 2 with BSA was mixed with 1 µl of 10 µM of the universal oligo

TTTTGCACCGACTCGGTGCCACTTTTTCAAGTTGATAACGGACTAGCCTTATTTT AACTTGCTATTTCTAGCTCTAAAA and 1 µl of 10 µM of the site-specific oligo TAATACGACTCACTATAGGCCTTGATGACAACTGGACGTTTTAGAGCTAGAAAT AGCAAG.

Table 3.24. Cycler conditions for annealing and extension of gRNA oligos.

Step	Temperature	Duration
1	95°C	5 mins
2	95°C to 85°C	2°C decrease/sec
3	85°C to 25°C	0.1°C decrease/sec
Halt		
Add the following to the 10 µl-mix for the extension step: 2.5 µl dNTPs (10µM), 2 µl 10X NEB buffer 2.1, 0.2 µl 100x BSA, 0.5 µl T4 DNA polymerase, and 4.8 µl dH2O		
4	12°C	20 mins
5	4°C	∞

GeneJET PCR purification kit was used to clean-up the PCR product and eluted into 30 µl dH2O. To confirm the successful annealing and extension, the sample was run a 3% agarose gel. The gRNA was then synthesized using a MEGA short script T7 kit following manufacturer's protocol.

50 pg of gRNA together with 150 pg of Cas9 mRNA were injected into one-cell stage zebrafish embryos and raised to adulthood. To identify fish carrying germline mutations (F0), fish were outcrossed to wild types. Mutants were identified by PCR using PrimeStar (Takara) using the program conditions as mentioned above in section 3.2.3.2., followed by restriction digest of the amplicon with NEB Ms1I enzyme. These F1's are raised and the mutation site was sequenced to identify the type of mutation. The F1 fish bearing the mutation of interest was further outcrossed to generate F2.

F2 zebrafish were in-crossed to give the first generation of global homozygous mutants.

Generation of zebrafish *emilin2a* mutant lines

emilin2a^{bns556} full locus deletion allele was generated using the CRISPR/Cas9 technology. Two gRNAs with the sequences AGCAGTGCGGACCAAGGCCA and TACCCGTCAAGTCTGTTCCA targeting exon 1 and exon 9 respectively, were generated.

gRNAs were transcribed as follows:

1. Oligo annealing

Oligos were diluted to 1 mM and incubated with 1 µl of T4 ligase buffer at 95°C for 5 minutes and at RT overnight.

2. Linearization of pT7-gRNA plasmid

pT7 plasmid was linearized using a BsmBI restriction enzyme. The linearized plasmid was run on a gel and purified.

3. Cloning dsOligos into pT7-gRNA vector

Annealed oligos were then cloned into the linear pT7-gRNA plasmid using a T4 ligase enzyme. Competent cells were then transformed with the cloned plasmid as described previously and plated onto LB plates. Two clones are picked the next day and cultured into a liquid LB culture overnight. Plasmids are then isolated and purified and sent for sequencing using M13 forward plasmids.

4. Transcription of gRNA

Positive gRNA clones are then linearized using BamHI enzymes and purified. gRNA was *in vitro* transcribed using a T7 MEGAshortscript kit. gRNA was then purified using a Zymo research kit.

50 pg of gRNA along with 150 pg of Cas9 mRNA were injected into one-cell stage zebrafish embryos and raised to adulthood. To identify fish carrying germline mutations (F0), fish were outcrossed to wild types. Mutants were identified by PCR using the DyNAmo Flash SYBR Green qPCR master mix (Thermo Fisher Scientific and the following program:

Step	Temperature	Duration	No. of cycles
PCR cycling	50°C	2 mins	1
	95°C	10 mins	
	95°C	10 secs	40
	60°C	30 secs	

These F1's are raised and- further outcrossed to generate F2. F2 zebrafish were in-crossed to give the first generation of global homozygous mutants.

3.2.5. Tissue dissociation and cell sorting

Ventricles of adult zebrafish were dissected and tissue was dissociated using the Pierce Primary Cardiomyocyte Isolation kit (Thermo Fisher Scientific (Cat# 88281)). Each biological sample was incubated in 100 µl of Enzyme 1 and 5 µl of Enzyme 2. Samples were gently shaken (300 rpm) ar 30ºCf or 30-45 minutes, with periodic pipetting. Enzymes were then deactivated by re-suspending the cells in 1X HBSS with 0.25% BSA. Cell suspension was passed through a 40 um nylon mesh. Cells were sorted using the BD FACSAria™ III (BD Biosciences) instrument. Dead cells were excluded by DAPI (Sigma (Cat#D954)) positive cells using 30mW 405nm excitation paired with 450/50 nm band pass filter. For sorting epicardium-derived cells (*Tg(tcf21:*mCherry*)*$^{+}$), mCherry fluorescence was measured with 50mW 561nm excitation paired with 610/20nm band pass filter; for coronary endothelial cells (*Tg(-0.8flt1:*RFP*)*$^{+}$), cardiomyocytes (*Tg(myl7:*DsRed*)*$^{+}$) and non-cardiomyocytes (*Tg(myl7:*DsRed*)*$^{-}$) RFP and DsRed fluorescence were measured with 50mW 561 nm excitation paired with a and 586/15 band pass filter. Sorted cells were re-suspended in 500 µl of Trizol for subsequent RNA extraction.

3.2.6. Gene expression

Ventricles of WT and *Tg(hsp70l:sflt4)* zebrafish were dissected at 24 hpci for RNA sequencing. Each biological replicate constituted of 3 ventricles. A miRNeasy micro kit (QIAGEN) was used to isolate RNA, along with DNase on-column digestion (DNase-Free DNase Set, QIAGEN). LabChip Gx Touch 24 (Perkin Elmer) was used to verify total RNA and library integrity. A total of 500 ng of RNA was used for VAHTS

Stranded mRNA-seq Library was prepared using manufacturer's instructions (Vazyme). NextSeq500 instrument (Illumina) using v2 chemistry was used for sequencing, leading to an average of 43M reads per library with 1x75bp single end setup. Quality, adapter content and duplication rates of raw reads were assessed with FastQC (available online at http://www.bioinformatics.babraham.ac.uk/ projects/fastqc). Reads displaying a quality drop below a mean of Q20 in a window of 10 nucleotides (Bolger et al., 2014) were trimmed using Trimmomatic version 0.38. Subsequent analysis was performed on reads between 30 and 150 nucleotides. Trimmed and filtered reads were aligned against the Ensembl Zebrafish genome version DanRer11 (GRCz11.92) using STAR 2.6.1d with the parameter "outFilterMismatchNoverLmax 0.1" to increase the maximum ratio of mismatches to mapped length to 10% (Dobin et al., 2013). Counting of the number of reads aligning to genes was done using featureCounts 1.6.3 tool from the Subread package (Liao et al., 2014). Reads mapping partly inside exons were admitted and aggregated per gene, while reads overlapping to multiple regions were excluded from following analysis. DESeq2 version 1.18.1 (Love et al., 2014) was used to identify differentially expressed genes. 17221 genes were tested. Only genes with a minimum fold change of ±0.585 and a Benjamini-Hochberg corrected *P*-value ≤0.05 were and a minimum combined mean of 5 reads deemed to be significantly differentially expressed. Log2 fold change of 0.585 reflects a 1.5 fold up or down regulation and constitutes a robust cut off to eliminate minor changes. The Ensembl annotation was enriched with UniProt data (release 06.06.2014) based on Ensembl gene identifiers (Activities at the Universal Protein Resource (UniProt)). The top 50 most significantly differentially expressed genes between both conditions were plotted in a heatmap. DESeq2 (1.18.1) normalized expression counts of these genes were averaged per condition and plotted in R studio (1.4.1717) using the ComplexHeatmap package, using z-scores with Canberra distance and hierarchical clustering. Z-score, the number of standard deviations that a value is above or below the mean of all values, was generated by inserting the normalized reads into R studio, which calculates the Z-score using the scale() function.

3.2.7. Histology

3.2.7.1. *in situ* hybridization

Dissected hearts were fixated in sterile 4% PFA at 4˚C overnight. Hearts were rinsed in PBS twice for 5 minutes, followed by 2 minutes washes of a gradient of ethanol in DEPC-water: 50%, 70%, 80%, 95% and 100% at RT. Hearts were washed in 50% xylene in ethanol and in 100% xylene for 30 minutes at RT. Hearts were then washed three times in 100% paraffin at 50˚C for one hour, embedded in paraffin and stored at 4˚C. Samples were cut into 8 µm sections and stored at RT.

Day 1:

Sections were first washed twice in xylene for 10 minutes, followed by rehydration in an ethanol gradient in DEPC-water for 2 minutes: 100%, 95%, 80%, 70% and 50%. Slides were then washed for 5 minutes with TBST, twice. Slides were fixed for 20 minutes in sterile 4% PFA, followed by two brief washes in TBST. 0.5 µg/mL Proteinase K diluted in TBS + 2 mM CaCl2 was added on sections for 15 minutes at 37˚C, followed by a 5 minutes wash in cold Tris/Glycine (Tris 50 mM pH7.4, 50 mM Glycine) to stop the reaction. This step is followed by a brief wash twice in TBST, and refixed in sterile 4% PFA for 5 minutes, followed by a brief wash in TBST. Slides were submerged in triethanolamine (0.1 M, pH 8.0) along with the addition of drops of acetic anhydride to reach 0.25% under agitation for 12 minutes. Slides were washed in TBST twice, followed by pre-hybridization of sections using a hybridization buffer at 60˚C - 65˚C for 1 hour. Probes (1 µg/ml in hybridization buffer) were denatured at 60˚C - 65˚C for 15 minutes and applied to sections at 60˚C - 65˚C overnight.

Day 2:

50% formamide in 2X SSC was used to wash the slides for 30 minutes at 60˚C - 65˚C. Slides were stringently washed in 60˚C - 65˚C for 15 minutes once at 2X SSC and twice with 0.1X SSC, followed by TBST wash at RT. Slides were washed in 37˚C for 15 minutes once at 2X SSC and twice at 1X SSC, followed by TBST wash at RT. Blocking solution (TBST + 0.5% BSA) was applied to slides for at least 1 hour at RT. Anti-digoxigenin (1:1000 in blocking solution) was added to slides at RT for 2-3 hours. Slides were then rinsed 5 times in TBST. Pre-filtered BM Purple (Roche) was added to slides and incubated in humid chamber in the dark for a maximum of 2 hours. After appearance of signal, slides were rinsed with TBST, fixed in 4% PFA for 5 minutes, and mounted.

3.2.7.2. Immunohistochemistry

Hearts were dissected and fixed in 4% PFA for one hour at RT, followed by a brief wash in PBS. Hearts were then preserved in 30% (w/v) sucrose in 1X PBS O/N at 4ºC. Hearts were then embedded in O.C.T (Tissue-Tek) and stored at -80ºC, and cut into 8 µm sections and stored at -20ºC.

Day 1:

Frozen slides were first brought to RT. Slides were then washed twice in PBST (1X PBS+0.01% Triton-X) for 5 minutes. Slides were then rinsed in distilled water twice for 5 minutes. Slides were immersed in 10% hydrogen peroxide in methanol for one hour at RT. Slides were then washed in water twice for 5 minutes, followed by two washes with PBST for 5 minutes. Blocking Solution was then added to the slides for 1 hour at RT. Primary antibodies were then applied on the sections and left O/N at 4ºC.

Day 2:

Slides were washed in PBST 3 times for 10 minutes. Secondary antibodies were then applied to sections and left at RT for 3 hours. Slides were then washed in PBST 3 times for 10 minutes, followed by a wash in PBST+ DAPI (1:1000). Slides were then mounted using a fluorescent mounting medium and left to dry.

3.2.7.3. Acid Fucshin Orange G (A.F.O.G)

Hearts were dissected and fixed in 4% PFA for one hour at room temperature, followed by a brief wash in PBS. Hearts were then preserved in 30% (w/v) sucrose in 1X PBS O/N at 4ºC. Hearts were then embedded in O.C.T (Tissue-Tek) and stored at -80ºC, and sectioned into 8 µm sections and stored at -20ºC.

Slides are fixed in Bouin's solution at 60ºC in a couplin jar for 2 hours. Slides are then left to cool at RT for 5 minutes. Slides are then transferred to a new couplin jar and put under running tap water until the yellow color becomes clear. 1-2 drops of Phosphomolybdic acid are then added on sections and left for 7 minutes. Slides are washed in deionized water. 1-2 drops of A.F.O.G reagent are added on sections and left for 5 minutes. Slides are washed in deionized water 3 times till the color reaches the needed intensity. Slides are washed with 95% ethanol for 30 seconds, and in 100% ethanol for 30 seconds. Slides are washed in Roti-Histol for 5 minutes. Slides are then mounted using Entellan and left to dry.

3.2.8. Imaging and quantification

IHC:

For each biological replicate, imaging and quantification was performed on 3 non-superficial non-consecutive midsagittal sections. A LSM700 microscope (Zeiss) was used to acquire confocal images.

cEC proliferation analysis:

For cEC proliferation analysis, the ZEN Blue software was used to count and calculate the percentage of proliferating cECs was calculated as a ratio from the total number of cECs in the injured tissue and in 200 µm of the injury border zone.

CM dedifferentiation and proliferation analysis:

For CM dedifferentiation and proliferation analysis, the ZEN Blue software was used to count and calculate the percentage of dedifferentiating/proliferating CMs was calculated as a ratio from the total number of CM in 100 µm of the injury border zone.

Coronary coverage analysis:

The percentage fluorescence intensity was from wholemount images of at least 4 biological replicates per condition. Percentage fluorescence in the injured tissue was calculated as a ratio from background fluorescence.

For wholemount imaging of Qdots, a Lightsheet Z.1 microscope (Zeiss) was used. Images were processed using the ZEN Blue Software.

A.F.O.G:

Images were taken using a Nikon SMZ25 stereomicroscope. The scar area in 3 non-consecutive sections per ventricle of at least 4 biological replicates per condition was used. Scar area was calculated as a ratio from total ventricle area using ImageJ software.

in situ hybridization:

Images were acquired and processed using a Nikon SMZ25 stereomicroscope.

3.2.9. Cell Culture techniques

Human umbilical vein endothelial cells (HUVECs) were used until a maximum of six passages. An endothelial basal medium (EBM-2, Lonza) supplemented with fetal bovine serum, hydrocortisone, human basic fibroblast growth factor, vascular endothelial growth factor, R3-insulin-like growth factor, ascorbic acid, human

epidermal growth factor, GA-1000 and heparin (EGM-2 BulletKit, Lonza) and 100 units/ml penicillin and 100 µg/ml streptomycin was used to culture HUVECs. For scratch assay experiments, cells were seeded in a 24-well plate at a density of 30,000 cells per well. After 24 hours from seeding, scratch experiment was performed with the use of a pipette tip. At 6 hours post scratch cells were lysed with 10% beta mercaptoethanol (Gibco) in lysis buffer (Invitrogen). RNA was extracted for subsequent RT-qPCR analysis. For RNA interference experiments in HUVECs, cells were first seeded in 24-well plate until reaching a confluence of 80%. A Lipofectamine RNAiMAX reagent was then used (Invitrogen (Cat# 13778030)) following manufacturer's standard protocol (final siRNA concentration used: 10 pmol/well) for transfecting cells. Pools of siRNA duplexes (Mission esiRNA, Sigma (Cat# EHU013781)) were used to target *VEGFC*. After 24 hours of transfection, cells were lysed with 10% beta mercaptoethanol (Gibco) in lysis buffer (Invitrogen). RNA was then extracted for subsequent RT-qPCR analysis.

3.2.10. Randomization and Statistical analysis

Randomization was performed in experiments in which mutant and WT sibling zebrafish were used. Randomization was performed as follows: mutants and WT siblings were housed in the one tank, used for the experiment and then subsequently genotyped. Blinding was not performed in experiments involving drug treatments (i.e., 4-OHT vs. EtOH, or DMSO vs SB25002) due to the difficulty to distinguish between control and experimental groups. Similarly, no blinding was performed in zebrafish carrying heat shock driven transgenes as they were fluorescently sorted in larval stages. Ventricles in which the injury was smaller than 20% were excluded from the experiments. Sample size was determined based on previous publications in the field. Data of cEC proliferation, percentage fluorescence intensity, CM dedifferentiation and proliferation, as well as percentage of scar area relative to the area of the ventricle was assessed for normal distribution using the Shapiro-Wilks normality test using a threshold alpha value= 0.05. Accordingly, Student’s t-test or the non-parametric Mann–Whitney test were used for comparative statistics as stated in the figure legends. For RT-qPCR experiments, at least 4 biological replicates were used. For cell sorting, at least 15 ventricles were combined per sample. Mann–Whitney non-parametric test was used to analyze all RT-qPCR expression data. Error bars represent mean ± SD and bars represent median value.

4. RESULTS

Note: Parts of this section have been published and used *verbatim* from the following article in the journal *Circulation Research*.

[**El-Sammak, H.**, Yang, B., Guenther, S., Chen, W., Marín-Juez, R., and Stainier, D.Y.R. (2022). A Vegfc-Emilin2a-Cxcl8a Signaling Axis Required for Zebrafish Cardiac Regeneration. Circ. Res. *130*, 1014–1029.]

The author's contribution in the paper as follows:
H.E.-S, R.M.-J. and D.Y.R.S. designed experiments, H.E.-S. and S.G. performed experiments, H.E.-S, B.Y. and W.C. developed and provided unpublished transgenic and mutant lines. H.E.-S., S.G., R.M.-J. and D.Y.R.S. analyzed data. H.E.-S, R.M.-J. and D.Y.R.S. wrote the manuscript, with input from all the authors.

4.1. *vegfc* is expressed by coronary endothelial cells during cardiac regeneration in zebrafish

Previous studies have shown that *vegfc* is upregulated in the adult zebrafish ventricle after cardiac injury (Lai et al., 2017; Lien et al., 2006). Furthermore, *vegfc* regulates the sprouting of intersegmental vessels during zebrafish development (Hogan et al., 2009a, 2009b). These observations led me to hypothesize that Vegfc signaling might also play a role in regulating endothelial cells (ECs) during cardiac regeneration. To investigate the temporal expression levels of *vegfc*, I performed RT-qPCR analysis on injured adult zebrafish ventricles at different time points after cardiac cryoinjury and compared them to sham-operated ventricles as controls. I detected a significant upregulation in the expression of *vegfc* at 48, 96 hpci (hours post cryoinjury) and 7 days post cryoinjury (dpci) (**Figure 4.1 A**). Notably, the peak in expression was at 96 hpci, which overlaps with the peak of coronary endothelial cell (cEC) proliferation (Marín-Juez et al., 2019). Next, to gain information on the spatial expression pattern of *vegfc*, I performed *in situ* hybridization on heart sections in uninjured ventricles and at 96 hpci. I could not detect any signal in uninjured ventricles, but observed *vegfc* expression at 96 hpci in the boundary of the injured tissue where cECs and epicardium-derived cells (EPDCs) are found (**Figure 4.1 B**). To confirm the source of the signal, I sorted cECs using the *Tg(-0.8flt1:RFP)* line and EPDCs using the

Tg(tcf21:mCherry) line at 96 hps (hours post sham) and 96 hpci and analyzed *vegfc* expression in both cell types by RT-qPCR (**Figure 4.1 C,D**). I found a significant upregulation in the expression of *vegfc* in cECs, but not EPDCs at 96 hpci (**Figure 4.1 E**). Moreover, to assess whether cardiomyocytes (CMs) express *vegfc* during cardiac regeneration, I sorted them using the *Tg(myl7:DsRed)* line at 96 hps and 96 hpci and found no *vegfc* upregulation (**Figure 4.1 F**). Altogether, these data show that *vegfc* is highly upregulated at the peak of cEC proliferation suggesting that cECs might be a source of Vegfc during cardiac regeneration in zebrafish.

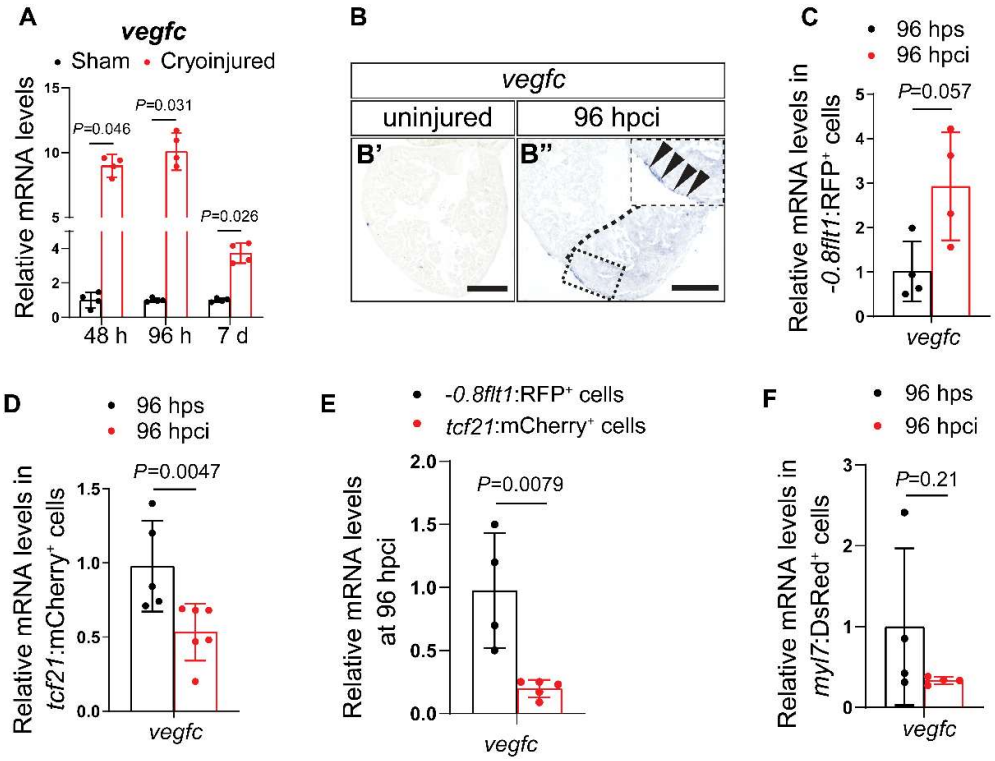

Figure 4.1: Expression pattern of *vegfc* after cardiac cryoinjury in zebrafish.

A. RT-qPCR analysis of mRNA expression of *vegfc* at 48 and 96 hpci and 7 dpci normalized to sham-operated ventricles (n=4); h: hpci, d: dpci. **B.** *in situ* hybridization for *vegfc* on paraffin sections of uninjured **(B')** and 96 hpci **(B'')** hearts. Arrowheads point to *vegfc* expression. **C.** RT-qPCR analysis of mRNA expression of *vegfc* in sorted *-0.8flt1*:RFP$^+$ cells (cECs) at 96 hpci normalized to sham-operated ventricles (96 hps) (n=4). **D.** RT-qPCR analysis of mRNA expression of *vegfc* in sorted *tcf21*:mCherry$^+$ cells (EPDCs) at 96 hpci (n=5) normalized to sham-operated ventricles (96 hps) (n=6). **E.** RT-qPCR analysis of mRNA expression of *vegfc* at 96 hpci in sorted *tcf21*:mCherry$^+$ cells (EPDCs) (n=5) normalized to sorted *flt1:*RFP$^+$ cells (cECs) (n=4). **F.** RT-qPCR analysis of mRNA expression of *vegfc* in sorted *myl7:*DsRed$^+$ cells (CMs) (n=4) at 96 hpci normalized to sham-operated ventricles (96 hps) (n=4). Black **(B)**

dotted lines mark the injured area. Statistical tests: Non-parametric Mann-Whitney test **(A,C,D,E,F)**. Scale bars: 100 µm **(B)**. [Adapted and reprinted with permission from (El-Sammak et al., 2022)].

4.2. Blocking Vegfc signaling impairs cardiac regeneration in zebrafish

4.2.1. Optimization of heat shock treatment to block Vegfc signaling

The observation that *vegfc* peaks in expression at 96 hpci when cECs are highly proliferative (Marín-Juez et al., 2019), and that it is expressed in cECs during cardiac regeneration, led me to hypothesize that Vegfc signaling might play a role in coronary revascularization after cardiac injury in zebrafish. To test this hypothesis, I utilized a loss-of-function tool to block Vegfc signaling. I overexpressed the soluble form of Vegfr3/Flt4 (*sflt4*) under a heat shock promoter (Matsuoka et al., 2016). This soluble receptor encodes the extracellular domain while lacking the transmembrane and cytoplasmic tyrosine kinase domains, hence it acts as a decoy receptor and blocks Vegfc signaling (Matsuoka et al., 2016) (**Figure 4.2 A**). To optimize the heat shock treatment for adult zebrafish, I analyzed the expression levels of *sflt4* after different heat shock regimens and at different temperatures. I tried heat shocks once daily at 37ºC, twice daily at 37ºC, once daily at 39ºC, and twice daily at 39ºC. All of these treatments were well-tolerated by the fish. By RT-qPCR, I found that the highest *sflt4* expression is obtained when performing two heat shock per day at 39ºC (**Figure 4.2 B**). Hence, I used this regimen for all experiments involving heat shock treatments.

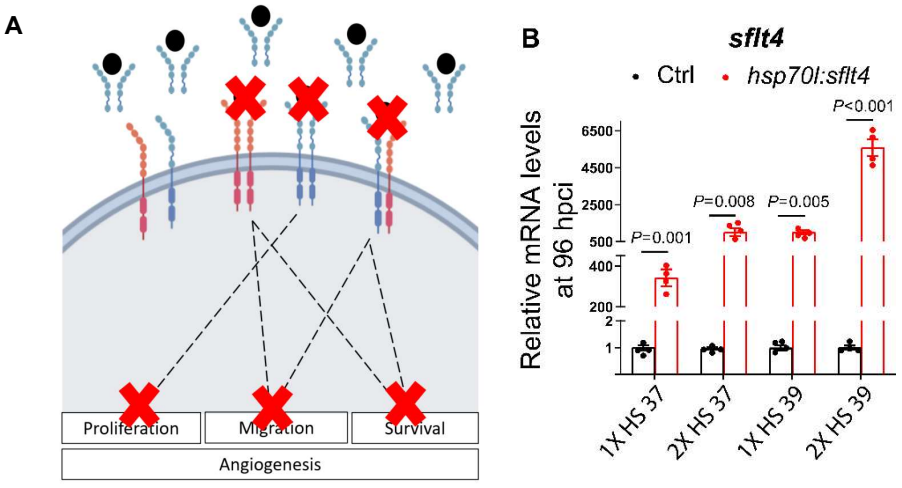

Figure 4.2: Optimization of the *Tg(hsp70l:sflt4)* line.

A. Schematic representation of how the *Tg(hsp70l:sflt4)* line works. **B.** RT-qPCR analysis of mRNA expression of *sflt4* at 96 hpci in *Tg(hsp70l:sflt4)* ventricles normalized to non-transgenic sibling (Ctrl) ventricles after different heat shock treatments (from left to right): once daily at 37˚C, twice daily at 37˚C, once daily at 39˚C, and twice daily at 39˚C (n=4). Statistical tests: Non-parametric Mann-Whitney test **(B)**. [Adapted and reprinted with permission from (El-Sammak et al., 2022)]

4.2.2. Vegfc signaling blockade leads to reduced coronary endothelial cell proliferation during cardiac regeneration in zebrafish

To visualize cECs, I utilized two transgenic lines throughout the study, namely, the *Tg(-0.8flt1:RFP)* line and the *Tg(flt1:Mmu.Fos-GFP)* line which label cECs (**Figure 4.3 A**). I blocked Vegfc signaling using the *Tg(hsp70l:sflt4); Tg(-0.8flt1:RFP)* line by performing heat shock treatments twice daily until 96 hpci. *Tg(-0.8flt1:RFP)* sibling controls were also subjected to the same treatment. Using PCNA as a proliferation marker, I analyzed cEC proliferation at 96 hpci and observed a significant reduction in the proliferation of these cells when blocking Vegfc signaling (**Figure 4.3 B,C**).

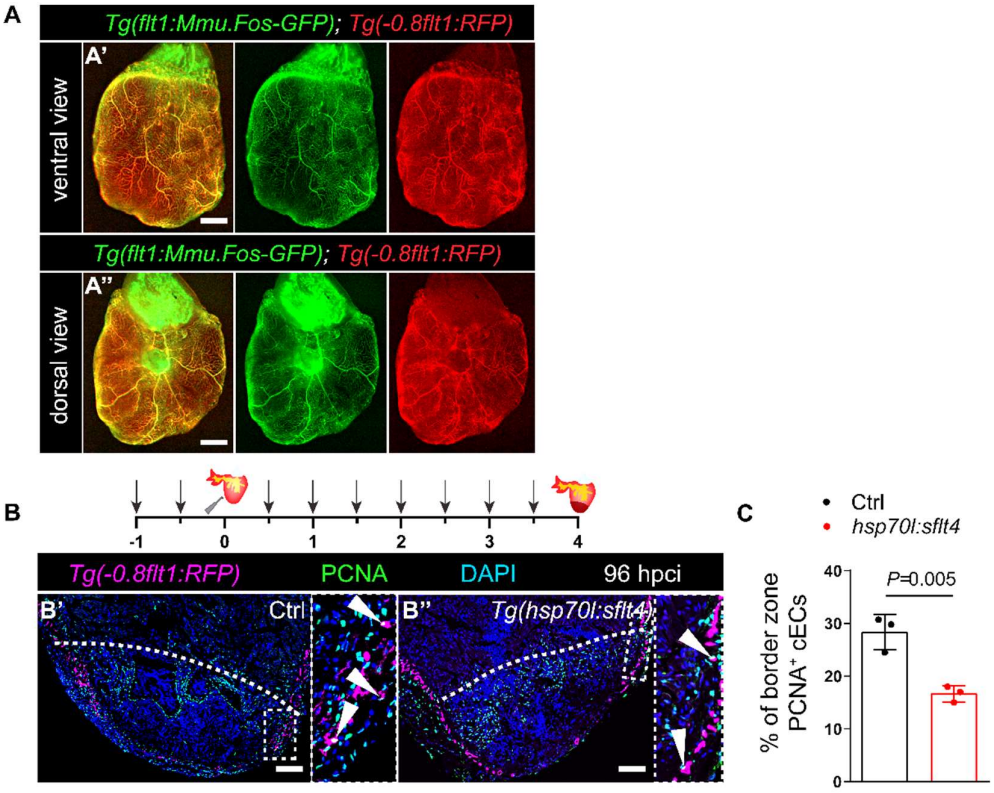

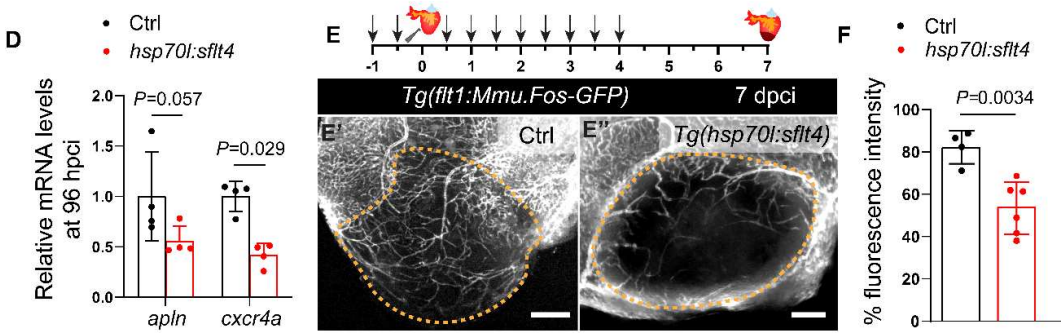

Figure 4.3: Vegfc signaling is essential for coronary revascularization after cardiac injury in zebrafish.

A. Wholemount images of uninjured ventricles of a *Tg(-0.8flt1:RFP); Tg(flt1:Mmu.Fos-GFP)* zebrafish, displaying ventral **(A')** and dorsal **(A'')** views. **B.** Illustration of heat shocks (arrows) and cardiac cryoinjury. Sections of cryoinjured ventricles at 96 hpci of *Tg(0.8flt1:RFP)* (Ctrl) **(B')** and *Tg(hsp70l:sflt4); Tg(-0.8flt1:RFP)* **(B'')** zebrafish immunostained for for RFP (coronaries, magenta), PCNA (proliferation marker, green), and DNA (DAPI, blue). Arrowheads point to PCNA$^+$ cECs. **C.** Percentage of PCNA$^+$ cECs in the injured area and border zone of *Tg(-0.8flt1RFP)* (Ctrl) (n=3) and *Tg(hsp70l:sflt4); Tg(-0.8flt1:RFP)* (n=3) ventricles at 96 hpci. **D.** RT-qPCR analysis of mRNA expression of *apln* and *cxcr4a* at 96 hpci in *Tg(hsp70l:sflt4)* ventricles normalized to non-transgenic sibling (Ctrl) ventricles (n=4). **E.** Illustration of heat shocks (arrows) and cardiac cryoinjury. Wholemount images of cryoinjured hearts at 7 dpci of sibling *Tg(flt1:Mmu.Fos-GFP)* (Ctrl) **(E')** and *Tg(hsp70l:sflt4); Tg(flt1:Mmu.Fos-GFP)* **(E'')** zebrafish. **F.** Percentage of GFP fluorescence intensity in the injured area of *Tg(flt1:Mmu.Fos-GFP)* (Ctrl) (n=4) and *Tg(hsp70l:sflt4); Tg(flt1:Mmu.Fos-GFP)* (n=6) hearts at 7 dpci. White **(B)**, and orange **(E)** dotted lines mark the injured area. Statistical tests: Non-parametric Mann-Whitney test **(D)**, Student's t-test **(C,F)**. Scale bars: 200 µm (**A,E**), 100 µm **(B)**. [Adapted and reprinted with permission from (El-Sammak et al., 2022)]

In addition, *Tg(hsp70l:sflt4)* ventricles showed a decreased expression of *apln* and *cxcr4a* (**Figure 4.3 D**), two factors known for their known role in promoting coronary revascularization in zebrafish (Marín-Juez et al., 2019). Moreover, I analyzed the coronary coverage at 7 dpci (a time point where we expect coronaries to fully cover the injured area (Marín-Juez et al., 2016, 2019)) in *Tg(hsp70l:sflt4); Tg(flt1:Mmu.Fos-GFP)* and *Tg(flt1:Mmu.Fos.GFP)* sibling controls, and observed that blocking Vegfc signaling significantly impairs coronary vessel coverage during cardiac regeneration

(**Figure 4.3 E,F**). Altogether, these results suggest that Vegfc signaling is essential for coronary revascularization after cardiac injury in zebrafish.

Since Flt4 (Vegfr3) is activated by both ligands, Vegfc and Vegfd (Jeltsch et al., 1997; Stacker et al., 1999), I wanted to confirm that the reduced coronary phenotype is due to blockage of Vegfc signaling and not Vegfd. To this end, I performed cryoinjuries on hypomorphic *vegfc*$^{-/-}$ (Le Guen et al., 2014) ventricles as well as *vegfd*$^{-/-}$ (Gancz et al., 2019) ventricles, and detected reduced cEC proliferation at 96 hpci in *vegfc*$^{-/-}$ ventricles but no change in *vegfd*$^{-/-}$ injured ventricles (**Figures 4.4 A,B**). These findings suggest that the reduced coronary revascularization phenotype observed in *Tg(hsp70:sflt4)* ventricles is due to blockage of Vegfc signaling and not Vegfd. Moreover, these results are consistent with previous studies which reported impaired cardiac regeneration phenotype in *vegfc*$^{+/-}$ zebrafish, while *vegfd*$^{-/-}$ ventricles did not display a cardiac regeneration phenotype (Gancz et al., 2019; Vivien et al., 2019).

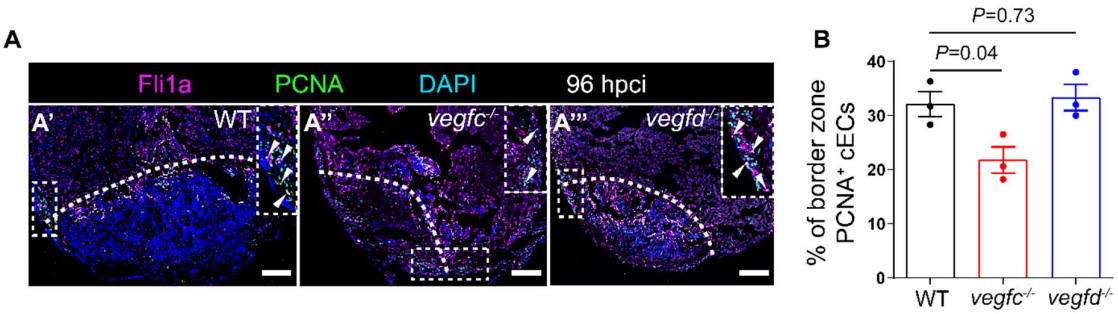

Figure 4.4: *vegfc* mutants display reduced coronary endothelial cell proliferation. A. Sections of cryoinjured ventricles of WT **(A')**, *vegfc*$^{-/-}$ **(A'')** and *vegfd*$^{-/-}$ **(A''')** zebrafish at 96 hpci immunostained for Fli1a (endothelial cells, magenta), PCNA (proliferation marker, green), and DNA (DAPI, blue). Arrowheads point to PCNA^{+} cECs. **F.** Percentage of PCNA^{+} cECs in the injured tissue and border zone of WT (n=3), *vegfc*$^{-/-}$ (n=3) and *vegfd*$^{-/-}$ (n=3) ventricles at 96 hpci (n=3). White **(A)** dotted lines mark the injured area. Statistical test: Student's t-test **(B)**. Scale Bars: 100 µm **(A)**. [Adapted and reprinted with permission from (El-Sammak et al., 2022)]

4.2.2.1. Reduced coronary revascularization phenotype is independent of ventricular lymphatics

Previous studies have shown that injecting VEGFC in adult mice increased lymphangiogenesis and enhanced cardiac function after myocardial infarction (Klotz

et al., 2015). Moreover, recent work has highlighted the importance of Vegfc in promoting lymphangiogenesis during cardiac regeneration in zebrafish (Gancz et al., 2019; Harrison et al., 2019). To assess whether the observed effects upon blockade of Vegfc signaling are caused by alterations in lymphatics, I used 27-28 mm long and 3-month-old zebrafish. These zebrafish have an established coronary network, but have not yet developed ventricular lymphatics (Gancz et al., 2019; Harrison et al., 2019). To confirm that 3-month-old zebrafish lack ventricular lymphatics, I injected Qdots intramyocardially in zebrafish. These Qdots are taken up by lymphatic ECs, and hence allows their visualization (Harrison et al., 2019). I injected Qdots into the ventricles of *Tg(flt1:Mmu.Fos-GFP); Tg(lyve1b:DsRed)* to visualize coronaries and lymphatics along with the Qdots. Indeed, I observed that 3-month-old zebrafish which lacked ventricular lymphatics had Qdots accumulated at the injection site, and were not cleared (**Figure 4.5 A'**). On the other hand, older zebrafish (6-month-old) which had lymphatics in their ventricles as visualized by the *Tg(lyve1b:DsRed)* line, were able to uptake and clear out the injected Qdots (**Figure 4.5 A''**). Next, to assure that manipulations with Vegfc signaling using the *Tg(hsp70l:sflt4)* during cardiac regeneration do not interfere with ventricular lymphatics in 3-month-old zebrafish, I performed Qdot injections in 3-month-old *Tg(hsp70l:sflt4); Tg(flt1:Mmu.Fos-GFP); Tg(lyve1b:DsRed)* and *Tg(flt1:Mmu.Fos-GFP); Tg(lyve1b:DsRed)* siblings and found that in both cases injected Qdots accumulated at the injection site at 7 dpci and were not taken up due to the lack of lymphatics in the ventricle (**Figure 4.5 B**). Next, to confirm that coronary revascularization is independent of lymphatics, I performed cryoinjuries on 3-month-old *Tg(hsp70l:sflt4); Tg(-0.8flt1:RFP)* and analyzed cEC proliferation at 96 hpci. Similar to previous observations on 8-month-old zebrafish, I observed reduced cEC proliferation in 3-month-old *Tg(hsp70l:sflt4); Tg(-0.8flt1:RFP)* when compared to their sibling controls (**Figure 4.5 C,D**). All of these findings indicate that the reduction in coronary revascularization observed upon Vegfc signaling block during cardiac regeneration is independent on the presence or lack of lymphatics in the ventricle. However, to use zebrafish that are devoid of ventricular lymphatics, I performed all experiments on 3-month-old zebrafish with a length of 28 mm throughout the whole study.

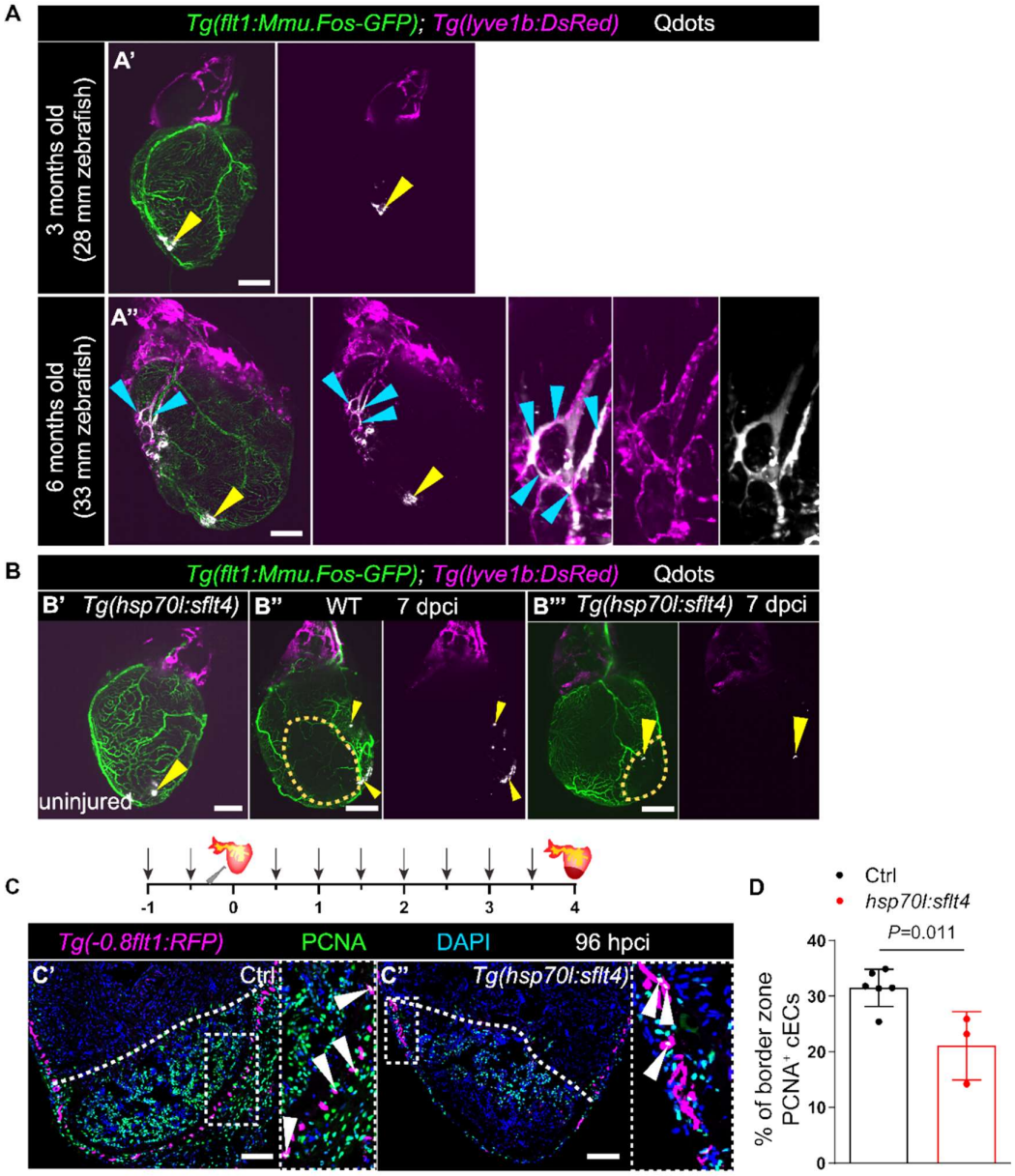

Figure 4.5: Blocking Vegfc signaling reduces coronary endothelial cell proliferation in a lymphatics independent manner.

A. Wholemount images of uninjured hearts of 3-month-old *Tg(lyve1b:DsRed); Tg(flt1:Mmu.Fos-GFP)* zebrafish **(A')** and uninjured ventricles of 6-month-old *Tg(lyve1b:DsRed); Tg(flt1:Mmu.Fos-GFP)* zebrafish **(A'')** after intramyocardial injection of Qdots. Yellow arrowheads point to the Qdots injection site. Blue arrowheads point to Qdots taken up by lymphatic vessels. **B.** Wholemount images of ventricles of 3-month-old uninjured *Tg(hsp70l:sflt4)*; *Tg(lyve1b:DsRed); Tg(flt1:Mmu.Fos-GFP)* zebrafish **(B')**, *Tg(lyve1b:DsRed); Tg(flt1:Mmu.Fos-GFP)* zebrafish at 7 dpci **(B'')** and *Tg(hsp70l:sflt4)*; *Tg(lyve1b:DsRed); Tg(flt1:Mmu.Fos-GFP)* zebrafish at 7 dpci **(B''')** after intramyocardial injection of Qdots.

Yellow arrowheads point to the Qdots injection site. **C.** Illustration of heat shocks (arrows) and cardiac cryoinjury. Sections of cryoinjured ventricles of *Tg(0.8flt1:RFP)* (Ctrl) **(C')** and *Tg(hsp70l:sflt4); Tg(-0.8flt1:RFP)* **(C'')** sibling zebrafish at 96 hpci immunostained for RFP (coronaries, magenta), PCNA (proliferation marker, green), and DNA (DAPI, blue). Arrowheads point to PCNA$^+$ cECs. **D.** Percentage of PCNA$^+$ cECs in the injured tissue and border zone of 3-month-old *Tg(-0.8flt1RFP)* (Ctrl) (n=6) and *Tg(hsp70l:sflt4); Tg(-0.8flt1:RFP)* (n=3) ventricles at 96 hpci. Orange **(B)** and white **(C)** dotted lines delineate the injured tissue. Statistical test: Student's t-test **(D)**. Scale Bars: 200 µm **(A,B)**, 100µm **(C)**. [Adapted and reprinted with permission from (El-Sammak et al., 2022)]

4.2.3. Reduced coronary revascularization leads to reduced muscle regeneration

Previous work has shown that coronaries provide support for CMs during development as well as regeneration (Marín-Juez et al., 2019) and that it is essential for scar resolution (Marín-Juez et al., 2016). These observations led me to hypothesize that the reduced coronary revascularization due to blocking Vegfc signaling could affect muscle regeneration. To this end, I used the *Tg(hsp70l:sflt4)* line to block Vegfc signaling until 96 hpci when cEC proliferation is at its highest levels. I then quantified CM dedifferentiation and proliferation at 7 dpci. Indeed, I observed a significant reduction in CM dedifferentiation as well as proliferation in *Tg(hsp70l:sflt4)* ventricles in comparison to their sibling WT (**Figure 4.6 A-D**). To better understand whether these CM phenotypes are due to Vegfc signaling block in CMs or due to reduced revascularization, I sorted CMs using the *Tg(myl7:DsRed)* line at 96 hps and 96 hpci and analyzed the expression of the different Vegf receptors, namely, *vegfr1*, *vegfr2* and *vegfr3*. I found no upregulation in expression levels of these receptors after cardiac injury (**Figure 4.6 E**). Moreover, I compared the expression levels of *vegfr1*, *vegfr2* and *vegfr3* at 96 hpci in CMs (*myl7*:DsRed$^+$ cells) and all other non-CMs in the ventricle (*myl7*:DsRed$^-$ cells) and found that these receptors are enriched in non-CMs in the ventricle after cardiac injury (**Figure 4.6 F**). These results suggest that the CM dedifferentiation and proliferation defects that I observe upon Vegfc signaling abrogation are likely due to reduced coronary revascularization.

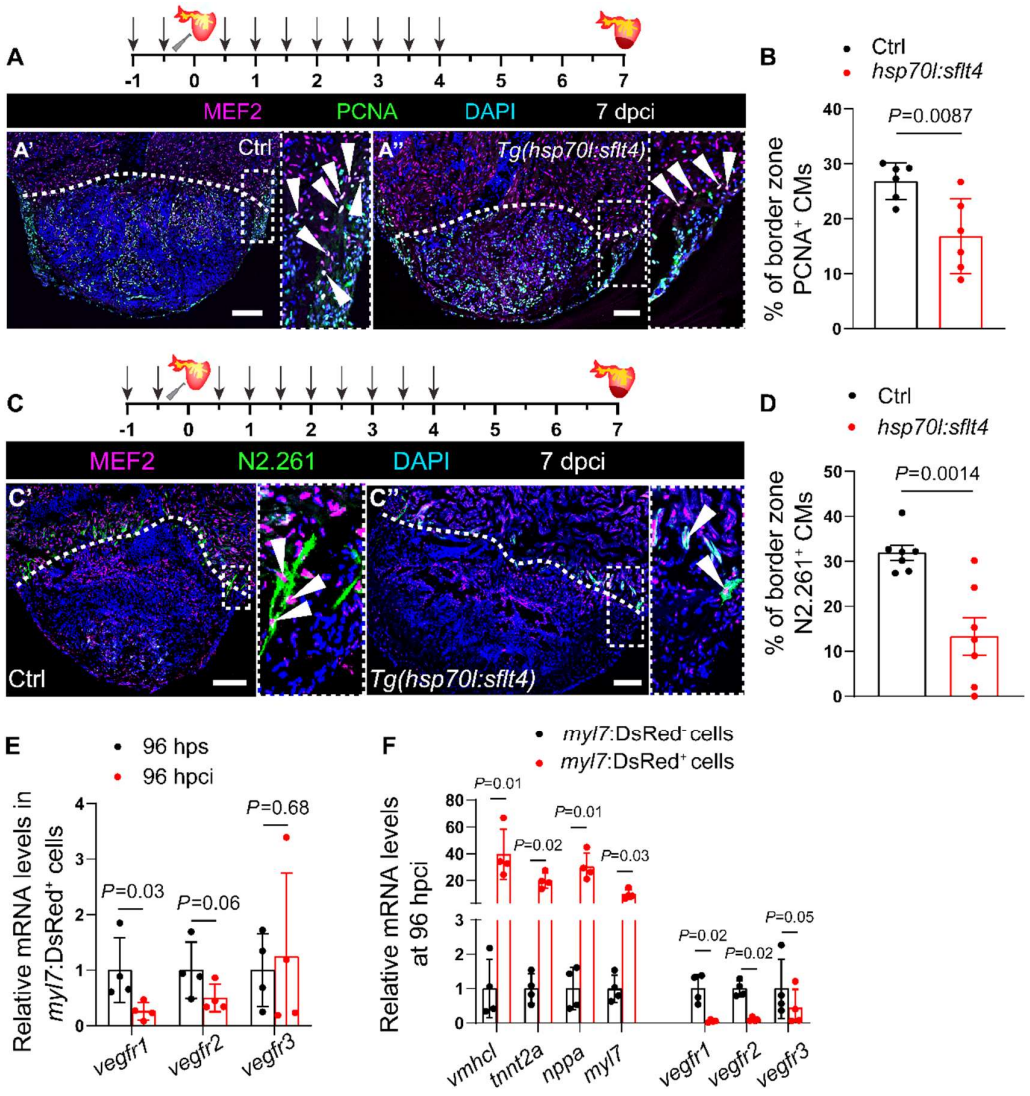

Figure 4.6: Blocking Vegfc signaling reduces cardiomyocyte dedifferentiation and proliferation after cardiac injury.

A. Illustration of heat shocks (arrows) and cardiac cryoinjury. Sections of cryoinjured ventricles at 7 dpci of non-transgenic sibling (Ctrl) **(A')** and *Tg(hsp70l:sflt4)* **(A'')** zebrafish immunostained for MEF2 (CMs, magenta), PCNA (proliferation marker, green), and DNA (DAPI, blue). Arrowheads point to PCNA$^+$ CMs. **B.** Percentage of PCNA$^+$ CMs in the border zone of non-transgenic sibling (Ctrl) (n=6) and *Tg(hsp70l:sflt4)* (n=6) ventricles at 7 dpci. **C.** Illustration of heat shocks (arrows) and cardiac cryoinjury. Sections of cryoinjured hearts at 7 dpci of non-transgenic sibling (Ctrl) **(C')** and *Tg(hsp70l:sflt4)* **(C'')** zebrafish immunostained for MEF2 (CMs, magenta), N2.261 (embryonic myosin heavy chain, green), and DNA (DAPI, blue). Arrowheads point to N2.261$^+$ CMs. **D.** Percentage of N2.261$^+$ CMs in the border zone

of non-transgenic sibling (Ctrl) (n=7) and *Tg(hsp70l:sflt4)* (n=7) ventricles at 7 dpci. **E.** RT-qPCR analysis of mRNA expression of *vegfr1*, *vegfr2* and *vegfr3* at 96 hpci in sorted *myl7*:DsRed^{+} cells (CMs) (n=4) normalized to sham-operated ventricles (96 hps) (n=4). **F.** RT-qPCR analysis of mRNA expression of *vegfr1*, *vegfr2* and *vegfr3* at 96 hpci in sorted *myl7:*DsRed^{+} cells (CMs) (n=4) normalized to *myl7:*DsRed^{-} cells (non-CMs) (n=4). White **(A,C)** dotted lines mark the injured area. Statistical test: Student's t-test **(B,D)**, Non-parametric Mann-Whitney test **(E,F)**. Scale bars: 100 µm **(A,C)**. [Adapted and reprinted with permission from (El-Sammak et al., 2022)]

Next, to assess if blocking Vegfc signaling affects scar resolution after cardiac injury in zebrafish, I used the same heat shock regimen to block Vegfc signaling until 96 hpci and assessed the scar size at 30 dpci using A.F.O.G staining which stains the muscle in orange, fibrin in red and collagen in blue, hence allows visualization of the scar. I found a significant increase in the scar size in *Tg(hsp70l:sflt4)* ventricles (**Figure 4.7 A,B**). In addition, ventricles with Vegfc sinaling block retained a profoundly larger scar at 90 dpci (a time point where the ventricle should be regenerated with minimal scarring) when compared to sibling WTs (**Figure 4.7 C,D**). Altogether, these findings suggest that Vegfc signaling is essential for coronary revascularization which supports CM proliferation and scar resolution during cardiac regeneration in zebrafish.

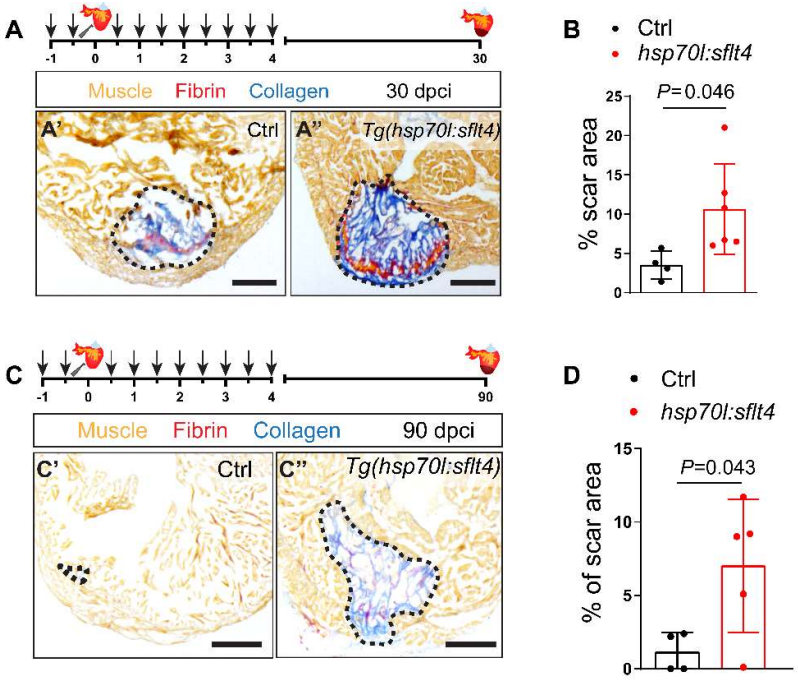

Figure 4.7: Blocking Vegfc signaling increases scarring after cardiac injury in zebrafish **A.** Illustration of heat shocks (arrows) and cardiac cryoinjury. A.F.O.G staining of cryosections of non-transgenic sibling (Ctrl) **(A')** and *Tg(hsp70l:sflt4)* **(A'')** hearts at 30 dpci. Orange: Muscle, red: Fibrin, blue: Collagen. **B.** Percentage of scar area normalized to ventricular area in non-transgenic sibling (Ctrl) (n=4) and *Tg(hsp70l:sflt4)* (n=5) ventricles at 30 dpci. **C.** Illustration of heat shocks (arrows) and cardiac cryoinjury. A.F.O.G staining of cryosections of non-transgenic sibling (Ctrl) **(C')** and *Tg(hsp70l:sflt4)* **(C'')** hearts at 90 dpci. Orange: Muscle, red: Fibrin, blue: Collagen. **D.** Percentage of scar area normalized to ventricular area in non-transgenic sibling (Ctrl) (n=4) and *Tg(hsp70l:sflt4)* (n=5) ventricles at 90 dpci. Black **(A,C)** dotted lines mark the injured area. Statistical test: Student's t-test **(B,D)**. Scale bars: 100 µm **(A,C)**. [Adapted and reprinted with permission from (El-Sammak et al., 2022)]

4.3. Identification of *emilin2a* is a downstream target of Vegfc signaling

4.3.1. Transcriptomic profiling of WT and *Tg(hsp70l:sflt4)* ventricles during cardiac regeneration

To understand the mechanism how Vegfc signaling promotes coronary revascularization during cardiac regeneration, I profiled the transcriptome of ventricles from WT and *Tg(hsp70l:sflt4)* zebrafish at 24 hpci to identify targets of Vegfc signaling (**Figure 4.8 A,B**). I then cross-referenced my dataset with a previously published one (Lai et al., 2017) to compare genes that are significantly downregulated in *Tg(hsp70l:sflt4)* with those that are significantly upregulated after cardiac injury in WT zebrafish ventricles (**Figure 4.8 C**). I was able to identify 10 genes that overlapped between these datasets. Next, I performed RT-qPCR analyses on all 10 genes to identify the ones that show a significant and consistent downregulation at 24 hpci (time point when the RNAseq was done) and at 96 hpci (time point where I observed the reduced coronary revascularization phenotype) when blocking Vegfc signaling (**Figure 4.8 D,E**). The only gene that showed a consistent downregulation at both time points was *emilin2a* (**Figure 4.9 A**).

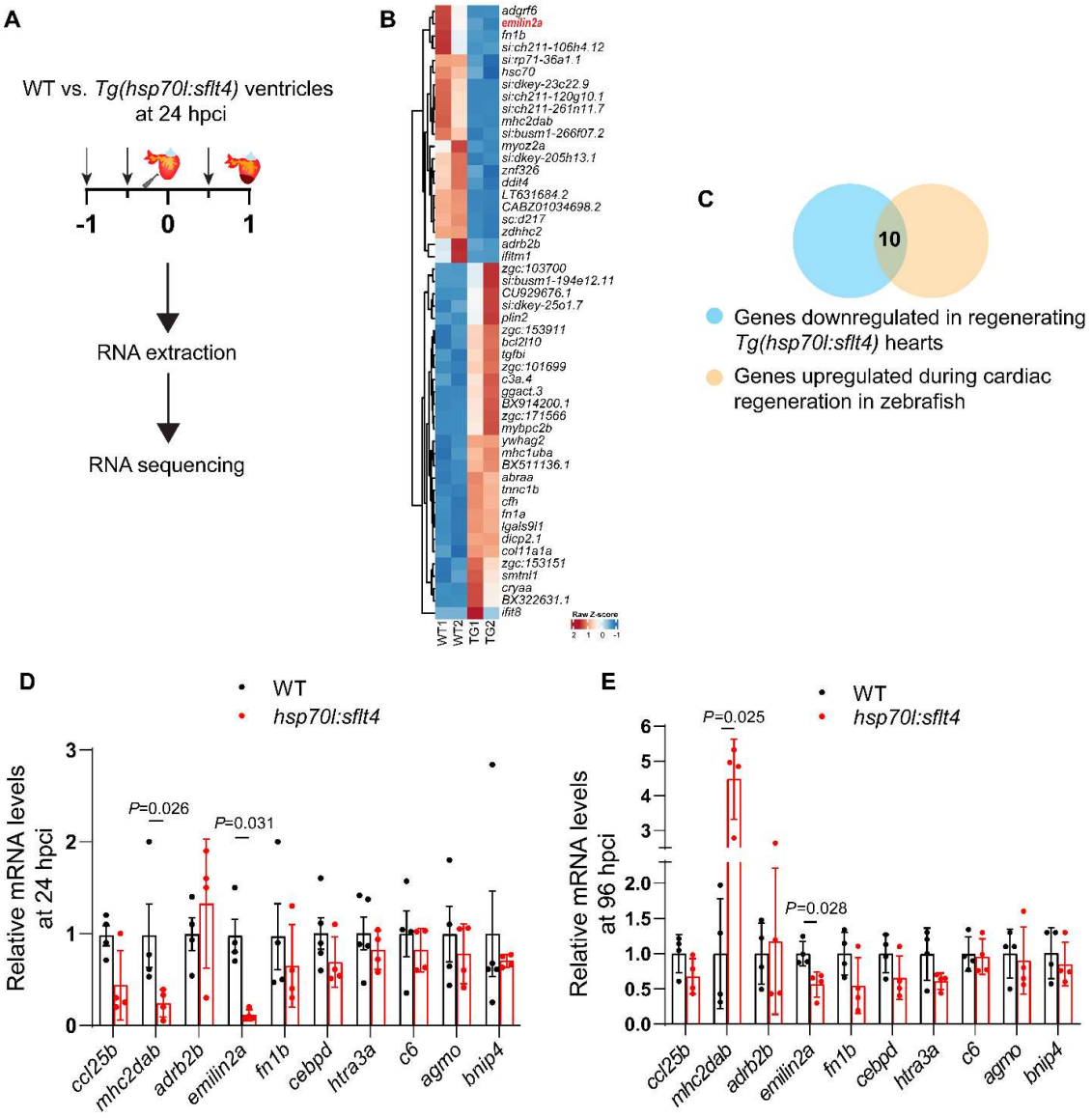

Figure 4.8: Identification of downstream targets of Vegfc signaling.

A. Illustration of the RNA sequencing experimental set up in WT vs. *Tg(hsp70l:sflt4)* ventricles at 24 hpci. **B.** Heat map displaying differentially expressed genes in non-transgenic sibling (WT) vs. *Tg(hsp70l:sflt4)* ventricles at 24 hpci. Genes are largely grouped into two clusters: one containing genes that are upregulated in *Tg(hsp70l:sflt4)* ventricles and the other containing genes that are downregulated in *Tg(hsp70l:sflt4)* ventricles. **C.** Cross-referencing of significantly downregulated genes in *Tg(hsp70l:sflt4)* at 24 hpci with genes upregulated during cardiac regeneration in WT zebrafish. **D.** RT-qPCR analysis of mRNA expression of 10 potential target genes of Vegfc signaling at 24 hpci in *Tg(hsp70l:sflt4)* ventricles (n=4) normalized to non-transgenic sibling (Ctrl) ventricles (n=4). **E.** RT-qPCR analysis of mRNA expression of 10 potential target genes of Vegfc signaling at 96 hpci in *Tg(hsp70l:sflt4)* ventricles (n=4) normalized to non-transgenic sibling (Ctrl) ventricles (n=4). Statistical tests:

Non-parametric Mann-Whitney test **(D,E)**. [Adapted and reprinted with permission from (El-Sammak et al., 2022)]

4.3.2. Emilin2a as a downstream target of Vegfc signaling

Since Vegfc signaling plays an important role in coronary revascularization, I reasoned that the reduction in *emilin2a* expression in *Tg(hsp70l:sflt4)* might be due to reduced coronary revascularization (**Figure 4.9 A**). To test this possibility, I analyzed the expression of *emilin2a* using RT-qPCR on uninjured adult ventricles of WT, *Tg(hsp70l:sflt4)* and *Tg(hsp70l:dn-vegfaa)* zebrafish, which is a global overexpression line of a dominant negative form of Vegfaa, that blocks coronary revascularization during cardiac regeneration in zebrafish (Marín-Juez et al., 2016; Rossi et al., 2016). *emilin2a* expression was reduced in *Tg(hsp70l:sflt4)* ventricles, whereas its expression in *Tg(hsp70l:dn-vegfaa)* was at similar levels as WT ventricles (**Figure 4.9 B**). These results suggest that *emilin2a* is a downstream target gene of Vegfc signaling and not simply a maker for endothelial cells. Moreover, to confirm that *emilin2a* is a downstream target of Vegfc signaling, I performed microinjections of *vegfc* mRNA into one-cell stage zebrafish embryos and analyzed the expression of *emilin2a*. I observed a significant increase in *emilin2a* expression at 48 hours post fertilization (hpf) following the injection of *vegfc* mRNA (**Figure 4.9 C**), further confirming that *emilin2a* is a downstream target of Vegfc signaling.

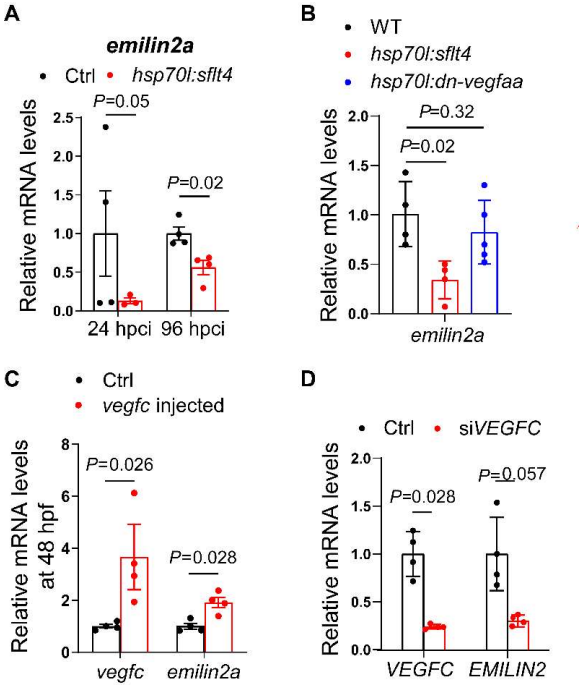

Figure 4.9: Validation of *emilin2a* as downstream target of Vegfc signaling.
A. RT-qPCR analysis of mRNA expression of *emilin2a* at 24 and 96 hpci in *Tg(hsp70l:sflt4)* ventricles normalized to non-transgenic sibling (Ctrl) ventricles (n=4). **B.** RT-qPCR analysis of mRNA expression of *emilin2a* in uninjured *Tg(hsp70l:sflt4)* (n=4) and *Tg(hsp70:dn-vegfaa)* adult ventricles (n=5) normalized to WT ventricles, after daily heat shocks for 3 days (n=4). **C.** RT-qPCR analysis of mRNA expression of *vegfc* and *emilin2a* at 48 hours post fertilization (hpf) following the injection of 75 pg of *vegfc* mRNA (n=4) normalized to un-injected (Ctrl) embryos (n=4). **D.** RT-qPCR analysis of *VEGFC* and *EMILIN2* mRNA expression in HUVECs after *siVEGFC* treatment (n=4) compared to scrambled control (n=4). Statistical tests: Non-parametric Mann-Whitney test **(A,B,C,D)**. [Adapted and reprinted with permission from (El-Sammak et al., 2022)]

Next, I tested whether EMILIN2 is a conserved downstream target for VEGFC signaling in humans. To this end, I knocked down *VEGFC* using siRNA in human umbilical vein endothelial cells (HUVECs), and analyzed the expression levels of *EMILIN2* using RT-qPCR. Notably, *EMILIN2* expression was reduced when blocking VEGFC signaling in HUVECs (**Figure 4.9 D**). These results suggest that VEGFC-EMILIN2 signaling axis is conserved in human ECs.

4.4. *emilin2a* is required for cardiac regeneration in zebrafish

EMILIN2 is an extracellular matrix (ECM) protein which belongs to the EMI domain endowed (EDEN) protein family, which comprises of EMILIN1, EMILIN2, MMRN1 and MMRN2 (Braghetta et al., 2004; Colombatti et al., 2012; Doliana et al., 2001). All of these proteins have an EMI domain at their N-terminus, and a gC1q domain at their C-terminus, and a unique domain which differs amongst the family members (**Figure 4.10**). These domains are important for their dimerization and their interactions with other proteins such as integrins (Bot et al., 2015; Doliana et al., 2000).

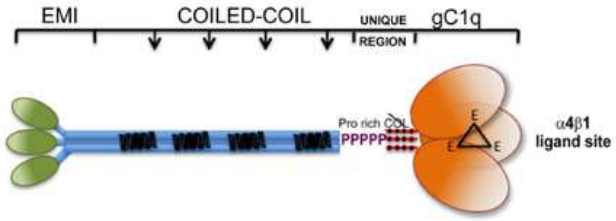

Figure 4.10: Schematic representation of the structure of EMILIN2 [Adapted from (Colombatti et al., 2012)], License: CC BY 4.0.

EMILIN2 in particular has been shown to promote angiogenesis. Addition of recombinant EMILIN2 increases sprouting of microvessels in cultured rat aortic rings. On the other hand, *Emilin2*$^{-/-}$ mice exhibit a reduction in the sprouting of microvessels in culture aortic rings (Paulitti et al., 2018). EMILIN2 is able to induce its angiogenic role in different types of cancer such as breast and gastric cancer cells (Andreuzzi et al., 2020; Marastoni et al., 2014). In zebrafish, *emilin2* is duplicated, resulting in *emilin2a* and *emilin2b*. *emilin2a* is expressed in the dorsal aorta and in intersegmental vessels at 24 hpf in zebrafish (Milanetto et al., 2008). However, no studies to date have investigated the role of *emilin2a* in zebrafish during cardiac regeneration.

4.4.1. Expression pattern of *emilin2a* during cardiac regeneration in zebrafish

To better understand the temporal expression dynamics of *emilin2a* after cardiac injury in zebrafish, I analyzed *emilin2a* expression by RT-qPCR analysis on WT zebrafish ventricles at different time points after cryoinjury and compared them to sham-operated hearts. I observed a significant increase in *emilin2a* expression at 96 hpci (**Figure 4.11 A**), coinciding with the peak of *vegfc* expression (**Figure 4.1 A**) and cEC proliferation (Marín-Juez et al., 2019). Next, to determine the spatial expression pattern, I performed *in situ* hybridization on heart sections and found that *emilin2a* is expressed at 96 hpci in the injured area where coronaries and EPDCs are found (**Figure 4.11 B**). To determine the source of *emilin2a* expression, I sorted both cell types, cECs using the *Tg(-0.8flt1:RFP)* line and EPDCs using the *Tg(tcf21:mCherry)* line at 96 hps and 96 hpci. I found that both cECs and EPDCs upregulate *emilin2a* expression at 96 hpci (**Figure 4.11 C**). When comparing *emilin2a* expression between both cell types, I observed a stronger upregulation in its expression in EPDCs at 96 hpci (**Figure 4.11 D**).

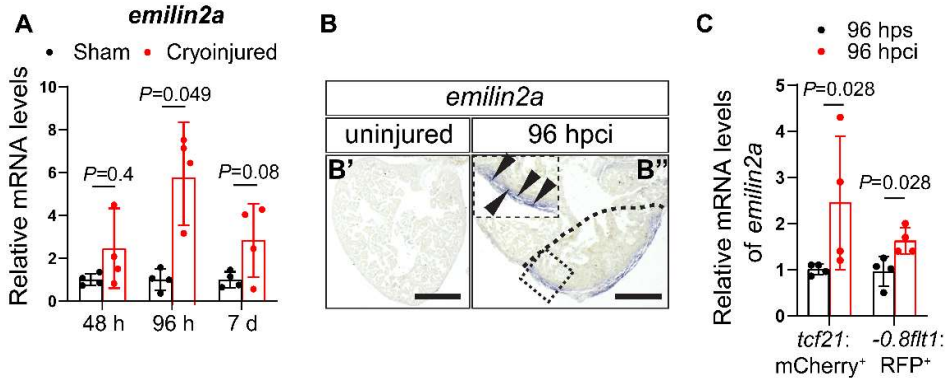

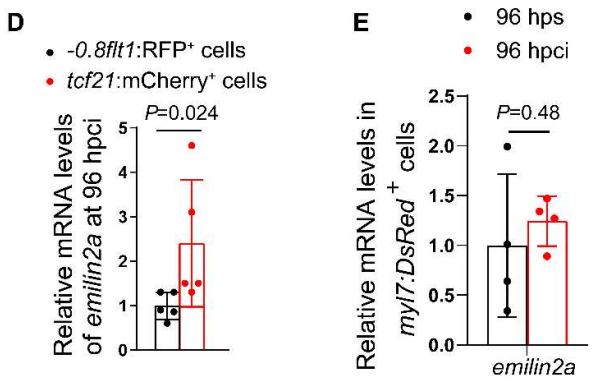

Figure 4.11: *emilin2a* expression levels during cardiac regeneration.

A. RT-qPCR analysis of mRNA expression of *emilin2a* at 48 and 96 hpci and 7 dpci in injured tissue normalized to sham-operated ventricles (n=4); h: hpci, d: dpci. **B.** *in situ* hybridization for *emilin2a* expression on paraffin sections of uninjured **(B')** and 96 hpci **(B'')** ventricles. Arrowheads point to *emilin2a* expression. **C.** RT-qPCR analysis of mRNA expression of *emilin2a* in sorted *tcf21*:mCherry^{+} cells (EPDCs) (n=4) and sorted *-0.8flt1*:RFP^{+} cells (cECs) (n=4) at 96 hpci normalized to 96 hps. **D.** RT-qPCR analysis of *emilin2a* mRNA expression at 96 hpci in sorted *tcf21*:mCherry^{+} cells (EPDCs) (n=5) normalized to sorted *-0.8flt1:*RFP^{+} cells (cECs) (n=5). **E.** RT-qPCR analysis of mRNA expression of *emilin2a* at 96 hpci in sorted *myl7:*DsRed^{+} cells (CMs) (n=4) normalized to 96 hps (n=4). Black **(B)** dotted lines mark the injured area. Statistical tests: Non-parametric Mann-Whitney test **(A,C,D,E)**. Scale bars: 100 µm **(B)**. [Adapted and reprinted with permission from (El-Sammak et al., 2022)]

To assess if CMs express *emilin2a*, I sorted them using the CM specific *Tg(myl7:DsRed)* line and could not detect *emilin2a* expression before and after injury (**Figure 4.11 E**). These data show that during cardiac regeneration in zebrafish, *emilin2a* is expressed in EPDCs and cECs, with EPDCs being the major source of expression.

4.4.2. Generation of *emilin2a* full locus deletion mutants

To investigate the role of *emilin2a* during cardiac regeneration in zebrafish, I generated an *emilin2a* mutant as a loss of function tool. Since the zebrafish genome consists of two paralogs of the *emilin2* gene; *emilin2a* and *emilin2b*, I generated a full locus deletion allele of *emilin2a* to avoid transcriptional adaptation response (El-Brolosy et al., 2019; Rossi et al., 2015). I used the CRISPR-Cas9 technology to target exons 1 and 9, thereby removing the 33 kb long *emilin2a* locus (**Figure 4.12 A**). I first tested the efficiency of each gRNA targeting each exon using high resolution melting curve

analysis (HRMA) (**Figure 4.12 B,C**). After identifying gRNAs that efficiently target exons 1 and 9, I co-injected both gRNAs and analyzed the loss of *emilin2a* in injected embryos using specific primers flanking the deleted region (**Figure 4.12 D,E**). To confirm the lack of *emilin2a* expression in adult hearts of the newly generated mutants, I performed RT-qPCR analysis in adult uninjured *emilin2a*$^{-/-}$ ventricles and compared *emilin2a* expression with *emilin2a*$^{+/+}$ siblings. Indeed, *emilin2a*$^{-/-}$ ventricles lacked *emilin2a* expression (**Figure 4.12 F**).

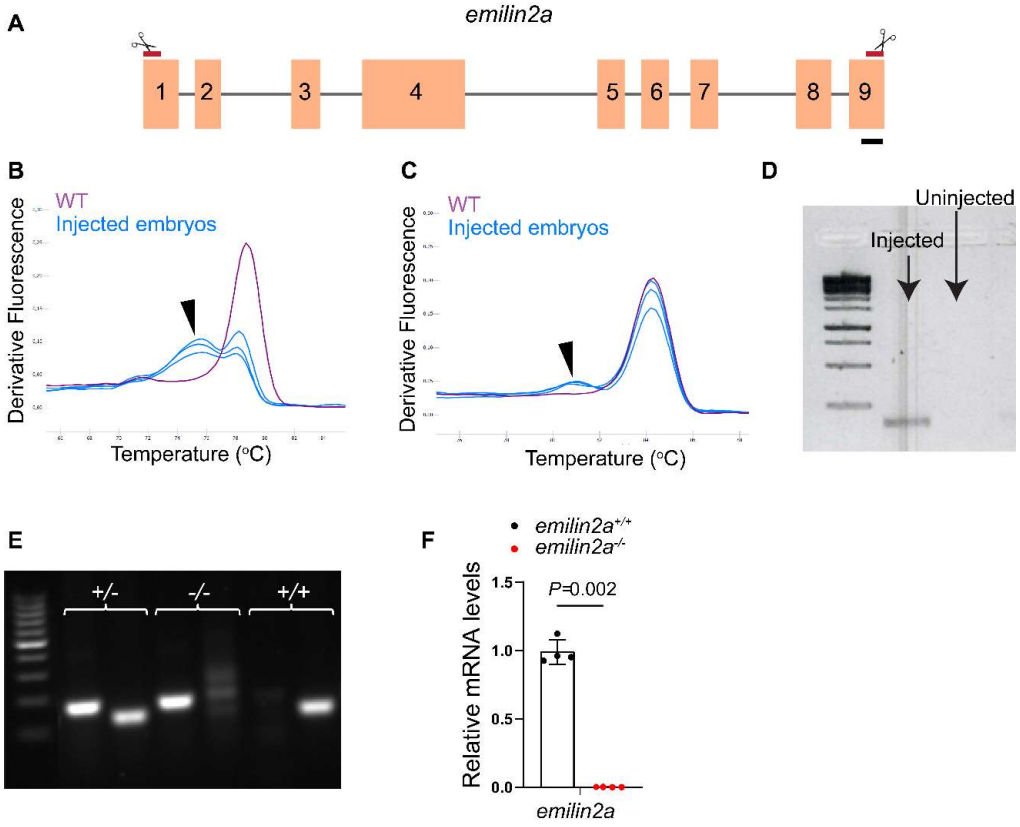

Figure 4.12: Generation of an *emilin2a* full locus deletion allele.

A. Illustration of the *emilin2a* locus showing the location of the gRNAs targeting exons 1 and 9 (red lines). **B.** High resolution melt analysis showing WT embryos at 24 hpf, uninjected (purple) and injected with 75 pg of gRNA targeting exon 1 (blue). **C.** High resolution melt analysis showing WT embryos at 24 hpf, uninjected (purple) and injected with 75 pg of gRNA targeting exon 9 (blue). **D.** DNA gel electrophoresis analysis of embryos at 24 hpf, uninjected and injected with the gRNAs targeting exons 1 and 9; DNA ladder =100 bp. **E.** DNA gel electrophoresis assay used to genotype the *emilin2a* full locus deletion allele; DNA ladder = 100 bp. **F.** RT-qPCR analysis of mRNA expression of *emilin2a* in uninjured ventricles of *emilin2a*$^{-/-}$ (n=4) normalized to *emilin2a*$^{+/+}$ uninjured ventricles (n=4). Statistical test: Non-

parametric Mann-Whitney test **(F)**. Scale bars: 1 kb **(A)**. [Adapted and reprinted with permission from (El-Sammak et al., 2022)].

Next, to analyze if *emilin2a* mutants exhibit any phenotype in physiological conditions, I characterized *emilin2a*$^{+/+}$ *and emilin2a*$^{-/-}$ larvae at 5 dpf and observed no obvious gross morphological defects (**Figure 4.13 A**). I then analyzed the gross morphology and the coronary network of the adult ventricle of these animals. Both *emilin2a*$^{+/+}$ *and emilin2a*$^{-/-}$ adult zebrafish displayed comparable ventricular size and coronary network conformation (**Figure 4.13 B,C**). These findings indicate that *emilin2a* mutants are not burdened and display no phenotype in physiological conditions.

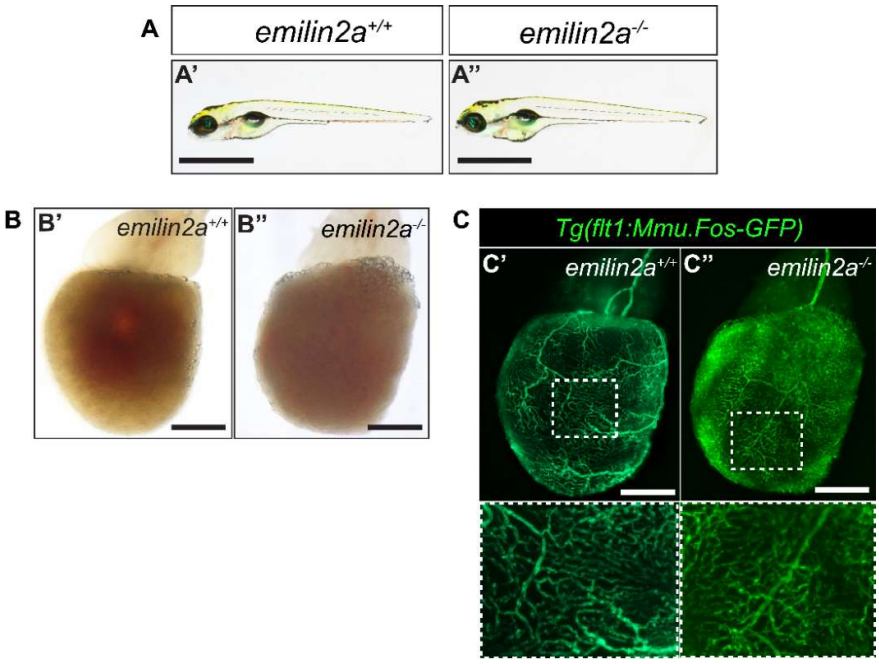

Figure 4.13: Characterization of *emilin2a*$^{-/-}$ full locus mutants.

A. Wholemount images of *emilin2a*$^{+/+}$ and *emilin2a*$^{-/-}$ sibling larvae at 5 dpf. **B.** Wholemount images of uninjured adult ventricles of *emilin2a*$^{+/+}$ **(B')** *emilin2a*$^{-/-}$ **(B'')** sibling zebrafish. **C.** Wholemount images of uninjured adult ventricles of *Tg(flt1:Mmu.Fos-GFP); emilin2a*$^{+/+}$ **(C')** and *Tg(flt1:Mmu.Fos-GFP); emilin2a*$^{-/-}$ **(C'')** sibling zebrafish. Scale bars: 500 µm **(A,B,C)**. [Adapted and reprinted with permission from (El-Sammak et al., 2022)]

4.4.3. *emilin2a* mutants exhibit impaired cardiac regeneration in zebrafish

Previous studies showing that EMILIN2 is required for microvessel sprouting in mouse cultured aortic rings (Paulitti et al., 2018), and the upregulation of *emilin2a* expression after cardiac injury motivated me to analyze the role of *emilin2a* in coronary

revascularization following cardiac injury in zebrafish. To this end, I performed cryoinjuries on the newly generated *emilin2a* mutants and analyzed the coronary revascularization response. cEC proliferation was significantly reduced at 96 hpci in *emilin2a*$^{-/-}$ ventricles in comparison with *emilin2a*$^{+/+}$ injured ventricles (**Figure 4.14 A,B**). Moreover, the coronary coverage in *emilin2a*$^{-/-}$ ventricles was significantly impaired at 7 dpci (**Figure 4.14 C,D**). Notably, I observed that *emilin2a* mutants exhibited these coronary revascularization defects while lacking ventricular lymphatics (**Figure 4.14 E**). Altogether, these findings indicate that *emilin2a* is required for coronary revascularization in zebrafish downstream of Vegfc signaling, and that its role in coronary revascularization is independent of lymphatics.

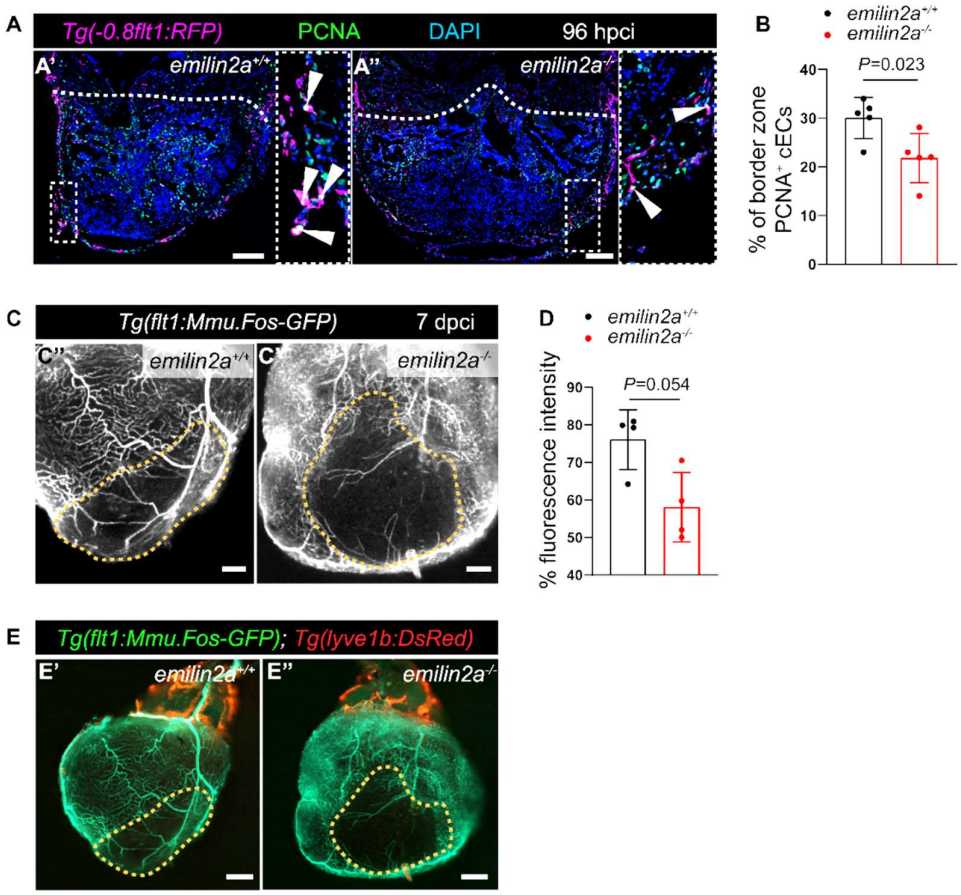

Figure 4.14: *emilin2a* mutants exhibit reduced coronary revascularization after cardiac injury in zebrafish.

A. Sections of cryoinjured hearts of *Tg(flt1:Mmu.Fos-GFP); emilin2a*$^{+/+}$ **(A')** and *Tg(flt1:Mmu.Fos-GFP); emilin2a*$^{-/-}$ **(A'')** sibling zebrafish at 96 hpci immunostained for GFP (coronaries, magenta), PCNA (proliferation marker, green), and DNA (DAPI, blue). Arrowheads point to PCNA^{+} cECs. **B.** Percentage of PCNA^{+} cECs in the injured tissue and

border zone of *Tg(flt1:Mmu.Fos-GFP); emilin2a*$^{+/+}$ (n=5) and *Tg(flt1:Mmu.Fos-GFP); emilin2a*$^{-/-}$ (n=5) ventricles at 96 hpci. **C.** Wholemount images of hearts of 7 dpci *Tg(flt1:Mmu.Fos-GFP); emilin2a*$^{+/+}$ **(C')** and *Tg(flt1:Mmu.Fos-GFP); emilin2a*$^{-/-}$ **(C'')** zebrafish. **D.** Percentage of GFP fluorescence intensity in the injured tissue of 7 dpci *Tg(flt1:Mmu.Fos-GFP); emilin2a*$^{+/+}$ (n=4) and *Tg(flt1:Mmu.Fos-GFP); emilin2a*$^{-/-}$ (n=4) hearts. **E.** Wholemount images of hearts of 7 dpci *Tg(flt1:Mmu.Fos-GFP); Tg(lyve1b:DsRed)*; *emilin2a*$^{+/+}$ **(E')** and *Tg(flt1:Mmu.Fos-GFP); Tg(lyve1b:DsRed); emilin2a*$^{-/-}$ **(E'')** sibling zebrafish. White **(A)**, and orange **(C,E)** dotted lines mark the injured area. Statistical tests: Student's t-test **(B,D)**. Scale Bars: 100 µm **(A)**, 200 µm **(C,E)**. [Adapted and reprinted with permission from (El-Sammak et al., 2022)]

Next, I hypothesized that the reduced coronary revascularization response exhibited in *emilin2a*$^{-/-}$ ventricles could also affect CM regeneration. To test this hypothesis, I cryoinjured *emilin2a*$^{+/+}$ and *emilin2a*$^{-/-}$ ventricles and analyzed CM proliferation at 7 dpci. I observed a significant reduction in CM proliferation in *emilin2a*$^{-/-}$ ventricles (**Figure 4.15 A,B**). Furthermore, *emilin2a*$^{-/-}$ ventricles had a significantly larger scar at 30 dpci (**Figure 4.15 C,D**), and retained this scar at 90 dpci, when cardiac regeneration is almost complete with very minimal scarring (**Figure 4.15 E,F**). These data indicate that *emilin2a* is required for cardiac regeneration in zebrafish.

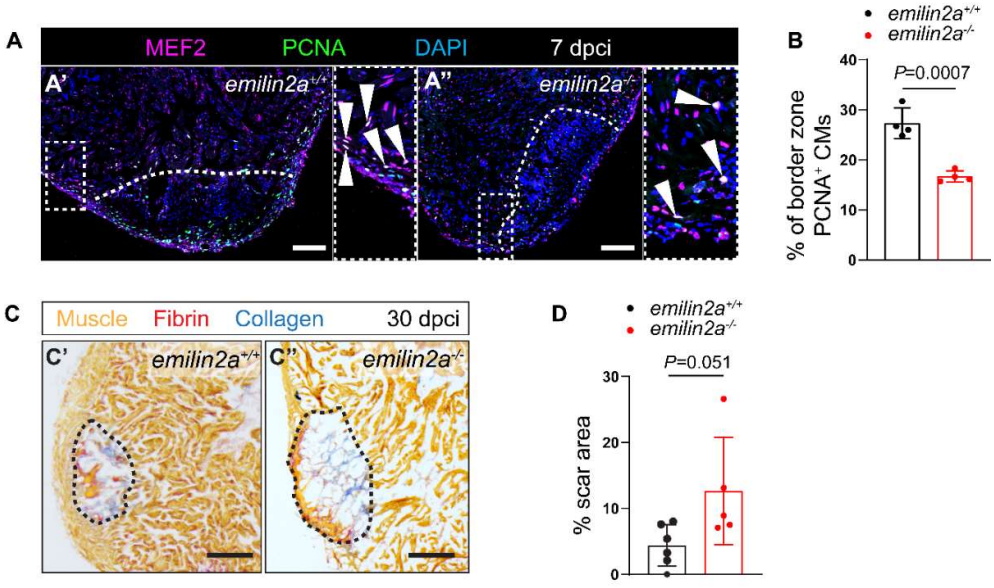

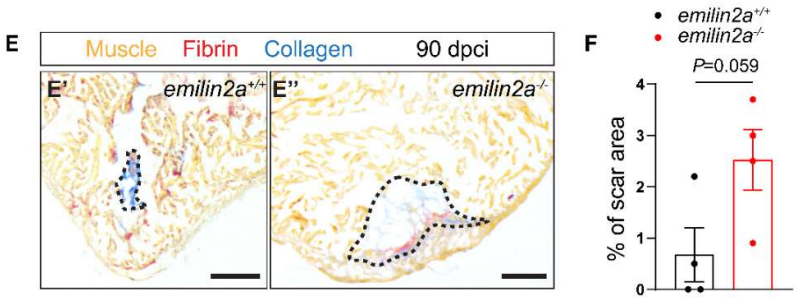

Figure 4.15: *emilin2a* mutants exhibit reduced muscle regeneration after cardiac injury in zebrafish.

A. Sections of cryoinjured ventricles of *emilin2a*$^{+/+}$ **(A')** and *emilin2a*$^{-/-}$ **(A'')** sibling zebrafish at 7 dpci immunostained for MEF2 (CMs, magenta), PCNA (proliferation marker, green), and DNA (DAPI, blue). Arrowheads point to PCNA^{+} CMs. **B.** Percentage of PCNA^{+} CMs in the border zone of *emilin2a*$^{+/+}$ (n=4) and *emilin2a*$^{-/-}$ (n=4) hearts at 7 dpci. **C.** A.F.O.G staining of cryosections of *emilin2a*$^{+/+}$ **(C')** and *emilin2a*$^{-/-}$**(C'')** hearts at 30 dpci. Orange: Muscle, red: Fibrin, blue: Collagen. **D.** Percentage of scar area normalized to ventricular area in *emilin2a*$^{+/+}$ (n=4) and *emilin2a*$^{-/-}$ (n=4) hearts at 30 dpci. **E.** A.F.O.G staining of cryosections of *emilin2a*$^{+/+}$ **(E')** and *emilin2a*$^{-/-}$**(E'')** hearts at 90 dpci. Orange: Muscle, red: Fibrin, blue: Collagen. **F.** Percentage of scar area normalized to ventricular area in *emilin2a*$^{+/+}$ (n=4) and *emilin2a*$^{-/-}$ (n=4) ventricles at 90 dpci. Black **(C,E)**, and white **(A)** dotted lines mark the injured area. Statistical tests: Student's t-test **(B,D,E)**. Scale Bars: 100 µm **(A)**, 200 µm **(C,E)**. [Adapted and reprinted with permission from (El-Sammak et al., 2022)]

4.5. *emilin2a* can promote cardiac regeneration in zebrafish

Previous reports have shown that addition of recombinant EMILIN2 can promote microvessel sprouting in cultured rat aortic rings (Paulitti et al., 2018). This observation led to me test if EMILIN2 is also required by ECs in an *in vitro* injury setting. To this end, I performed a scratch assay on cultured HUVECs and analyzed the expression of EMILIN2 at 6 hours post scratch (hpsc) when cells migrate to cover the scratch. I detected a significant upregulation in the expression of *EMILIN2* following the scratch (**Figure 4.16 A**), indicating that EMILIN2 might be required for endothelial cells migration in an *in vitro* wound. Furthermore, previously published datasets comparing the transcriptome of the regenerative zebrafish ventricle and the non-regenerative medaka (*Oryzias latipes*) ventricle after cardiac injury show that

emilin2a is upregulated in zebrafish after injury but not in medaka which cannot regenerate its heart (Lai et al., 2017) (**Figure 4.16 B**).

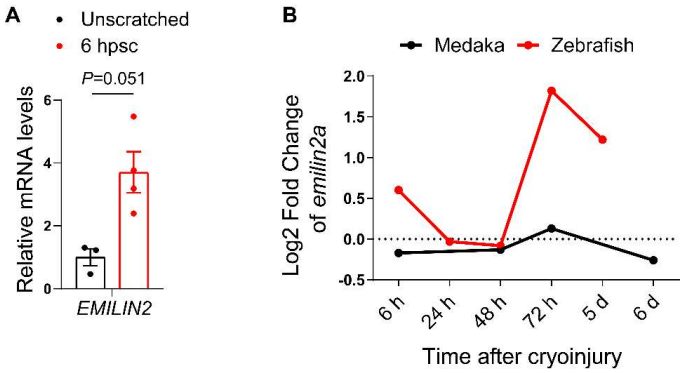

Figure 4.16: *emilin2a* expression in different injury models.

A. RT-qPCR analysis of the mRNA expression of *EMILIN2* in HUVECs at 6 hours post scratch (6 hpsc) (n=3) normalized to unscratched (n=4). **F.** *emilin2a* mRNA expression levels in zebrafish and medaka ventricles after cardiac cryoinjury normalized to sham operated ventricles (data from (Lai et al., 2017)); h: hpci; d: dpci. Statistical test: Non-parametric Mann-Whitney test **(A).** [Adapted and reprinted with permission from (El-Sammak et al., 2022)]

All of these lines of evidences, along with the data showing impaired cardiac regeneration in *emilin2a*$^{-/-}$ ventricles led me to hypothesize that Emilin2a can act as a pro-regenerative factor. I tested this hypothesis by attempting to answer two questions as described in the following sections:

1. Can Emilin2a rescue the cardiac regeneration phenotype observed when blocking Vegfc signaling?
2. Can Emilin2a promote cardiac regeneration?

4.5.1. Overexpressing *emilin2a* in epicardium-derived cells can rescue Vegfc signaling block

I set out to test the possibility that Emilin2a can rescue the Vegfc signaling block phenotype by generating a HOTCRE *emilin2a* line for a timely and tissue specific control over *emilin2a* expression (Hesselson et al., 2009). I generated the *Tg(hsp70l:loxP-CFP-loxP-emilin2a-p2A-mCherry)* which allows temporal control over the expression by heat shock treatments (**Figure 4.17 A**). Combining this line with a tissue specific CreERT2 line allows for tissue specific control over *emilin2a* expression as well as additional temporal control with tamoxifen administration to induce

recombination (**Figure 4.17 B-D**). Using this approach, I performed tamoxifen injections and heat shocks before and after cardiac cryoinjury, respectively, on *Tg(hsp70l:sflt4); TgBAC(tcf21:CreERT2); Tg(hsp70l:loxP-CFP-loxP-emilin2a-p2A-mCherry)* zebrafish to overexpress *emilin2a* specifically in epicardium-derived cells while blocking Vegfc signaling during cardiac regeneration in zebrafish. And as a control experiment, I performed ethanol injections instead of tamoxifen so that recombination is not induced in those hearts, hence *emilin2a* expression is not induced and only Vegfc signaling is blocked (**Figure 4.18 A**).

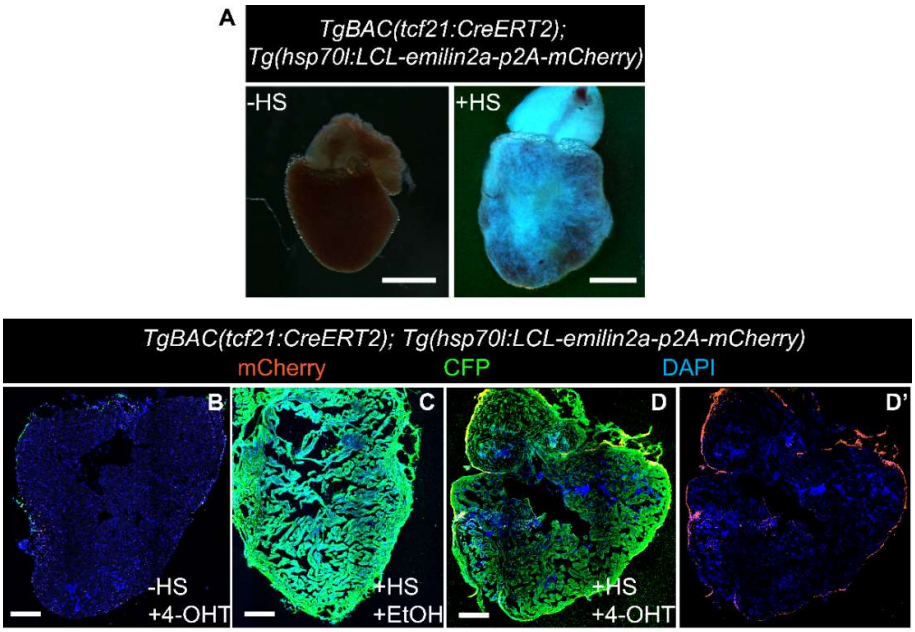

Figure 4.17: Validation of *TgBAC(tcf21:CreERT2); Tg(hsp70l:loxP-CFP-loxP-emilin2a-p2A-mCherry)* in adult zebrafish hearts.

A. Wholemount images of uninjured hearts of *TgBAC(tcf21:CreERT2); Tg(hsp70l:LCL-emilin2a-p2A-mCherry)* zebrafish without heat shocks (-HS) and after heat shocks (+HS). **B.** Immunostaining of sections of cryoinjured hearts of *TgBAC(tcf21:CreERT2); Tg(hsp70l:LCL-emilin2a-p2A-mCherry)* zebrafish without heat shock (-HS) and with tamoxifen injection (+4-OHT) **(C)**, with heat shock (+HS) and ethanol injection (+EtOH) **(D)** and with heat shock (+HS) and tamoxifen injections (+4-HT) **(D, D')**; sections are stained for mCherry (recombined EPDCs, orange), GFP (non-recombined tissue, green), and DNA (DAPI, blue). Scale Bars: 200 µm **(A)**, 100 µm **(B,C,D)**. [Adapted and reprinted with permission from (El-Sammak et al., 2022)]

I extracted the hearts at 96 hpci and quantified cEC proliferation, and observed increased cEC proliferation in ventricles in which Vegfc signaling was blocked and *emilin2a* was overexpressed in EPDCs (**Figure 4.18 A,B**). cEC proliferation in those hearts were comparable to those observed in WT hearts at 96 hpci (Marín-Juez et al., 2019). On the other hand, ventricles in which *emilin2a* was not induced showed cEC proliferation levels close to those observed when blocking Vegfc signaling in earlier experiments (**Figure 4.18 A,B**). Moreover overexpressing *emilin2a* in EPDCs also increased CM proliferation in *Tg(hsp70l:sflt4)* ventricles (**Figure 4.18 C,D**). Interestingly, when I performed the same experiment and analyzed the hearts at a later time point, 30 dpci, I found that overexpressing *emilin2a* in EPDCs was able to reduce the scar area in comparison to ventricles in which Vegfc signaling was blocked while *emilin2a* was not expressed (**Figure 4.18 E,F**). All of these findings suggest that Emilin2a was able to rescue the Vegfc signaling block phenotype and increase cEC proliferation to a comparable level as observed in WT hearts (Marín-Juez et al., 2019) and reduce scarring.

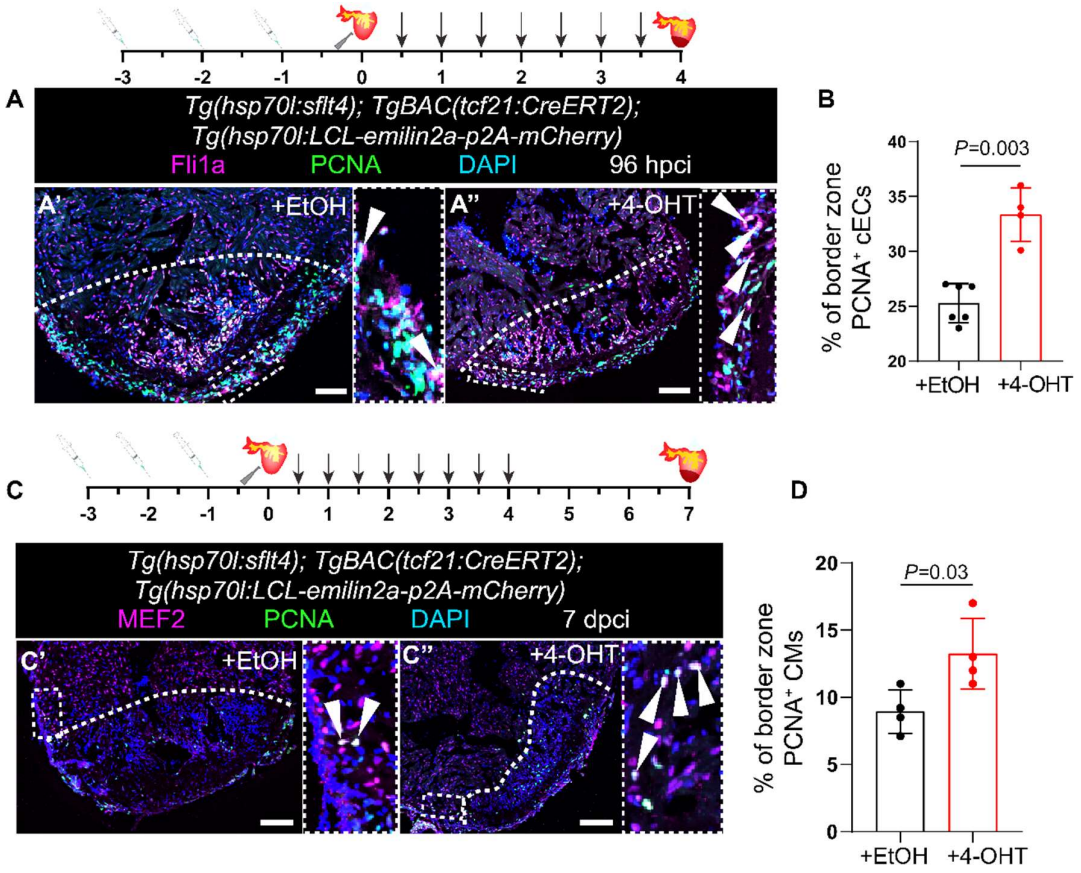

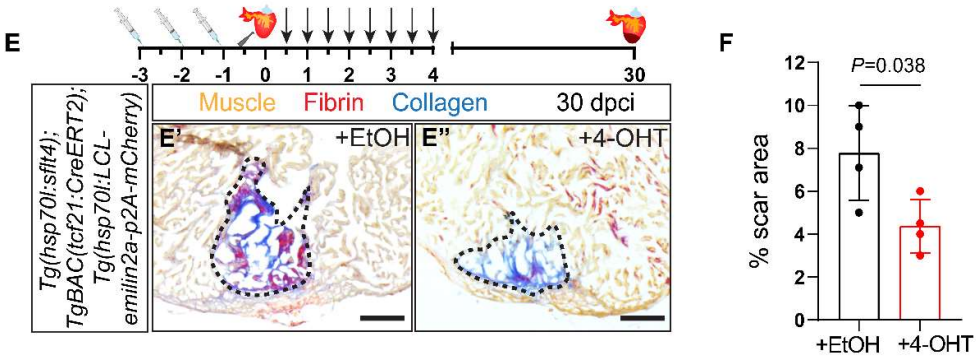

Figure 4.18: Overexpressing *emilin2a* in epicardium-derived cells can rescue Vegfc signaling block.

A. Illustration of Ethanol (EtOH) or 4-hydroxytamoxifen (4-OHT) injections followed by cryoinjury and heat shocks (arrows). Sections of cryoinjured hearts of *Tg(hsp70l:sflt4); TgBAC(tcf21:CreERT2); Tg(hsp70l:LCL-emilin2a-p2A-mCherry)* zebrafish injected with EtOH **(A')** or 4-OHT **(A'')** at 96 hpci immunostained for Fli1a (endothelial cells, magenta), PCNA (proliferation marker, white), and DNA (DAPI, blue). Arrowheads point to PCNA$^+$ cECs. **B.** Percentage of PCNA$^+$ cECs in the injured tissue and border zone of *Tg(hsp70l:sflt4); TgBAC(tcf21:CreERT2); Tg(hsp70l:LCL-emilin2a-mCherry)* at 96 hpci injected with EtOH (n=6) or 4-OHT (n=4). **C.** Illustration of Ethanol (EtOH) or 4-hydroxytamoxifen (4-OHT) injections followed by cryoinjury and heat shocks (arrows). Sections of cryoinjured hearts of *Tg(hsp70l:sflt4); TgBAC(tcf21:CreERT2); Tg(hsp70l:LCL-emilin2a-p2A-mCherry)* zebrafish injected with EtOH **(C')** or 4-OHT **(C'')** at 7 dpci immunostained for MEF2 (CMs, magenta), PCNA (proliferation marker, white), and DNA (DAPI, blue). Arrowheads point to PCNA$^+$ CMs. **D.** Percentage of PCNA$^+$ CMs in the border zone of *Tg(hsp70l:sflt4); TgBAC(tcf21:CreERT2); Tg(hsp70l:LCL-emilin2a-mCherry)* at 7 dpci injected with EtOH (n=4) or 4-OHT (n=4). **E.** Illustration of Ethanol (EtOH) or 4-hydroxytamoxifen (4-OHT) injections followed by cryoinjury and heat shocks (arrows). A.F.O.G staining of cryosections of injured ventricles of *Tg(hsp70l:sflt4); TgBAC(tcf21:CreERT2); Tg(hsp70l:LCL-emilin2a-p2A-mCherry)* zebrafish injected with EtOH **(E')** or 4-OHT **(E'')** at 30 dpci. Orange: Muscle, red: Fibrin, blue: Collagen. **F.** Percentage of scar area normalized to ventricular area in *Tg(hsp70l:sflt4); TgBAC(tcf21:CreERT2); Tg(hsp70l:LCL-emilin2a-mCherry)* at 30 dpci injected with EtOH (n=4) or 4-OHT (n=4). White **(A,C)**, and Black **(E)** dotted lines mark the injured area. Statistical test: Student's t-test **(B,D,F)**. Scale Bars: 100 µm **(A,C)**, 200 µm **(E)**. [Adapted and reprinted with permission from (El-Sammak et al., 2022)].

4.5.2. Overexpression of *emilin2a* promotes cardiac regeneration in zebrafish

The findings that Emilin2a was able to rescue the Vegfc signaling block phenotype and restore cEC proliferation levels to that of WT (**Figure 4.18**) motivated me to test the possibility that Emilin2a can act as a pro-regenerative molecule and promote cardiac regeneration. To this end, I generated a transgenic *emilin2a* line to overexpress *emilin2a* globally under the heat shock promoter. I cryoinjured *Tg(hsp70l:emilin2a)* zebrafish ventricles, performed heat shock treatments twice daily and extracted the hearts at 96 hpci. There was a profound increase in cEC proliferation levels in *Tg(hsp70l:emilin2a)* ventricles compared with sibling WT (**Figure 4.19 A,B**), and a marginal increase in coronary coverage at 7 dpci (**Figure 4.19 C,D**). Since Emilin2a is a target of Vegfc signaling, it is possible that the pro-regenerative effects observed upon *emilin2a* induction are associated with increased lymphangiogenesis. To test this possibility, I analyzed lymphatic ECs at 7 dpci when overexpressing *emilin2a* and could not detect any change in the ventricular lymphatic coverage (**Figure 4.19 E**), suggesting that the coronary effects mediated by Emilin2a are independent of lymphatics.

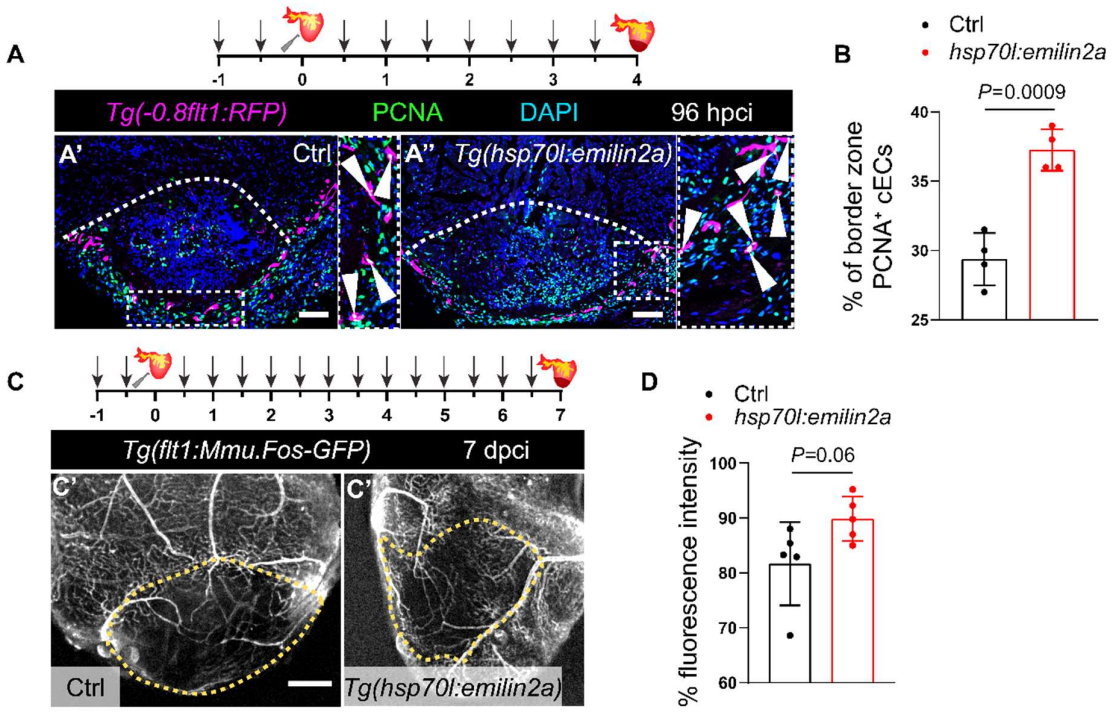

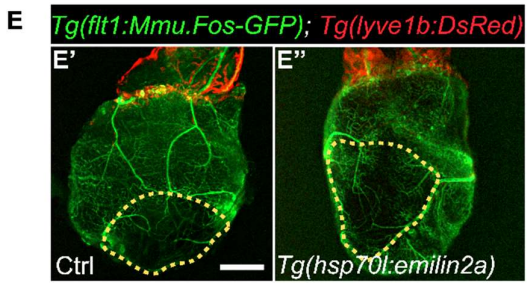

Figure 4.19: *emilin2a* overexpression increases coronary endothelial cell proliferation. **A.** Illustration of heat shocks (arrows) and cardiac cryoinjury. Sections of cryoinjured hearts of *Tg(0.8flt1:RFP)* (Ctrl) **(A')** and *Tg(hsp70l:emilin2a); Tg(-0.8flt1:RFP)* **(A'')** sibling zebrafish at 96 hpci immunostained for RFP (coronaries, magenta), PCNA (proliferation marker, green), and DNA (DAPI, blue). Arrowheads point to $PCNA^+$ cECs. **B.** Percentage of $PCNA^+$ cECs in the injured tissue and border zone of *Tg(-0.8flt1RFP)* (Ctrl) (n=4) and *Tg(hsp70l:emilin2a); Tg(-0.8flt1:RFP)* heart (n=4) at 96 hpci. **C.** Illustration of heat shocks (arrows) and cardiac cryoinjury. Wholemount images of heart of *Tg(flt1:Mmu.Fos-GFP)* (Ctrl) **(C')** and *Tg(hsp70l:emilin2a); Tg(flt1:Mmu.Fos-GFP)* **(C'')** zebrafish at 7 dpci. **D.** Percentage of GFP fluorescence intensity in the injured area of *Tg(flt1:Mmu.Fos-GFP)* (Ctrl) (n=5) and *Tg(hsp70l:emilin2a); Tg(flt1:Mmu.Fos-GFP)* (n=5) heart at 7 dpci. **E.** Wholemount images of ventricles of *Tg(flt1:Mmu.Fos-GFP); Tg(lyve1b:DsRed)* (Ctrl) **(E')** and *Tg(hsp70l:emilin2a); Tg(flt1:Mmu.Fos-GFP); Tg(lyve1b:DsRed)* **(E'')** zebrafish at 7 dpci. White **(A)**, and orange **(C,E)** dotted lines mark the injured area. White **(A)**, orange **(C,E)** dotted lines mark the injured area. Statistical test: Student's t-test **(B)**, Non-parametric Mann-Whitney test **(D)**. Scale Bars: 100 µm **(A)**, 200 µm **(C,E)**. [Adapted and reprinted with permission from (El-Sammak et al., 2022)].

Interestingly, increasing coronary revascularization by overexpressing *emilin2a* led to a significant increase in CM proliferation (**Figure 4.20 A,B**) and significantly enhanced scar resolution as evident by the reduced scar area in *Tg(hsp70l:emilin2a)* ventricles at 30 dpci (**Figure 4.20 C,D**). These results suggest that downstream of Vegfc signaling, epicardium-derived Emilin2a promotes cardiac regeneration in zebrafish.

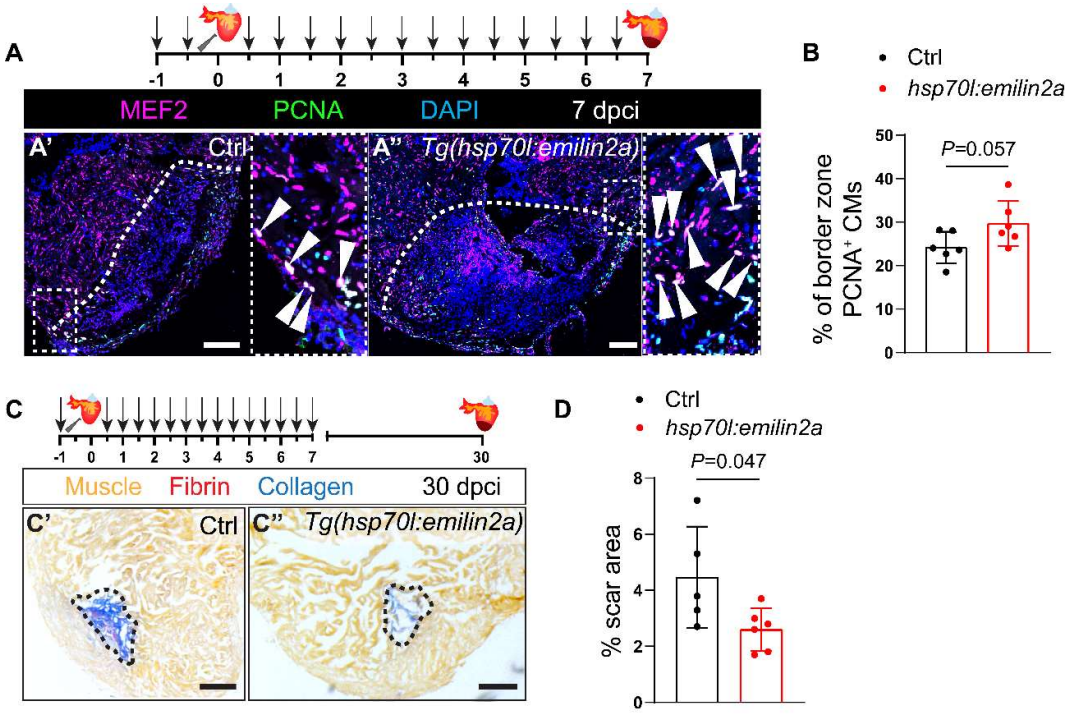

Figure 4.20: *emilin2a* overexpression promotes cardiac regeneration.

A. Illustration of heat shocks (arrows) and cardiac cryoinjury. Sections of cryoinjured hearts of non-transgenic sibling (Ctrl) **(A')** and *Tg(hsp70l:emilin2a)* **(A'')** zebrafish at 7 dpci immunostained for MEF2 (CMs, magenta), PCNA (proliferation marker, green), and DNA (DAPI, blue). Arrowheads point to PCNA$^+$ CMs. **B.** Percentage of PCNA$^+$ CMs in the border zone of non-transgenic sibling (Ctrl) (n=6) and *Tg(hsp70l:emilin2a)* (n=6) hearts at 7 dpci. **C.** Illustration of heat shocks (arrows) and cardiac cryoinjury. A.F.O.G staining of cryosections of non-transgenic sibling (Ctrl) **(C')** and *Tg(hsp70l:emilin2a)* **(C'')** hearts at 30 dpci. Orange: Muscle, red: Fibrin, blue: Collagen. **D.** Percentage of scar area normalized to ventricular area in non-transgenic sibling (Ctrl) (n=5) and *Tg(hsp70l:emilin2a)* (n=6) ventricles at 30 dpci. White **(A)**, black **(C)** dotted lines mark the injured area. Statistical tests: Student's t-test **(B,D)**. Scale Bars: 100 µm **(A)**, 200 µm **(C)**. [Adapted and reprinted with permission from (El-Sammak et al., 2022)]

4.6. *emilin2a* stimulates *cxcl8a* during cardiac regeneration in zebrafish

EMILIN2 exerts its angiogenic role in HUVECs as well as in gastric cancer cells by inducing the expression of the chemokine CXCL8 (IL-8) (Andreuzzi et al., 2020; Paulitti et al., 2018). CXCL8 is an inflammatory chemokine which binds to and activates G-

protein coupled receptors CXCR1 and CXCR2 (Murphy and Tiffany, 1991). CXCL8 has been extensively studied for its role in regulating neutrophils during wound healing (Ha et al., 2017). In zebrafish, Cxcl8a recruits neutrophils to the wound epithelium via Cxcr1, and recruits them away from the wound via Cxcr2 (De Oliveira et al., 2016; Powell et al., 2017). Besides its well-known role in neutrophils, several studies have highlighted a pro-angiogenic role of CXCL8 in HUVECs, intestinal ECs and in gastric cancer (Heidemann et al., 2003; Li et al., 2003; Shi and Wei, 2016). Moreover, addition of human recombinant CXCL8 induces neovascularization in rat and rabbit corneas (Koch et al., 1992; Strieter et al., 1992). In zebrafish, a study has previously shown that silencing of *cxcl8a* inhibited the development and sprouting of intersegmental vessels (Stoll et al., 2011). All of these reports collectively suggest that CXCL8 might be involved in wound healing and regeneration.

To test if Emilin2a can promote the expression of *cxcl8a* after cardiac injury in zebrafish, I analyzed *cxcl8a* expression by RT-qPCR in *emilin2a*$^{-/-}$ ventricles at 96 hpci and compared it to *emilin2a*$^{+/+}$ ventricles. I found that *cxcl8a* expression is significantly reduced in *emilin2a*$^{-/-}$ ventricles which lacked *emilin2a* expression (**Figure 4.21 A**). Moreover, when I overexpressed *emilin2a* using the *Tg(hsp70l:emilin2a)* line, I detected a significant increase in *cxcl8a* expression at 96 hpci (**Figure 4.21 B**).

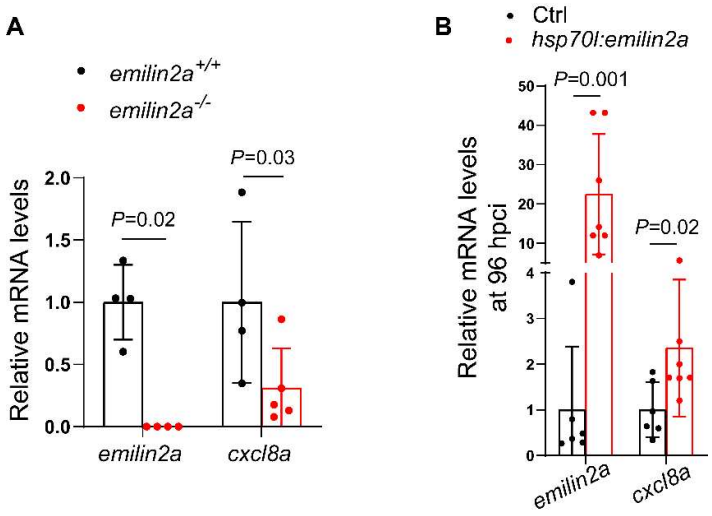

Figure 4.21: Emilin2a induces *cxcl8a* expression after cardiac injury in zebrafish. A. RT-qPCR analysis of mRNA expression of *emilin2a* and *cxcl8a* in *emilin2a*$^{-/-}$ ventricles normalized to *emilin2a*$^{+/+}$ hearts at 96 hpci (n=4-5). **B.** RT-qPCR analysis of mRNA expression of *emilin2a* and *cxcl8a* at 96 hpci in *Tg(hsp70l:emilin2a)* ventricles (n=7) normalized to non-

transgenic sibling (Ctrl) ventricles (n=6). Statistical tests: Non-parametric Mann-Whitney test **(A,B)**. [Adapted and reprinted with permission from (El-Sammak et al., 2022)]

These results suggest that Emilin2a induces *cxcl8a* expression in regenerating zebrafish ventricles and that *cxcl8a* might play a role in cardiac regeneration.

4.7. *cxcl8a* is required for cardiac regeneration in zebrafish

4.7.1. *cxcl8a* is expressed in epicardium-derived cells during cardiac regeneration

The observation that Emilin2a induces the expression of *cxcl8a* after cardiac injury in zebrafish made me hypothesize that Cxcl8a might be playing a role in regulating coronary proliferation during cardiac regeneration in zebrafish. I first set out to detect which cell type(s) might be expressing *cxcl8a* during cardiac regeneration in zebrafish. I performed *in situ* hybridization on heart sections and found that *cxcl8a* is expressed at 96 hpci at the periphery of the injury where cECs and EPDCs are found (**Figure 4.22 A**). To confirm the source of the signal, I sorted cECs and EPDCs before and after injury. I could not detect *cxcl8a* expression in cECs, but detected a significant upregulation of *cxcl8a* expression in EPDCs at 96 hpci (**Figure 4.22 B-D**). To confirm that *cxcl8a* acts downstream of Vegfc, I examined the expression of *cxcl8a* in *Tg(hsp70l:sflt4)* ventricle, and found that *cxcl8a* expression is significantly downregulated when blocking Vegfc signaling (**Figure 4.22 E**). Conversely, when I injected *vegfc* mRNA into zebrafish embryos at one-cell stage, *cxcl8a* was highly upregulated at 48 hpf (**Figure 4.22 F**).
These findings suggest that downstream of Vegfc signaling, Emilin2a promotes *cxcl8a* expression in EPDCs during cardiac regeneration in zebrafish.

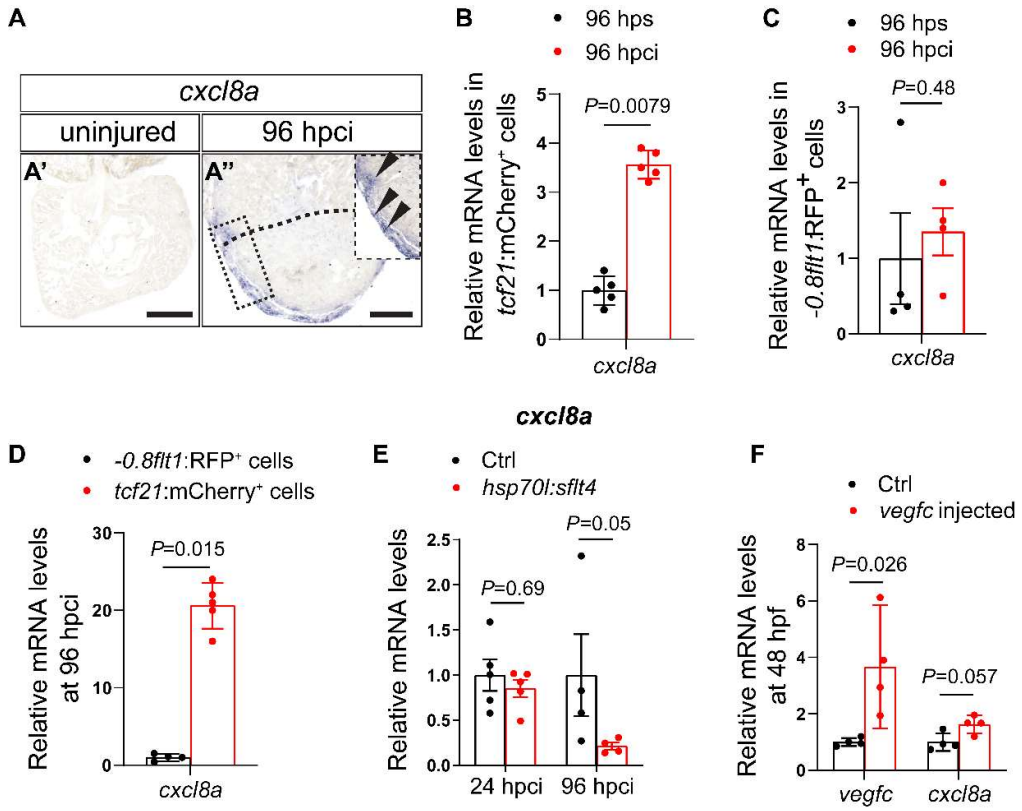

Figure 4.22: *cxcl8a* expression pattern during cardiac regeneration in zebrafish. **A.** *in situ* hybridization for *cxcl8a* expression on paraffin sections of uninjured **(A')** and 96 hpci **(A'')** hearts. Arrowheads point to *cxcl8a* expression. **B.** RT-qPCR analysis of mRNA expression of *cxcl8a* in sorted *tcf21*:mCherry^{+} (EPDCs) (n=5) at 96 hpci normalized to 96 hps. **C.** RT-qPCR analysis of mRNA expression of *cxcl8a* in sorted *-0.8flt1*:RFP^{+} cells (cECs) at 96 hpci (n=4) normalized to sham-operated ventricles (96 hps) (n=4). **D.** RT-qPCR analysis of mRNA expression of *cxcl8a* in sorted *tcf21*:mCherry^{+} cells (EPDCs) (n=5) at 96 hpci normalized to sorted *-0.8flt1:*RFP^{+} cells (cECs) (n=4). **E.** RT-qPCR analysis of mRNA expression of *cxcl8a* at 24 and 96 hpci in *Tg(hsp70l:sflt4)* hearts (n=4-5) normalized to non-transgenic (Ctrl) hearts (n=4-5). **F.** RT-qPCR analysis of mRNA expression of *vegfc* and *cxcl8a* at 48 hpf following the injection at the one-cell stage of 75 pg of *vegfc* mRNA (n=4) normalized to uninjected embryos (Ctrl) (n=4). Black **(A)** dotted lines mark the injured area. Statistical test: Non-parametric Mann-Whitney test **(B,C,D,E,F)**. [Adapted and reprinted with permission from (El-Sammak et al., 2022)]

4.7.2. *cxcl8a* mutants display impaired cardiac regeneration phenotype

To understand the role of *cxcl8a* during cardiac regeneration, a *cxcl8a* mutant was generated using the CRISPR-Cas9 technology, targeting exon 3 (**Figure 4.23 A,B**).

In silico analysis predicts that this mutation results in the deletion of 31 amino acids in the C-terminal domain responsible for dimerization of Cxcl8a and its binding to the receptors (Clark-Lewis et al., 1991).

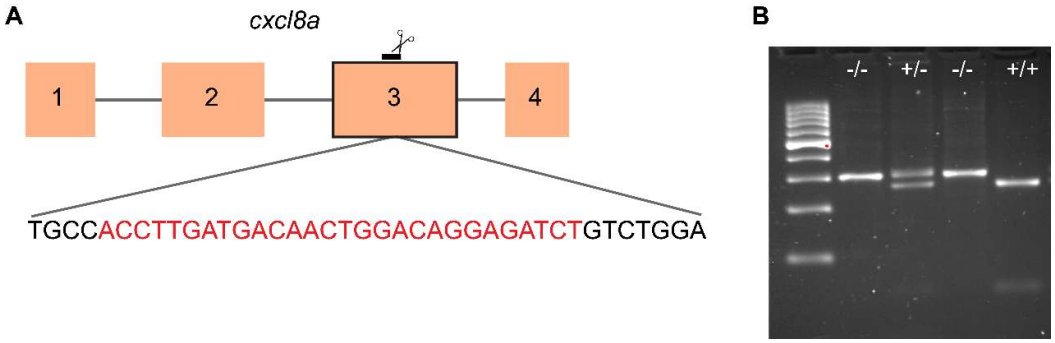

Figure 4.23: Generation of *cxcl8a* mutant.

A. Schematic representation of the *cxcl8a* gene showing the deleted bases in red. **B.** DNA gel electrophoresis assay used to genotype the *cxcl8a* mutation; DNA ladder = 100 bp. [Adapted and reprinted with permission from (El-Sammak et al., 2022)]

I performed cryoinjuries on *cxcl8a*$^{+/+}$ and *cxcl8a*$^{-/-}$ ventricles and analyzed cEC proliferation at 96 hpci. I found that *cxcl8a*$^{-/-}$ ventricles exhibit a significant reduction in cEC proliferation (**Figure 4.24 A,B**). Furthermore, they also exhibited reduced coronary coverage at 7 dpci while lacking ventricular lymphatics (**Figure 4.24 C-E**).

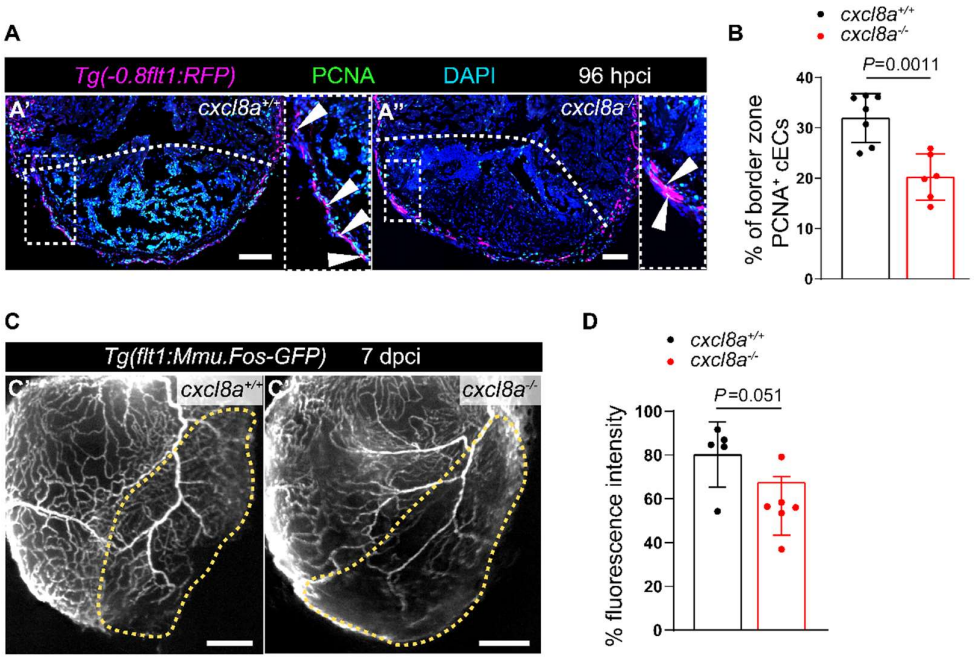

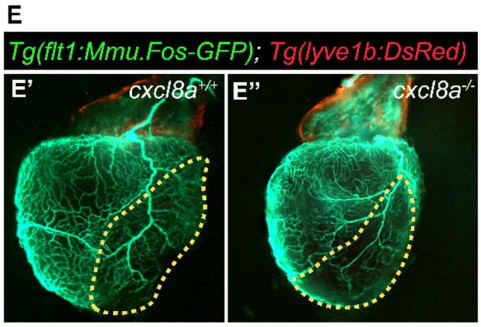

Figure 4.24: *cxcl8a* is important for coronary revascularization in the absence of ventricular lymphatics.

A. Sections of cryoinjured hearts of *Tg(flt1:Mmu.Fos-GFP); cxcl8a*$^{+/+}$ **(A')** and *Tg(flt1:Mmu.Fos-GFP); cxcl8a*$^{-/-}$ **(A'')** sibling zebrafish at 96 hpci immunostained for GFP (coronaries, magenta), PCNA (proliferation marker, green), and DNA (DAPI, blue). Arrowheads point to PCNA^{+} cECs. **B.** Percentage of PCNA^{+} cECs in the injured tissue and border zone of *cxcl8a*$^{+/+}$ (n=7) and *cxcl8a*$^{-/-}$ (n=6) hearts at 96 hpci. **C.** Wholemount images of hearts of *Tg(flt1:Mmu.Fos-GFP); cxcl8a*$^{+/+}$ **(C')** and *Tg(flt1:Mmu.Fos-GFP); cxcl8a*$^{-/-}$ **(C'')** zebrafish at 7 dpci. **D.** Percentage of GFP fluorescence intensity in the injured tissue of *Tg(flt1:Mmu.Fos-GFP); cxcl8a*$^{+/+}$ (n=5) and *Tg(flt1:Mmu.Fos-GFP); cxcl8a*$^{-/-}$ (n=6) hearts at 7 dpci. **E.** Wholemount images of hearts of 7 dpci *Tg(flt1:Mmu.Fos-GFP); Tg(lyve1b:DsRed); cxcl8a*$^{+/+}$ **(E')** and *Tg(flt1:Mmu.Fos-GFP); Tg(lyve1b:DsRed); cxcl8a*$^{-/-}$ **(E'')** sibling zebrafish. White **(A)**, orange **(C,E)** dotted line mark the injured area. Statistical tests: Student's t-test **(B)**, Non-parametric Mann-Whitney test **(D)**. Scale Bars: 100 µm **(A)**, 200 µm **(C)**. [Adapted and reprinted with permission from (El-Sammak et al., 2022)]

Notably, when I examined the scar resolution in these mutants, I observed that while *cxcl8a*$^{-/-}$ ventricles showed a slightly larger scar in comparison to sibling ventricles at 30 dpci (**Figure 4.25 A,B**), they retained a much larger scar at 90 dpci (**Figure 4.25 C,D**). Altogether, these findings indicate that Cxcl8a plays an important role in coronary revascularization during cardiac regeneration in zebrafish.

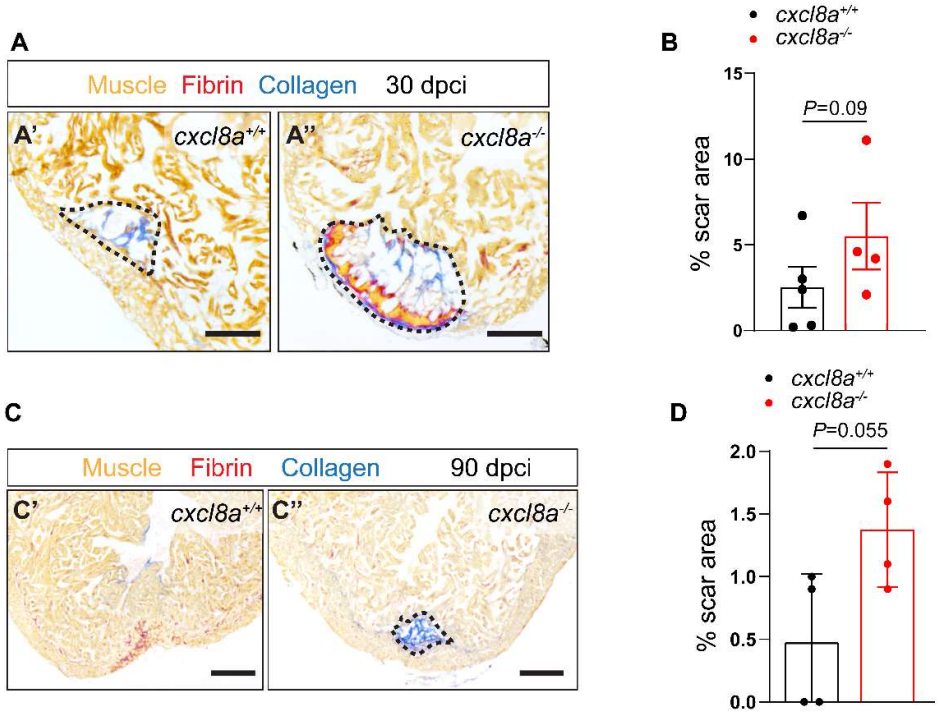

Figure 4.25: *cxcl8a* is required for cardiac regeneration in zebrafish.

A. A.F.O.G staining of cryosections of *cxcl8a*$^{+/+}$ **(A')** and *cxcl8a*$^{-/-}$ **(A'')** hearts at 30 dpci. Orange: Muscle, red: Fibrin, blue: Collagen. **B.** Percentage of scar area normalized to ventricular area in *cxcl8a*$^{+/+}$ (n=5) and *cxcl8a*$^{-/-}$ (n=4) hearts at 30 dpci. **C.** A.F.O.G staining of cryosections of *cxcl8a*$^{+/+}$ **(C')** and *cxcl8a*$^{-/-}$ **(C'')** hearts at 90 dpci. Orange: Muscle, red: Fibrin, blue: Collagen. **D.** Percentage of scar area normalized to ventricular area in *cxcl8a*$^{+/+}$ (n=5) and *cxcl8a*$^{-/-}$ (n=4) hearts at 90 dpci. Black **(A,C)** dotted lines mark the injured area. Statistical tests: Student's t-test **(B,D)**. Scale Bars: 200 µm **(A,C)**. [Adapted and reprinted with permission from (El-Sammak et al., 2022)]

4.8. Cxcl8a signals through Cxcr1 receptors to promote cardiac regeneration in zebrafish

4.8.1. *cxcr1* is expressed in regenerating coronary endothelial cells

The findings that *cxcl8a* is expressed in EPDCs during cardiac regeneration and that the mutants exhibit a reduction in coronary revascularization made me reason that the receptor(s) activated by Cxcl8a is/are expressed in coronaries. To test this possibility, I sorted cECs before and after injury using the *Tg(-0.8flt1:RFP)* line. I analyzed the expression of both receptors, *cxcr1* and *cxcr2* by RT-qPCR, and found that *cxcr1* is significantly upregulated in coronaries after injury, while *cxcr2* expression was almost

non-detectable (**Figure 4.26 A**). Furthermore, I performed *in situ* hybridization of *cxcr1* on heart sections and was able to confirm that indeed *cxcr1* is expressed in coronaries during cardiac regeneration (**Figure 4.26 B**).

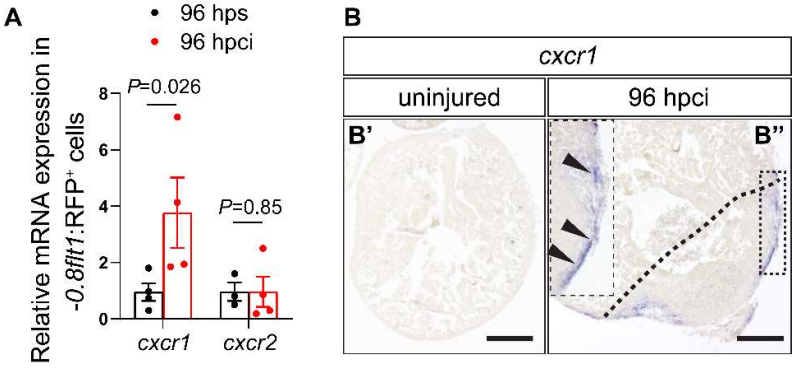

Figure 4.26: *cxcr1* is expressed in regenerating coronary endothelial cells. A. RT-qPCR analysis of mRNA expression of *cxcr1* and *cxcr2* in sorted *-0.8flt1*:RFP^{+} cells (cECs) (n=3-4) at 96 hpci normalized to 96 hps. **B.** *in situ* hybridization for *cxcr1* expression on paraffin sections of uninjured **(B')** and 96 hpci **(B'')** hearts. Arrowheads point to *cxcr1* expression. Black **(B)** dotted lines mark the injured area. Statistical tests: Non-parametric Mann-Whitney test **(A)**. Scale Bars: 200 µm **(B)**. [Adapted and reprinted with permission from (El-Sammak et al., 2022)]

4.8.2. *cxcr1* mutants exhibit impaired coronary revascularization and scar resolution following cardiac injury

To investigate if Cxcr1 signaling is at play during coronary revascularization, I used a pharmacological inhibitor (SB225002) to block Cxcr1 signaling (White et al., 1998). I performed IP-injections of the inhibitor in *Tg(-0.8flt1:RFP)* zebrafish and used DMSO as a control. I analyzed the coronary coverage at 7 dpci, and found a significant reduction when blocking Cxcr1 signaling (**Figure 4.27 A,B**). Since SB225002 blocks both Cxcr1 and Cxcr2, I performed cardiac cryoinjuries on *cxcr1*$^{-/-}$ ventricles to delineate the role of *cxcr1* specifically. cEC proliferation at 96 hpci and the coronary coverage at 7 dpci were significantly reduced in *cxcr1*$^{-/-}$ ventricles (**Figure 4.27 C-F**).

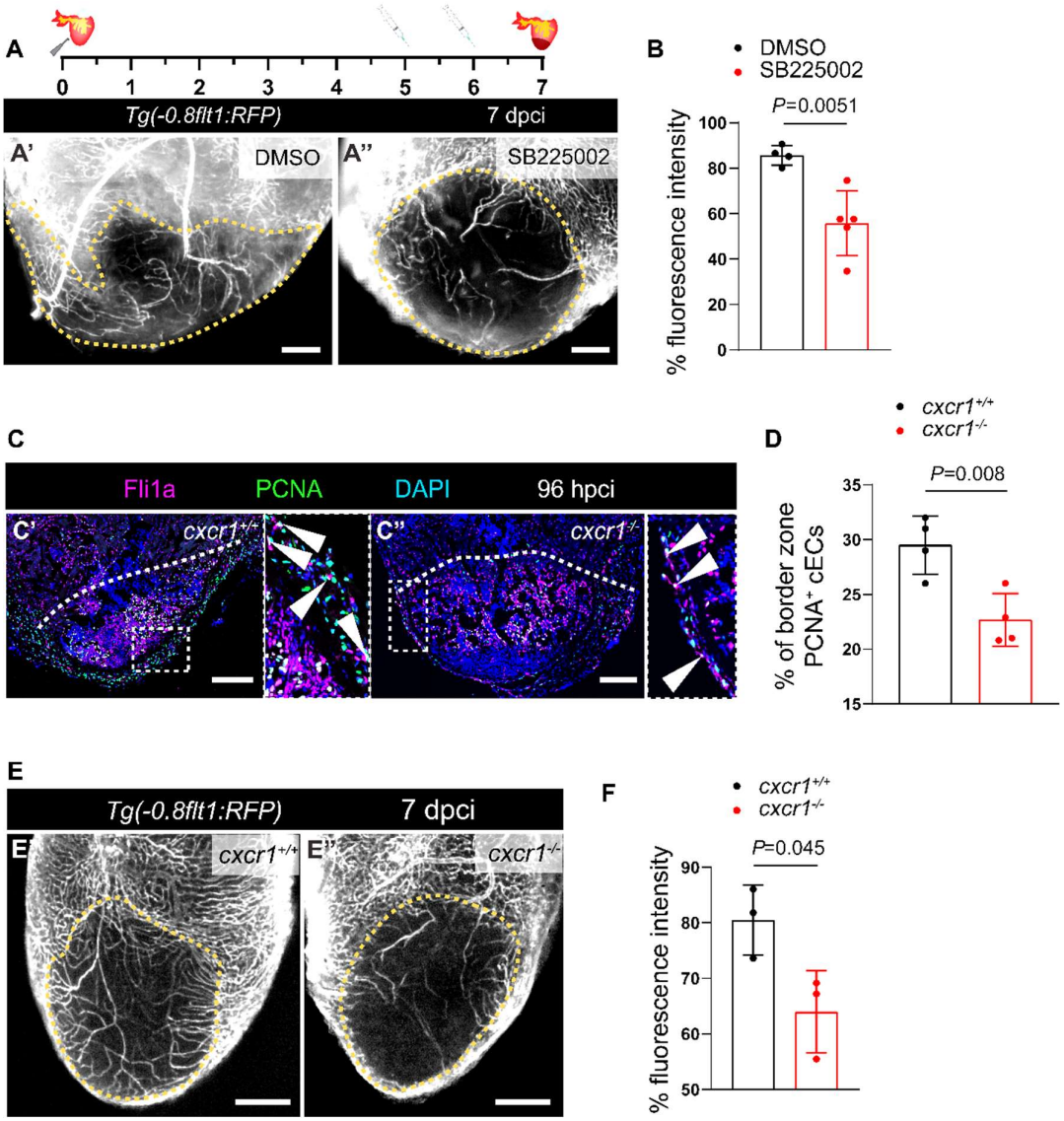

Figure 4.27: Cxcl8a-Cxcr1 signaling is required for revascularization after cardiac injury in zebrafish.

A. Illustration of intraperitoneal injections of DMSO or 0.01 mM SB225002 and cardiac cryoinjury. Wholemount images of 7 dpci *Tg(0.8flt1:RFP)* zebrafish hearts following injections with DMSO as control **(A')** or 0.01 mM SB225002 **(A'')**. **B.** Percentage of RFP fluorescence intensity in the injured tissue of 7 dpci *Tg(-0.8flt1:RFP)* hearts after injections with DMSO (n=4) or SB225002 (n=5). **C.** Sections of cryoinjured hearts of *cxcr1*$^{+/+}$ **(C')** and *cxcr1*$^{-/-}$ **(C'')** sibling zebrafish at 96 hpci immunostained for Fli1a (endothelial cells, magenta), PCNA (proliferation marker, green), and DNA (DAPI, blue). Arrowheads point to PCNA^{+} cECs. **D.** Percentage of PCNA^{+} cECs in the injured tissue and border zone of *cxcr1*$^{+/+}$ (n=4) and *cxcr1*$^{-/-}$ (n=4) ventricles at 96 hpci. **E.** Wholemount images of hearts of *Tg(-0.8flt1:RFP); cxcr1*$^{+/+}$ **(E')** and *Tg(-0.8flt1:RFP); cxcr1*$^{-/-}$ **(E'')** sibling zebrafish at 7 dpci. **F.** Percentage of RFP fluorescence

intensity in the injured tissue of *Tg(-0.8flt1:RFP); cxcr1*$^{+/+}$ (n=3) and *Tg(-0.8flt1:RFP); cxcr1*$^{-/-}$ (n=3) hearts at 7 dpci. Orange **(A,E)** and white **(C)** dotted lines mark the injured area. Statistical tests: Student's t-test **(B,D,F)**. Scale bars: 200 µm **(C,E)**, 100 µm **(A)**. [Adapted and reprinted with permission from (El-Sammak et al., 2022)]

To test if *cxcr1* is important for muscle regeneration, I extracted *cxcr1*$^{+/+}$ and *cxcr1*$^{-/-}$ injured ventricles at 30 and 90 dpci to analyze the scar size. Although the scar size of *cxcr1*$^{-/-}$ ventricles were comparable to their *cxcr1*$^{+/+}$ siblings (**Figure 4.28 A,B**), *cxcr1*$^{-/-}$ ventricles retained a much larger scar at 90 dpci (**Figure 4.28 C,D**).

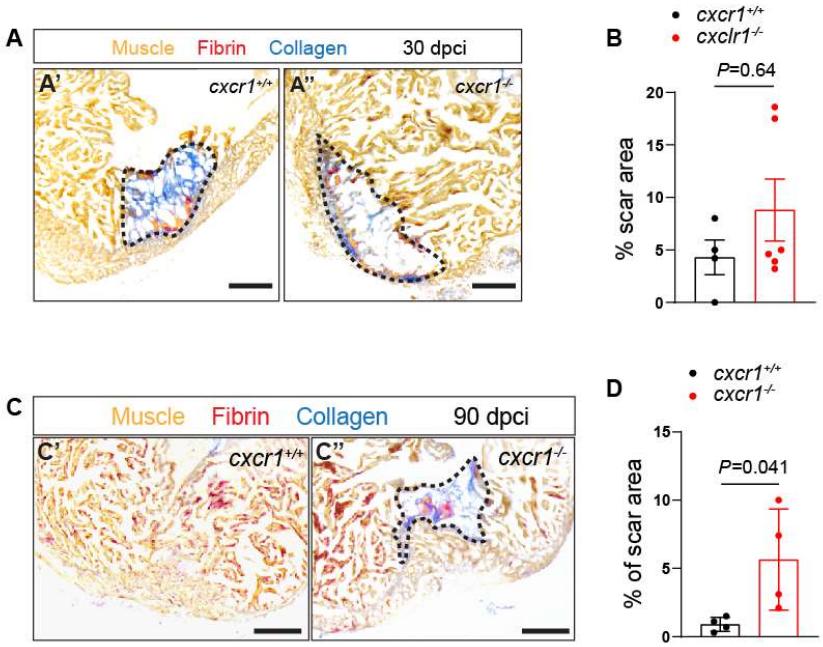

Figure 4.28: Cxcr1 signaling is required for cardiac regeneration in zebrafish.
A. A.F.O.G staining of cryosections of *cxcr1*$^{+/+}$ **(A')** and *cxcr1*$^{-/-}$ **(A'')** hearts at 30 dpci. Orange: Muscle, red: Fibrin, blue: Collagen. **B.** Percentage of scar area normalized to ventricular area in *cxcr1*$^{+/+}$ (n=4) and *cxcr1*$^{-/-}$ (n=6) hearts at 30 dpci. **C.** A.F.O.G staining of cryosections of *cxcr1*$^{+/+}$ **(C')** and *cxcr1*$^{-/-}$ **(C'')** hearts at 90 dpci. Orange: Muscle, red: Fibrin, blue: Collagen. **D.** Percentage of scar area normalized to ventricular area in *cxcr1*$^{+/+}$ (n=4) and *cxcr1*$^{-/-}$ (n=4) ventricles at 90 dpci. Black **(A,C)** dotted lines delineate the injured tissue. Statistical tests: Student's t-test **(B,D)**. Scale Bars: 200 µm **(A,C)**. [Adapted and reprinted with permission from (El-Sammak et al., 2022)]

Altogether these findings suggest that Cxcl8a-Cxcr1 signaling is essential for coronary revascularization in zebrafish, and that downstream of Vegfc signaling, Emilin2a

promotes Cxcl8a-Cxcr1 signaling to facilitate a crosstalk between EPDCs and cECs to enhance cardiac regeneration in zebrafish.

4.9. Proposed model

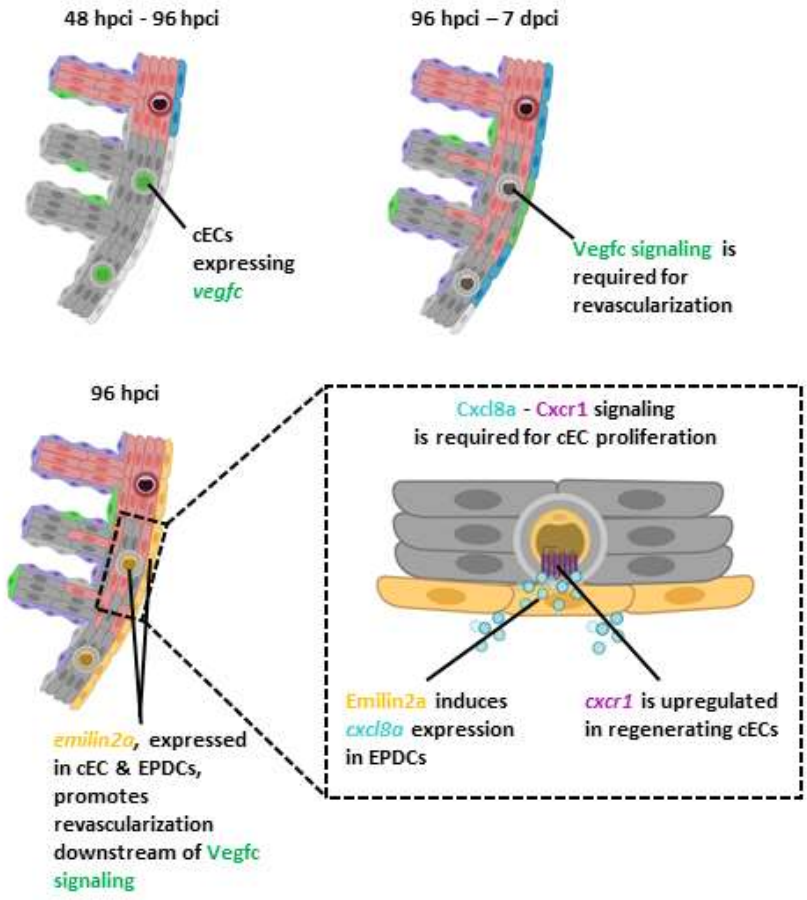

Figure 4.29: Proposed model describing the role of Vegfc signaling during cardiac regeneration in zebrafish.

vegfc is expressed in coronaries during cardiac regeneration. Vegfc promotes coronary revascularization by inducing *emilin2a* expression in EPDCs. Emilin2a acts as a pro-regenerative molecule that enhances cardiac regeneration. Mechanistically, Emilin2a promotes *cxcl8a* expression in EPDCs. Cxcl8a signals to regenerating coronaries via Cxcr1 receptors to facilitate revascularization and cardiac regeneration in zebrafish. [Adapted and reprinted with permission from (El-Sammak et al., 2022)]

5. DISCUSSION

Note: Parts of this section have been published as an article in the journal *Circulation Research*.

[**El-Sammak, H.**, Yang, B., Guenther, S., Chen, W., Marín-Juez, R., and Stainier, D.Y.R. (2022). A Vegfc-Emilin2a-Cxcl8a Signaling Axis Required for Zebrafish Cardiac Regeneration. Circ. Res. *130*, 1014–1029.]

5.1. The role of coronary endothelial cells following cardiac damage

Over the last years, the view of coronaries has changed from being merely blood vessels that supply the heart with nutrients and oxygenated red blood cells, to tools that are instrumental for the heart's development and its regeneration. One of the main factors that influence the poor regenerative potential of the adult mammalian heart is its inability to revascularize the injured tissue (Kocijan et al., 2021). Improving collateral artery formation in adult mammals improves cardiac function following injury (Das et al., 2019). Indeed, a recent study has shown that VEGFA-VEGFR2 signaling is important for cardiac growth. Deleting *Vegfr2* results in a reduction in coronary endothelial cell (cEC) and cardiomyocyte (CM) proliferation. Conversely, overexpressing *Vegfr2* increased cEC density and enhanced cardiac regeneration (Debenedittis et al., 2021). Moreover, stabilizing vessel-like structures in medaka, a fish species without cardiac regenerative capacity resulted in a reduction in scarring following cardiac injury (Lai et al., 2017).

In the same line of observations, the regenerative zebrafish heart, mounts a fast angiogenic response following injury to revascularize the damaged tissue, which is vital to support cardiac regeneration (Marín-Juez et al., 2016). Following cardiac injury, pre-existing cECs proliferate to give rise to new cECs and invade the injured area (Marín-Juez et al., 2016, 2019). Coronaries sprout superficially, i.e. along the surface of the ventricle, and intraventricularly intro the lumen (Marín-Juez et al., 2019). To date, no reports have indicated that endocardial cells give rise to cECs during coronary revascularization in zebrafish, however the endocardium is a source of Vegfaa signaling that is essential for intraventricular sprouting during this process (Marín-Juez et al., 2019). Blocking this process impairs cardiac regeneration and results in permanent fibrotic scarring (Marín-Juez et al., 2016, 2019). The observation

that improving coronary revascularization enhances cardiac regeneration motivated researchers to identify factors that promote this process.

Studies by Lai et al., and Lien et al., show that *vegfc* is upregulated following cardiac injury in zebrafish (Lai et al., 2017; Lien et al., 2006), but the role of Vegfc in regulating revascularization during cardiac regeneration is not yet known. In this project (1) I show that *vegfc* is expressed in coronaries after cardiac damage and that Vegfc signaling is essential for cardiac regeneration, (2) I identify *emilin2a* as a downstream target gene of Vegfc signaling. Moreover, (3) I show that Emilin2a is required for and can promote cardiac regeneration. Mechanistically, I found that (4) Emilin2a orchestrates a cross-talk between epicardium-derived cells and coronaries via Cxcl8a-Cxcr1 signaling to induce coronary revascularization during cardiac regeneration in zebrafish.

5.2. Vegfc is an angiocrine required for cardiac regeneration independent of lymphatics

In my PhD work, I show that Vegfc acts as an angiocrine to support cardiac regeneration in zebrafish. Angiocrines are paracrine molecules secreted by endothelial cells and have a multitude of effects on neighboring tissues (Rafii et al., 2016). Several studies have emphasized the important role of angiocrine molecules in development, tissue homeostasis, as well as repair (Rafii et al., 2016). For instance, endothelial cells (ECs) in liver sinusoids control the equilibrium between liver regeneration and fibrosis following injury injury, by the preferential stimulation of CXCR7 and CXCR4 receptors, respectively (Ding et al., 2014). Similarly, pulmonary capillary ECs secrete angiocrine factors after pneumonectomy, including MMP14 to promote regeneration of alveolar epithelial cells (Ding et al., 2011). Interestingly, it has been shown that VEGFC secreted by ECs induces neural stem cell proliferation in various contexts (Le Bras et al., 2006; Han et al., 2015).

The role of ECs extends in the heart during development and regeneration. It has been recently shown that the angiocrine molecule COL15A1 promotes CM proliferation in mice (Rhee et al., 2021). In zebrafish, the two endothelial compartments; the endocardium and coronaries play a vital role during heart development (Qi et al., 2022; Rasouli and Stainier, 2017) and regeneration (Kikuchi et al., 2011a; Lepilina et al., 2006; Marín-Juez et al., 2019; Münch et al., 2017).

In line with my findings that *vegfc* is expressed in cECs during cardiac regeneration in zebrafish, a previous study revealed that *Vegfc* is expressed in ECs in neonatal mice after cardiac injury, further confirming that Vegfc acts as an angiocrine following cardiac injury in regenerative settings (Quaife-Ryan et al., 2017). On the other hand, it has been very recently reported that macrophages are a source of VEGFC following cardiac injury in adult mice (Glinton et al., 2022). It would be interesting to investigate if VEGFC from different cellular sources contribute to a pleiotropic role to promote cardiac regeneration following injury.

Blocking Vegfc signaling caused defective coronary revascularization, as well as reduced CM dedifferentiation and proliferation. My findings suggest that Vegfc is not likely to signal directly to CMs. Hence, I hypothesize that the reduction in CM dedifferentiation and proliferation are secondary effects due to reduced coronary revascularization. Our group has previously shown that coronaries act as a scaffold to support CM development and regeneration (Marín-Juez et al., 2019). All of these findings support the idea that coronaries play a vital role in supporting cardiac regeneration in zebrafish and that Vegfc signaling is essential in this process. However, one cannot completely rule out the possibility that there might be direct Vegfc signaling in CMs to an extent. This possibility can be tested only by tissue specific loss-of-function approaches.

Vegfc signaling block resulted in the retention of a permanent fibrotic scar, similar to non-regenerative models such as medaka or adult mice. These observation are in line with previous studies reporting the importance of Vegfc signaling in cardiac regeneration in zebrafish (Gancz et al., 2019; Harrison et al., 2019). It has been previously shown that VEGFC is required for coronary development in mice (Chen et al., 2014a, 2014c). *Vegfc* knock out mice displayed defective coronary development and branching (Chen et al., 2014a). This observation and my results showing the significance of Vegfc in coronary revascularization in zebrafish suggests a role for VEGFC in promoting collateral formation following myocardial infarction in mammals. It would be interesting to test if overexpressing *Vegfc* in the non-regenerative adult mouse heart can induce the formation of collaterals and aid in scar resolution following cardiac injury.

In my PhD work, I describe for the first time a role of Vegfc signaling in promoting cardiac regeneration in zebrafish in a lymphatics independent manner. Several studies have investigated the role of Vegfc in inducing lymphangiogenesis during development as well as cardiac regeneration (Gancz et al., 2019; Le Guen et al., 2014; Harrison et al., 2019; Hogan et al., 2009a; Jeltsch et al., 1997; Klotz et al., 2015). Studies in mice have shown that injecting recombinant VEGFC promotes lymphangiogenesis in the ventricle following myocardial infarction (Klotz et al., 2015). It has been also shown that the lymphangiogenic response is necessary for the clearance of pro-inflammatory neutrophils and macrophages to help in cardiac repair (Vieira et al., 2018). Similarly in zebrafish (Gancz et al., 2019; Harrison et al., 2019), Vegfc is essential for lymphangiogenesis during cardiac regeneration which is important to clear out neutrophils (Harrison et al., 2019). To confirm that my observations are independent of lymphatics in the ventricles of 3-month-old fish, as well as when blocking Vegfc signaling, I used Qdots which provide a non-biased and reporter free visualization of lymphatics. Hence this study describes a novel role of Vegfc in promoting coronary revascularization in a lymphatic independent manner.

In zebrafish, Vegfc acts downstream of the transcription factor Hhex to promote lymphatic development (Gauvrit et al., 2018). It would be of great benefit to try to dissect the upstream regulators and stimuli that induce *vegfc* expression during cardiac regeneration and test if the same stimuli are conserved in promoting lymphangiogenesis and coronary revascularization in the heart.

5.3. Emilin2a acts as pro-regenerative molecule

To dissect the role of Vegfc signaling during cardiac regeneration in zebrafish, RNAseq was performed comparing WT ventricles and ventricles of *Tg(hsp70l:sflt4)* zebrafish at 24 hpci, and *emilin2a* was identified as a new potential target of Vegfc signaling. In this study, I show *emilin2a* is expressed in cECs and epicardium-derived cells (EPDCs), which suggests that during cardiac regeneration Vegfc signals to the same cells secreting it or to neighboring cells. Indeed, during zebrafish development, Vegfc acts in an autocrine and paracrine way to promote intersegmental vessel sprouting and venous sprouting, respectively (Villefranc et al., 2013). I hypothesize that Vegfc acts on cECs and EPDCs via Vegfr2 and Nrp1a receptors, respectively. In line with this hypothesis, a recent study has shown that *nrp1a* is expressed in EPDCs

during cardiac regeneration in zebrafish and that *nrp1a*$^{-/-}$ ventricles exhibited reduced number of cECs following injury (Lowe et al., 2019).

My findings show that not only is Emilin2a required for coronary revascularization, but also acts as a pro-angiogenic molecule during cardiac regeneration. These results goin line with previous studies reporting an angiogenic role of EMILIN2 by activating EGFR in HUVECs (Andreuzzi et al., 2020; Marastoni et al., 2014; Paulitti et al., 2018). Interestingly EMILIN2 promotes angiogenesis in tumors while inhibiting the migration of cancer cells (Mongiat et al., 2010), suggesting that it has a cell-specific role.

Notably, overexpressing *emilin2a* also enhanced the regeneration response in zebrafish. On the other hand, *emilin2a* is not expressed in non-regenerative models such as medaka as well as in adult mouse hearts following cardiac injury (Lai et al., 2017; Quaife-Ryan et al., 2017). Furthermore, *EMILIN2* expression was induced in HUVECs after a scratch, suggesting that EMILIN2 might be required for EC migration. I also showed that *EMILIN2* is an effector of VEGFC signaling in HUVECs. These findings and observations suggest a pro-regenerative role of Emilin2a, and that VEGFC-EMILIN2 signaling axis is conserved in human ECs, hence supporting future studies into the role of VEGFC and EMILIN2 in patients following myocardial infarction. It would indeed be very interesting to test if overexpressing *Emilin2* can enhance regeneration in adult mouse hearts following myocardial infarction.

5.4. Vegfc signaling modulates an ECM milieu necessary for cardiac regeneration

Besides *emilin2a*, 20 genes that were differentially expressed in *Tg(hsp70l:sflt4)* ventricles encode for extra cellular matrix (ECM) proteins. The role of ECM molecules in regulating several aspects of cardiac development and regeneration has been highlighted in several studies (Rienks et al., 2014). For instance, a recent study has shown that the ECM molecule Agrin can improve the cardiac output and promote cardiac regeneration in non-regenerative adult mouse hearts as well as in pigs following myocardial infarction (Baehr et al., 2020; Bassat et al., 2017). Several ECM molecules are also essential in regulating the division and proliferation of CMs (Wu et al., 2020). ECM molecules are also vital in regulating angiogenesis in different contexts (Mongiat et al., 2016). For instance, several proteoglycans have been shown to promote angiogenesis in cancer cells by interacting with different growth factors

including VEGFA, FGF2, FGF7, FGF9 and PDGF (Mongiat et al., 2016). Interestingly, *prelp,* one of the genes encoding for a proteoglycan is downregulated in *Tg(hsp70l:sflt4)* ventricles. In addition, one of the ECM genes downregulated in *Tg(hsp70l:sflt4)* ventricles is *fibronectin* (*fn1b*). It has been previously shown that fibronectin is essential for cardiac regeneration in zebrafish (Wang et al., 2013). In addition, fibronectin has also been implicated with angiogenesis (Astrof and Hynes, 2009; Chiu et al., 2012; Zhou et al., 2008), as blocking fibronectin polymerization impairs EC proliferation and tube formation (Zhou et al., 2008).

In this study, I hypothesize that Vegfc signaling promotes coronary revascularization by providing a permissive extracellular environment that facilitates cardiac regeneration. This study also puts emphasis on the importance of understanding the ECM composition and how fine tuning of these component in adequate levels could have beneficial therapeutic outcome.

5.5. Vegfc signaling orchestrates a coronary-epicardial crosstalk in cardiac regeneration via Cxcl8a-Cxcr1 signaling

Similar to HUVECs and gastric cancer cells (Andreuzzi et al., 2020; Paulitti et al., 2018), I showed in this study that Emilin2a induces the expression of the pro-inflammatory chemokine *cxcl8a* in EPDCs. One hypothesis how the extracellular Emilin2a induces *cxcl8a* expression is by binding and activating Egfr (Paulitti et al., 2018). Indeed previous transcriptomic analyses show that receptor *egfr* is expressed in EPDCs (Sánchez-Iranzo et al., 2018). However, experiments including immunostaining of Emilin2a and Egfr as well as Co-IP are needed to confirm this hypothesis.

In this study, I show that Cxcl8a is required for coronary proliferation during cardiac regeneration in zebrafish. These results are in line with previous studies reporting an angiogenic role of CXCL8 (Heidemann et al., 2003; Koch et al., 1992; Li et al., 2003; Matsuo et al., 2009; Shi and Wei, 2016; Strieter et al., 1992). Besides its role in promoting EC proliferation and migration, CXCL8 is a pro-inflammatory chemokine that has various implications with wound healing, especially neutrophil trafficking after an injury (Fox et al., 2005; Matsuo et al., 2009; S.T. et al., 2010). In zebrafish, Cxcl8a is a regulator of neutrophil recruitment and retraction by activating the G-protein coupled receptors, Cxcr1 and Cxcr2 (De Oliveira et al., 2016; Powell et al., 2017).

The findings presented in my PhD work suggest a cross-talk between cECs and EPDCs mediated by Cxcl8a-Cxcr1 signaling. It has been previously shown that in the context of cardiac regeneration, epicardial cells upregulate the expression of factors relevant to CM proliferation and coronary revascularization (Lepilina et al., 2006). Several studies have shown that retinoic acid from epicardium (and endocardium) is essential for CM proliferation in zebrafish (Kikuchi et al., 2011a) and in the mouse heart (Bilbija et al., 2012) following cardiac injury. Importantly, a recent study by Marín-Juez has shown that EPDCs closely interact with cECs via Cxcl12b-Cxcr4a signaling to promote coronary revascularization (Marín-Juez et al., 2019). Similar observation on these intercellular communication between EPDCs and other cells in the heart is also observed in mice (Virag et al., 2007; Zhou et al., 2011).

In view of the observations that CXCL8 signaling regulates neutrophil trafficking (Fox et al., 2005; Matsuo et al., 2009; S.T. et al., 2010) and that VEGFC is expressed in part in macrophages in the mouse heart following MI (Glinton et al., 2022), it would be interesting to test if VEGFC can mediate cellular interactions between immune cells and coronaries and how these interactions could affect the regenerative outcome following cardiac injury. I speculate that VEGFC plays a pleiotropic role during cardiac regeneration, and that it can modulate immune cells and their interactions with coronaries to promote revascularization. The concept of immune cell-mediated angiogenesis has been previously discussed in different contexts. For instance, a study by Gerri and colleagues has shown that macrophages play an important role in promoting angiogenesis in the developing zebrafish embryo via Hif1α (Gerri et al., 2017). Importantly, the role of macrophages in promoting angiogenesis following MI , as well as enhancing scar resolution has been previously reported (Ferraro et al., 2019; Guo et al., 2018). The angiogenic role of macrophages has been mostly associated with anti-inflammatory M2 macrophages (Jetten et al., 2014). Besides macrophages, angiogenesis has also been associated with neutrophils in tumors via several signaling pathways and cytokines including CXCL8 (Kolaczkowska and Kubes, 2012; Tazzyman et al., 2009). Neutrophils also mediate inflammatory induced angiogenesis in corneas (Gong and Koh, 2010). However, the role of neutrophils in promoting revascularization in the heart has not been investigated before. It would be interesting to test if downstream of Vegfc signaling, Cxcl8a can regulate neutrophils and their interactions with coronaries. Neutrophils are often associated with a pro-

inflammatory phase following tissue injury. Another interesting point would be to test if there are differences between pro- and anti-inflammatory mediated angiogenesis in the context of cardiac regeneration, could these differences lead to a diversity in coronaries with respect to endothelial cell plasticity, leakage and maturity.

5.6. Future Outlook

This study emphasizes the important role of angiocrine molecules in modulating an ECM milieu permissive of coronary revascularization. It also highlights the importance of intercellular communication between different cells types to promote cardiac regeneration. Several questions remain open and addressing them would be of great benefit to the cardiac regeneration field. It would be interesting to know if *vegfc* is expressed in a specific subtype of cECs, and how cEC heterogeneity contributes to revascularization. The role of perivascular cells in cardiac regeneration in zebrafish has stared gaining attention (Kapuria et al., 2022), and future studies about these cell types would add to our understanding of the cardiac vascular network, its maturity and stability, and how we can utilize these parameters to promote cardiac regeneration. The role of ECM in development as well as in regeneration has gained increasing attention over the last years. It would be of great value to dissect the ECM composition in the regenerating zebrafish heart, and test how manipulating these components could benefit the adult mammalian heart. Another interesting idea would be to test if Vegfc signaling regulates immune cells and modulate their interaction with coronaries. In a more general view, further studies on the cellular and molecular interactions between immune cells and ECs in the heart can help us gain a deeper understanding on the various factors that modulate coronary revascularization and how we can manipulate these interactions to promote cardiac regeneration. Lastly, the main aim of understanding all of these different factors and pathways is to ultimately promote CM regeneration. With endothelial cells being one of the most abundant and heterogeneous cell types in the heart, investigations on how the different endothelial compartments (i.e. endocardium, coronaries and lymphatics) affect different aspects of CM including proliferation, dedifferentiation, maturation and protrusion will help us devise precise and better therapeutic approaches to enhance the regeneration of the adult mammalian heart following MI.

6. CONCLUSION

Following are the conclusions from my findings for each specific aim.

Aim 1: Determine the expression dynamics of *vegfc* during cardiac regeneration in zebrafish.

I show that *vegfc* acts as an angiocrine molecule that is expressed in cECs during cardiac regeneration in zebrafish and that its expression peaks at the peak of cEC proliferation, suggesting a role in coronary revascularization.

Aim 2: Investigate the role of Vegfc signaling during cardiac regeneration.

Using loss-of-function tools, I found that Vegfc signaling is essential for coronary revascularization, and that a blockade in Vegfc signaling resulted in reduced CM dedifferentiation and proliferation. Moreover, blocking Vegfc signaling impaired scar resolution.

Aim 3: Understand the mechanism how Vegfc regulates cardiac regeneration.

Using transcriptomic and expression analyses, I identified *emilin2a* as an effector of Vegfc signaling. Using tissue-specific gain-of-function tools, overexpressing *emilin2a* rescued the Vegfc signaling block during cardiac regeneration. Moreover, I generated new loss- and gain-of function tools, and found that Emilin2a is required for cardiac regeneration and overexpressing it promotes coronary revascularization and cardiac regeneration. I investigated in depth the mechanism how Emilin2a promotes coronary revascularization, and found that Emilin2a orchestrates an epicardial-coronary crosstalk via Cxcl8a-Cxcr1 signaling to facilitate coronary revascularization and cardiac regeneration in zebrafish.

Altogether, I propose that Vegfc signaling promotes coronary revascularization by regulating matrisome-associated factors to facilitate cardiac regeneration in adult zebrafish, with possible implications to promote cardiac regeneration in the adult mammalian heart.

7. SUMMARY

7.1. Introduction

Ischemic cardiac diseases that are caused due to blockage of coronary arteries represent the world's leading cause of death. These coronary occlusions lead to the death of the downstream tissues (Pfeffer and Braunwald, 1990), which causes the heart to undergo remodeling and replace the lost tissue with a fibrotic scar that compromises the contractile efficiency of the heart hence leading to myocardial infarction (Talman and Ruskoaho, 2016). Unfortunately, the adult mammalian heart cannot regenerate and restore the lost tissue due to several factors including the poor ability of cardiomyocytes (CMs) to enter cell cycle and divide, the presence and abundance of activated myofibroblasts which deposit fibrotic extra cellular matrix (ECM) components, as well as the poor angiogenic potential of the heart to re-perfuse the damaged tissue (Kocijan et al., 2021; Travers et al., 2016; Tzahor and Poss, 2017). Several studies have shown that increasing the revascularization capability of the heart may hold great therapeutic potential. Recent work by Das and colleagues has shown that improving collateral artery formation in adult mouse hearts led to an improvement in the cardiac output (Das et al., 2019). Along the same lines, a recent study showed that improving revascularization in adult mouse hearts enhanced CM proliferation (Debenedittis et al., 2021). All of these evidences suggest that angiogenic therapy might be key to improving the adult mammalian heart's regenerative ability. However, clinical trials have proven that injecting angiogenic factors is ineffective (Robich et al., 2011). These and other evidences motivated researchers to study coronary revascularization in model organisms that have an endogenous regenerative ability to understand the mechanisms regulating this process.

The adult zebrafish has a remarkable capability to regenerate the heart after injury (Poss et al., 2002). One of the initial responses that take place after cardiac is coronary revascularization (Marín-Juez et al., 2016). Hindering this process perturbs CM proliferation and results in the retention of a permanent fibrotic scar (Marín-Juez et al., 2016, 2019). Therefore, identifying factors that aid in this process might be of high clinical benefit.

One of the angiogenic factors that gets upregulated in response to cardiac injury in zebrafish is the vascular endothelial growth factor C (*vegfc*) (Lai et al., 2017; Lien et

al., 2006). Vegfc is a master regulator of lymphatic development in zebrafish and mice (Karaman et al., 2018; Oh et al., 1997; Secker and Harvey, 2015). Moreover, the role of Vegfc in promoting lymphangiogenesis extends to regenerative settings as well (Gancz et al., 2019; Harrison et al., 2019; Klaourakis et al., 2021; Klotz et al., 2015). It has been previously shown that injecting recombinant VEGFC induces lymphangiogenesis in the adult mouse heart, which improved clearance of immune cells and enhanced cardiac function following MI (Klotz et al., 2015; Vieira et al., 2018). Moreover, recent studies in zebrafish have shown that Vegfc is required for lymphangiogenesis following cardiac injury, and blocking this process results in increased scarring (Gancz et al., 2019; Harrison et al., 2019).

Vegfc is also essential in regulating angiogenic sprouting. In zebrafish, *vegfc* knockdown experiments revealed its important role in inducing intersegmental vessel sprouting (Le Guen et al., 2014; Villefranc et al., 2013). Moreover, VEGFC also induces microvessel sprouting in chick embryos as well as in mouse corneas (Cao et al., 1998). In the heart, the lack of *Vegfc,* resulted in defective coronary development, with reduced branching (Chen et al., 2014a, 2014c). All of these findings suggest a critical role of VEGFC in promoting angiogenesis. However, the mechanisms how VEGFC regulates coronary revascularization following cardiac injury remain unknown.

In this study, I show that *vegfc* is expressed by coronaries following cardiac injury and that it is essential for coronary revascularization and cardiac regeneration by promoting the expression of *emilin2a*. Emilin2a acts as a pro-regenerative molecule that promotes revascularization during cardiac regeneration in zebrafish. Mechanistically, Emilin2a regulates an epicardial-coronary crosstalk via Cxcl8a-Cxcr1 signaling to promote coronary revascularization during cardiac regeneration in zebrafish.

7.2. Results

7.2.1. *vegfc* is expressed in coronary endothelial cells and is required for cardiac regeneration in zebrafish

I first analyzed the expression dynamics of *vegfc* during cardiac regeneration. To this end, I performed RT-qPCR analyses and compared *vegfc* expression in cryoinjured ventricles in comparison to sham operated ones at different time points. I observed that *vegfc* is upregulated as early as 48 hours post cryoinjury (hpci) and peaks in

expression at 96 hpci (**Figure 4.1 A**). Next, to determine the cellular source of this signal, I performed *in situ* hybridization on heart sections and found that *vegfc* is specifically expressed in the injured area at the periphery of the tissue (**Figure 4.1 B**). To further analyze the source of expression, I sorted coronary endothelial cells (cECs), epicardium-derived cells (EPDCs) and CMs, and checked *vegfc* expression in these cell types after cryoinjury. Interestingly, I found that *vegfc* is expressed by cECs after cardiac injury, but not in EPDCs or CMs (**Figure 4.1 C-F**).

The observations that *vegfc* is expressed in cECs and peaks in expression at 96 hpci, when coronaries are at a peak in their proliferation (Marín-Juez et al., 2019), made me hypothesize that *vegfc* might play a role in coronary revascularization during cardiac regeneration. To test this hypothesis, I optimized and made use of the *Tg(hsp70l:sflt4)* loss-of-function line where I can overexpress the soluble form of Vegfr3 (Flt4) under a heat shock promoter, thereby blocking Vegfc signaling (**Figure 4.2**). Blocking Vegfc signaling leads to a significant reduced cEC proliferation at 96 hpci (**Figure 4.3 B,C**). Moreover, when I analyzed those hearts at 7 days post cryoinjury (dpci), when we expect coronaries to fully cover the injured area (Marín-Juez et al., 2016, 2019), I observed a significant reduction in the coronary coverage (**Figure 4.3 E,F**), further suggesting that Vegfc signaling plays an important role in coronary revascularization. Previous studies have shown that coronaries act as scaffold supporting CM regeneration (Debenedittis et al., 2021; Marín-Juez et al., 2019). Hence, I wanted to test if the reduced coronary revascularization when blocking Vegfc signaling has an effect on cardiac muscle regeneration. I analyzed CM dedifferentiation and proliferation at 7 dpci, and observed that indeed blocking Vegfc signaling led to a significant decrease in CM dedifferentiation and proliferation (**Figure 4.6 A-D**). Moreover, hearts with Vegfc signaling bloackade retained a larger scar at 90 dpci, when almost complete cardiac regeneration is expected (**Figure 4.7**). To test the possibility that the CM phenotypes are due to direct Vegfc signaling on CM, I sorted CMs before and after injury and analyzed the expression levels of *vegfr1*, *vegfr2* and *vegfr3*. I found low expression of all the three receptors in CM, further suggesting that it is unlikely that Vegfc directly signals to CMs (**Figure 4.6 E,F**). However, this possibility cannot be completely ruled out without tissue-specific loss-of-function experiments.

7.2.2. Vegfc signaling is essential for coronary revascularization in a lymphatic independent manner

Vegfc is a master regulator of lymphangiogenesis in zebrafish in developmental and regeneration contexts (Gancz et al., 2019; Harrison et al., 2019; Hogan et al., 2009a, 2009b; Küchler et al., 2006; Villefranc et al., 2013). To exclude the possibility that the *Tg(hsp70l:sflt4)* line blocked lymphatics during my experiments, I used 3-month-old fish which lack ventricular lymphatics while having an established coronary network. To confirm that 3-month-old zebrafish hearts lack lymphatics, I performed intramyocardial injections of Qdots, which are absorbed by lymphatics (Harrison et al., 2019). Indeed, I found that 3-month-old zebrafish ventricles did not clear the injected Qdots, further confirming that 3-month-old zebrafish ventricles lack a lymphatic network and that the observed reduced coronary revascularization phenotype is independent of lymphatics (**Figure 4.5 A,B**).

7.2.3. The extracellular matrix protein Emilin2a is an effector of Vegfc signaling

To better understand the mechanism how Vegfc signaling regulates coronary revascularization, RNA sequencing was performed to compare the transcriptome of WT ventricles and those of *Tg(hsp70l:sflt4)* zebrafish at 24 hpci (**Figure 4.8 A,B**). After thorough analysis and validation of several potential targets (**Figure 4.8 C-E**), one of the genes that showed a consistent downregulation in *Tg(hsp70l:sflt4)* at 24 hpci (when the RNAseq was performed) and at 96 hpci (when the reduced cEC phenotype is observed) was *emilin2a* (**Figure 4.9 A**).

I then reasoned that the reduced *emilin2a* expression in *Tg(hsp70l:sflt4)* might be due to reduced revascularization. To assess this possibility, I used the *Tg(hsp70l:dn-vegfaa)* line which exhibits reduced coronary revascularization after cardiac injury (Marín-Juez et al., 2016). I analyzed *emilin2a* expression in uninjured ventricles of WT, *Tg(hsp70:sflt4)* and *Tg(hsp70l:dn-vegfaa)* zebrafish. I observed decreased expression of *emilin2a* in uninjured *Tg(hsp70l:sflt4)* ventricles but not in *Tg(hsp70l:dn-vegfaa)* (**Figure 4.9 B**). Furthermore, I performed *vegfc* mRNA injections in one-cell stage zebrafish embryos and observed a significant upregulation of *emilin2a* expression, hence confirming that *emilin2a* is a downstream target of Vegfc signaling (**Figure 4.9 C**). Interestingly, knockdown of *VEGFC* in HUVECs led to a significant

decrease in *EMILIN2* expression (**Figure 4.9 D**), suggesting that the VEGFC-EMILIN2 signaling axis is conserved in human endothelial cells.

7.2.4. *emilin2a* is required for coronary revascularization during cardiac regeneration in zebrafish

Emilin2a is an ECM protein that has been shown to promote angiogenic sprouting *in vitro* (Paulitti et al., 2018). *emilin2a* is expressed in the dorsal aorta of developing zebrafish embryos at 24 hours post fertilization (hpf) (Milanetto et al., 2008). However, the role of Emilin2a in cardiac regeneration has not been explored yet.

I first examined the expression levels of *emilin2a* in regenerating zebrafish ventricles at several time points after injury and observed a significant upregulation in its expression at 96 hpci (**Figure 4.11 A**), overlapping with the peak of cEC proliferation (Marín-Juez et al., 2019) and *vegfc* expression (**Figure 4.1 A**). Next, by means of *in situ* hybridization on heart sections, I found that *emilin2a* is expressed in the injured area by both cECs and EPDCs (**Figure 4.11 B**). However, when comparing *emilin2a* expression in both cell types by RT-qPCR, EPDCs showed a higher increase in its expression at 96 hpci (**Figure 4.11 C-E**).

To study the role of *emilin2a* in cardiac regeneration in zebrafish, I used the CRISPR-Cas9 technology to generate a full locus *emilin2a* mutant (**Figure 4.12**). I injured *emilin2a*$^{-/-}$ ventricles and analyzed coronary revascularization at 96 hpci. *emilin2a*$^{-/-}$ ventricles exhibited a decreased cEC proliferation at 96 hpci, as well as a reduction in coronary coverage at 7 dpci, while lacking ventricular lymphatics (**Figure 4.14**). Next, I wanted to test the possibility if *emilin2a*$^{-/-}$ ventricles displayed defective cardiac regeneration. I analyzed CM proliferation and scar resolution in *emilin2a*$^{-/-}$ ventricles and their sibling WTs (**Figure 4.15 A,B**). Interestingly, *emilin2a*$^{-/-}$ ventricles displayed reduction in CM proliferation levels and retained a larger scar at 90 dpci (**Figure 4.15 E,F**). Altogether, these findings suggest that the ECM molecule Emilin2a is required for coronary revascularization and cardiac regeneration in zebrafish.

7.2.5. Emilin2a promotes cardiac regeneration

The findings that *emilin2a* acts downstream of Vegfc signaling and is required for coronary revascularization led me to reason that overexpressing *emilin2a* can rescue the reduced coronary revascularization phenotype due to the Vegfc signaling block. To test this possibility, I generated the *Tg(hsp70l:loxP-CFP-loxP-emiln2a-p2A-*

mCherry) line. Combining this line with the *TgBAC(tcf21:CreERT2)* line allows spatial and timely control over the expression of *emilin2a* in EPDCs during cardiac regeneration (**Figure 4.17**). I used the *Tg(hsp70l:sflt4)* line to block Vegfc signaling and overexpressed *emilin2a* in EPDCs. Indeed, overexpressing *emilin2a* was able to increase cEC proliferation and restore it to WT levels in *Tg(hsp70l:sflt4)* ventricles (**Figure 4.18**). Hence, overexpression of *emilin2a* in EPDCs rescued the Vegfc signaling block.

In view of these findings, I hypothesized that *emilin2a* can promote cardiac regeneration. To assess this hypothesis, I generated a global heat shock line to overexpress *emilin2a*. I analyzed several important aspects of cardiac regeneration and found that overexpressing *emilin2a* led to a profound increase in cEC proliferation at 96 hpci and increased coronary coverage at 7 dpci, while lacking lymphatics in the ventricle (**Figure 4.19**). Importantly, overexpression of *emilin2a* also led to increased CM proliferation at 7 dpci as well as reduced scar area at 30 dpci (**Figure 4.20**). Altogether, these results suggest that epicardium-derived *emilin2a* promotes cardiac regeneration downstream of Vegfc signaling.

7.2.6. Emilin2a promotes epicardial *cxcl8a* expression during cardiac regeneration

Previous studies showed that EMILIN2 stimulates the expression of the chemokine *CXCL8* to promote the proliferation and migration of endothelial cell *in vitro* (Andreuzzi et al., 2020; Paulitti et al., 2018). To gain a more mechanistic understanding into how Emilin2a promotes coronary revascularization in zebrafish, I performed RT-qPCR analysis on *emilin2a*$^{-/-}$ ventricles at 96 hpci, and detected a profound decrease in *cxcl8a* expression (**Figure 4.21 A**). Similarly, *cxcl8a* expression was upregulated upon overexpressing *emilin2a* at 96 hpci, using the *Tg(hsp70l:emilin2a)* line (**Figure 4.21 B**), suggesting that indeed, Emilin2a induces the expression of *cxcl8a* during cardiac regeneration in zebrafish. Using *in situ* hybridization on heart sections, I found that *cxcl8a* is expressed in EPDCs in the injured area (**Figure 4.22 A**). To confirm the source of *cxcl8a* signal, I analyzed *cxcl8a* expression in sorted EPDCs and cECs and observed that EPDCs express *cxcl8a* after cardiac injury, but not cECs, confirming the *in situ* hybridization findings (**Figure 4.22 B-D**). Altogether, these data suggest that Emilin2a induces epicardial *cxcl8a* expression, downstream of Vegfc siganling.

7.2.7. Cxcl8a-Cxcr1 signaling is required for coronary revascularization and cardiac regeneration in zebrafish

The pro-inflammatory chemokine Cxcl8a has been previously implicated with neutrophil recruitment and wound healing (Fox et al., 2005; De Oliveira et al., 2016). To investigate if the increased *cxcl8a* expression plays a role during cardiac regeneration, a *cxcl8a* mutant was generated targeting the dimerization and receptor binding domain (**Figure 4.23**). cEC proliferation was significantly reduced in *cxcl8a*$^{-/-}$ ventricles at 96 hpci (**Figure 4.24**). Moreover, these mutants also displayed reduced coronary coverage at 7 dpci, as well as increased scar area at 90 dpci (**Figure 4.25**). In view of the results that *cxcl8a* is expressed in EPDCs and the mutants exhibit defective coronary revascularization, I reasoned that the receptor(s) activated by Cxcl8a are expressed in cECs. Cxcl8a can bind and activate the G-protein coupled receptors Cxcr1 and Cxcr2 (Ha et al., 2017). To this end, I sorted cECs using the *Tg(-0.8flt1:RFP)* line and analyzed the expression of both *cxcr1* and *cxcr2* receptors. *cxcr1* was significantly upregulated in sorted cECs after cardiac injury, while the expression of *cxcr2* was very low in cECs before and after injury (**Figure 4.26**).

To investigate if the receptor Cxcr1 plays a role during cardiac regeneration, I injured *cxcr1*$^{-/-}$ ventricles and observed reduced cEC proliferation and coronary coverage (**Figure 4.27**). I also analyzed the cardiac regeneration response. Although the scar size of *cxcr1*$^{-/-}$ ventricles was similar to sibling WTs at 30 dpci, these mutants displayed a significantly larger scar at 90 dpci, suggesting that Cxcr1 signaling is needed for cardiac regeneration (**Figure 4.28**).

Overall, these results suggest that Cxcl8a-Cxcr1 signaling regulates a cellular crosstalk between cECs and EPDCs to facilitate coronary revascularization during cardiac regeneration in zebrafish.

7.3. Discussion and Conclusion

The zebrafish heart revascularizes the injured area rapidly following cardiac damage (Marín-Juez et al., 2016). In this project, I showed that Vegfc signaling is required for coronary revascularization. I have identified *emilin2a* as a new downstream target of Vegfc signaling during cardiac regeneration. Emilin2a was able to promote revascularization and promote cardiac regeneration in zebrafish. Downstream of Vegfc signaling, Emilin2a regulates a crosstalk between EPDCs and coronaries via

Cxcl8a-Cxcr1 signaling to facilitate coronary revascularization and cardiac regeneration.

This study provides mechanistic insight on how endothelial cells support cardiac regeneration. Indeed, the role of endothelial cells in maintaining tissue development and homeostasis has been well documented in several tissues and organs (Rafii et al., 2016). Endothelial cells secrete different factors that act in a paracrine (angiocrine) manner to support neighboring tissues. Here, I show that Vegfc is secreted by cECs also acts in an angiocrine manner to support cardiac regeneration.

Vegfc is a well-known regulator of lymphangiogenesis during development and regeneration (Klaourakis et al., 2021). Here, I show a novel mechanism of how Vegfc signaling promotes cardiac regeneration in a lymphatic independent manner, hence laying a strong base for future research to study the clinical potential of Vegfc signaling in enhancing collateral formation in patients following MI.

As a part of this project, I showed that the extra ECM molecule Emilin2a enhances cardiac regeneration. Besides Emilin2a, Vegfc signaling adjusts the composition of various ECM component (**Table 10.2**), thereby providing a suitable microenvironment that is permissive for cardiac regeneration. This study emphasizes the need to investigate how alterations of the ECM components could be beneficial in promoting tissue regeneration (Mongiat et al., 2016).

Mechanistically, Emilin2a regulates cellular communication between EPDCs and cECs via Cxcl8a-Cxcr1 signaling to promote coronary revascularization. Indeed, previous studies have shown that epicardial-coronary signaling is critical for cardiac regeneration (Marín-Juez et al., 2019; Zhou et al., 2011). Given the importance of cellular communication during cardiac regeneration, more work is needed to further understand the molecular mechanisms that govern communication between the different cellular compartments in the heart including CMs, EPDCs, cECs as well as the different immune cells, and how these interactions regulate cardiac regeneration.

Altogether, this work provides new mechanistic insights into how Vegfc signaling regulates key aspects of the regenerative response by modulating ECM factors to provide a milieu that facilitates cardiac regeneration.

8. ZUSAMMENFASSUNG

8.1. Einleitung

Ischämische Herzerkrankungen, die durch einen Verschluss der Koronararterien verursacht werden, stellen weltweit die häufigste Todesursache dar. Das durch die Koronarverschlüsse unterversorgte Gewebe stirbt ab (Pfeffer and Braunwald, 1990), wodurch das Herz einen Umbau durchmacht und das verlorene Gewebe durch eine fibrotische Narbe ersetzt, die die kontraktile Effizienz des Herzens beeinträchtigt und somit zu einem Myokardinfarkt führt (Talman and Ruskoaho, 2016). Leider kann sich das erwachsene Säugetierherz nicht regenerieren und das verlorene Gewebe wiederherstellen, was auf mehrere Faktoren zurückzuführen ist, darunter die geringe Fähigkeit von Kardiomyozyten (KM), in den Zellzyklus einzutreten und sich zu teilen, das Vorhandensein und die Fülle aktivierter Myofibroblasten, die fibrotische extrazelluläre Matrix (EZM)-Komponenten ablagern, sowie das geringe angiogene Potenzial des Herzens, das Infarktgewebe zu revaskularisieren (Kocijan et al., 2021; Travers et al., 2016; Tzahor and Poss, 2017). Mehrere Studien haben gezeigt, dass eine Verbesserung der Revaskularisierungsfähigkeit des Herzens ein großes therapeutisches Potenzial haben könnte. Jüngste Arbeiten von Das und Kollegen haben gezeigt, dass die Verbesserung der Bildung von Kollateralarterien im Herzen erwachsener Mäuse zu einer Verbesserung der Herzleistung führt (Das et al., 2019). Im gleichen Sinne zeigte eine neuere Studie, dass die Verbesserung der Revaskularisierung im Herzen erwachsener Mäuse die Proliferation von KM (Debenedittis et al., 2021). All diese Erkenntnisse deuten darauf hin, dass eine angiogene Therapie der Schlüssel zur Verbesserung der Regenerationsfähigkeit des erwachsenen Säugetierherzens sein könnte. Klinische Studien haben jedoch gezeigt, dass die Injektion angiogener Faktoren unwirksam ist (Robich et al., 2011). Dies veranlasste die Forscher, die Revaskularisierung der Herzkranzgefäße in Modellorganismen zu untersuchen, die über eine endogene Regenerationsfähigkeit verfügen, um die Mechanismen zu verstehen, die diesen Prozess steuern.

Der erwachsene Zebrafisch verfügt über eine bemerkenswerte Fähigkeit, das Herz nach einer Verletzung zu regenerieren (Poss et al., 2002). Eine der frühesten Reaktionen nach einer Herzverletzung ist die koronare Revaskularisierung (Marín-Juez et al., 2016). Die Blockierung dieses Prozesses führt zu einer verminderten

Proliferation des Herzmuskels und zur Bildung einer dauerhaften fibrotischen Narbe. (Marín-Juez et al., 2016, 2019). Daher könnte die Identifizierung von Faktoren, die diesen Prozess unterstützen, von großem klinischen Nutzen sein.

Einer der angiogenen Faktoren, der nach einer Herzverletzung in Zebrafischen hochreguliert wird, ist der vaskuläre endotheliale Wachstumsfaktor C (*vegfc*) (Lai et al., 2017; Lien et al., 2006). Vegfc ist ein Hauptregulator der lymphatischen Entwicklung in Zebrafischen und Mäusen (Karaman et al., 2018; Oh et al., 1997; Secker and Harvey, 2015). Darüber hinaus erstreckt sich die Rolle von Vegfc bei der Förderung der Lymphangiogenese auch auf regenerative Situationen (Gancz et al., 2019; Harrison et al., 2019; Klaourakis et al., 2021; Klotz et al., 2015). Es wurde bereits gezeigt, dass die Injektion von rekombinantem VEGFC die Lymphangiogenese im erwachsenen Mäuseherz induziert, was die zeitgemäße Entfernung von Immunzellen verbessert und die Herzfunktion nach einem Herzinfarkt erhöht. (Klotz et al., 2015; Vieira et al., 2018). Darüber hinaus haben jüngste Studien an Zebrafischen gezeigt, dass Vegfc für die Lymphangiogenese nach einer Herzverletzung erforderlich ist und dass die Blockierung dieses Prozesses zu einer verstärkten Narbenbildung führt (Gancz et al., 2019; Harrison et al., 2019).

Vegfc ist auch für die Regulierung der angiogenen Gefäßwachstums wichtig. In Zebrafischen haben Knockdown-Experimente gezeigt, dass *Vegfc eine* wichtige Rolle bei der Bildung der intersegmentalen Gefäße spielt (Le Guen et al., 2014; Villefranc et al., 2013). Darüber hinaus induziert VEGFC auch die Ausbreitung von Mikrogefäßen in Kükenembryonen und in der Hornhaut von Mäusen (Cao et al., 1998). Im Herzen führte *das* Fehlen von *Vegfc* zu einer gestörten Entwicklung der Herzkranzgefäße mit reduzierten Verzweigungen. (Chen et al., 2014a, 2014b). Alle diese Befunde deuten auf eine entscheidende Rolle von VEGFC bei der Förderung der Angiogenese hin. Die Mechanismen, wie VEGFC die koronare Revaskularisierung nach einer Herzverletzung reguliert, sind jedoch noch unbekannt.

In dieser Arbeit zeige ich, dass *vegfc* nach einer Herzverletzung in den Herzkranzgefäßen exprimiert wird und dass Vegfc-Signale für die koronare Revaskularisierung und die Regeneration des Herzens wichtig sind, indem sie die Expression des EZM-Gens *Emilin2a* fördern. Emilin2a wirkt als pro-regeneratives Molekül, das die koronare Revaskularisierung und die Herzregeneration im Zebrafisch fördert. Mechanistisch gesehen induziert Emilin2a die epikardiale *cxcl8a*-Expression,

während sein Rezeptor *cxcr1* in den Koronargefäßen exprimiert wird. Die Cxcl8a-Cxcr1-Signalübertragung reguliert einen epikardialen-koronaren Crosstalk, um die koronare Revaskularisierung während der Herzregeneration in Zebrafischen zu erleichtern.

8.2. Ergebnisse

8.2.1. *vegfc* wird in Koronarendothelzellen exprimiert und ist für die Herzregeneration im Zebrafisch erforderlich

Zunächst analysierte ich die Expressionsdynamik von *vegfc* während der Herzregeneration. Zu diesem Zweck führte ich RT-qPCR-Analysen durch und verglich die vegfc-Expression in kryoverletzten Ventrikeln im Vergleich zu scheinoperierten Ventrikeln zu verschiedenen Zeitpunkten. Ich beobachtete, dass *vegfc bereits ab* 48 hpci (= hours post cryo injury / Stunden nach Kryoverletzung) hochreguliert wird und die Expression bei 96 hpci ihren Höhepunkt erreicht (**Abbildung 4.1 A**). Um die zelluläre Quelle dieses Signals zu bestimmen, führte ich anschließend eine In-situ-Hybridisierung an Herzschnitten durch und stellte fest, dass *vegfc* spezifisch im verletzten Bereich an der Peripherie des Gewebes exprimiert wird (**Abbildung 4.1 B**). Um die Quelle der Expression weiter zu analysieren, sortierte ich cECs(= coronary endothelial cells / Koronargefäßendothelzellen), EPDCs (= epithelial derived cells / vom Epithel stammende Zellen) und KMs und überprüfte die *vegfc*-Expression in diesen Zelltypen nach der Kryoverletzung. Interessanterweise stellte ich fest, dass *vegfc* nach einer Herzverletzung von cECs exprimiert wird, nicht aber von EPDCs oder KMs (**Abbildung 4.1 C-F**).

Die Beobachtungen, dass *vegfc* in cECs exprimiert wird und die Expression bei 96 hpci ihren Höhepunkt erreicht, wenn die Proliferation der Koronargefäße ihren Höhepunkt erreicht (Marín-Juez et al., 2019) veranlasste mich zu der Hypothese, dass *vegfc* eine Rolle bei der koronaren Revaskularisierung während der Herzregeneration spielen könnte. Um diese Hypothese zu testen, optimierte ich die *Tg(hsp70l:sflt4)* Funktionsverlust-Linie, mithilfe der ich die lösliche Form von Vegfr3 (Flt4) unter einem Hitzeschockpromotor überexprimieren kann, wodurch die Vegfc-Signalisierung blockiert wird (**Abbildung 4.2**). Ich habe festgestellt, dass die Blockierung der Vegfc-Signalübertragung zu einer signifikanten Verringerung der cEC-Proliferation bei 96 hpci führt (**Abbildung 4.3 B,C**). Bei der Analyse dieser Herzen im Alter von 7 dpci,

wenn die Koronargefäße während der unbeeinflussten Herzregeneration den verletzten Bereich vollständig bedecken (Marín-Juez et al., 2016, 2019) beobachtete ich eine signifikante Verringerung der Koronarabdeckung (**Abbildung 4.3 E,F**), was ein weiterer Hinweis darauf ist, dass Vegfc-Signale für die koronare Revaskularisierung erforderlich sind.

Frühere Studien haben gezeigt, dass die Koronargefäße als Gerüst für die KM-Regeneration dienen (Debenedittis et al., 2021; Marín-Juez et al., 2019). Daher wollte ich testen, ob die verringerte koronare Revaskularisierung bei Blockierung der Vegfc-Signalübertragung eine Auswirkung auf die Herzmuskelregeneration hat. Ich analysierte die KM-Dedifferenzierung und -Proliferation bei 7 dpci und stellte fest, dass die Blockierung des Vegfc-Signals tatsächlich zu einer signifikanten Verringerung der KM-Dedifferenzierung und -Proliferation führte (**Abbildung 4.6 A-D**). Darüber hinaus behielten die Herzen, in denen die Vegfc-Signalübertragung blockiert war, eine größere Narbe bei 90 dpci, einem Zeitpunkt, zu dem eine fast vollständige Herzregeneration erwartet wird (**Abbildung 4.7**). Um die Möglichkeit zu prüfen, dass die KM-Phänotypen auf eine direkte Vegfc-Signalübertragung auf KM zurückzuführen sind, habe ich KM vor und nach der Verletzung sortiert und die Expression von *vegfr1*, *vegfr2* und *vegfr3* analysiert. Ich fand eine geringe Expression aller drei Rezeptoren in KMs, was darauf hindeutet, dass es unwahrscheinlich ist, dass Vegfc direkt Signale an die KMs sendet (**Abbildung 4.6 E,F**). Diese Möglichkeit kann jedoch ohne gewebespezifische Experimente zum Funktionsverlust nicht vollständig ausgeschlossen werden.

8.2.2. Vegfc-Signalisierung ist für die koronare Revaskularisierung unabhängig vom Lymphsystem erforderlich

Vegfc ist ein Hauptregulator der Lymphangiogenese während der Entwicklung und Regeneration im Zebrafisch (Gancz et al., 2019; Harrison et al., 2019; Hogan et al., 2009a, 2009b; Küchler et al., 2006; Villefranc et al., 2013). Um die Möglichkeit auszuschließen, dass die *Tg(hsp70l:sflt4)*-Linie die Lymphgefäße während meiner Experimente blockiert hat, habe ich 3 Monate alte Fische verwendet, die noch keine ventrikulären Lymphgefäße, aber ein etabliertes Koronarnetz aufweisen. Um zu bestätigen, dass 3 Monate alten Zebrafischherzen Lymphgefäße fehlen, habe ich intramyokardiale Injektionen von Qdots durchgeführt, die von den Lymphgefäßen absorbiert und wieder ausgeschieden werden (Harrison et al., 2019). Tatsächlich

stellte ich fest, dass 3 Monate alte Zebrafischventrikel die injizierten Qdots nicht absorbierten. Dies bestätigt, dass 3 Monate alten Zebrafischventrikeln ein lymphatisches Netzwerk fehlt und dass der beobachtete Phänotyp der reduzierten koronaren Revaskularisierung unabhängig vom Vorhandensein oder Fehlen von Lymphgefäßen ist (**Abbildung 4.5 A,B**).

8.2.3. Das extrazelluläre Matrixprotein Emilin2a ist ein downstream Target der Vegfc-Signalübertragung

Um einen Einblick in den Mechanismus zu erhalten, wie die Vegfc-Signalgebung die koronare Revaskularisierung reguliert, wurde eine RNA-Sequenzierung durchgeführt, um das Transkriptom von WT-Ventrikeln mit dem von *Tg(hsp70l:sflt4)*-Zebrafischen bei 24 hpci zu vergleichen (**Abbildung 4.8 A,B**). Nach gründlicher Analyse und Validierung mehrerer potenzieller Targets (**Abbildung 4.8 C-E**) war *emilin2a* eines der Gene, die Behandlung durch *Tg(hsp70l:sflt4)* bei 24 hpci (als die RNAseq durchgeführt wurde) und bei 96 hpci (als ein reduzierter cEC-Phänotyp beobachtet wurde) eine konsistente Herabregulierung zeigten (**Abbildung 4.9 A**).
Ich schloss daraus, dass die verminderte Expression von *emilin2a* in *Tg(hsp70l:sflt4)* auf eine verminderte Revaskularisierung zurückzuführen sein könnte. Um diese Möglichkeit zu testen, habe ich die *Tg(hsp70l:dn-vegfaa)*-Linie verwendet, die nach einer Herzverletzung eine verminderte koronare Revaskularisierung aufweist (Marín-Juez et al., 2016). Ich analysierte die Expression von *emilin2a* in unverletzten Ventrikeln von WT, *Tg(hsp70:sflt4)* und *Tg(hsp70l:dn-vegfaa)* Zebrafischen. Ich beobachtete eine signifikante Verringerung der *emilin2a*-Expression in unverletzten *Tg(hsp70l:sflt4)*-Ventrikeln, aber nicht in *Tg(hsp70l:dn-vegfaa)* (**Abbildung 4.9 B**). Darüber hinaus habe ich Vegfc-mRNA-Injektionen in Zebrafisch-Embryonen im Ein-Zell-Stadium durchgeführt und eine signifikante Hochregulierung der *emilin2a*-Expression beobachtet, was bestätigt, dass *emilin2a* ein nachgeschaltetes Ziel der Vegfc-Signalwirkung ist (Abbildung 4**.9 C**). Interessanterweise führte der Knockdown von *VEGFC* in HUVECs zu einer signifikanten Abnahme der *EMILIN2*-Expression (**Abbildung 4.9 D**), was darauf hindeutet, dass die VEGFC-EMILIN2-Signalachse in menschlichen Endothelzellen konserviert ist.

8.2.4. *emilin2a* ist für die koronare Revaskularisierung während der Herzregeneration im Zebrafisch erforderlich

Emilin2a ist ein EZM-Protein, von dem gezeigt wurde, dass es die angiogene Gefäßentwicklung *in vitro* induziert (Paulitti et al., 2018). In Zebrafisch-Embryonen wird *emilin2a* in der dorsalen Aorta bei 24 hpf exprimiert (Milanetto et al., 2008). Die Rolle von Emilin2a bei der Regeneration des Herzens wurde jedoch noch nicht untersucht.

Zunächst untersuchte ich das Expressionsmuster von *emilin2a* in sich regenerierenden Zebrafischventrikeln zu verschiedenen Zeitpunkten nach der Verletzung und beobachtete eine signifikante Hochregulierung der Expression bei 96 hpci (**Abbildung 4.11 A**), die mit dem Höhepunkt der cEC-Proliferation (Marín-Juez et al., 2019) und der *vegfc*-Expression (**Abbildung 4.1 A**). Durch *in situ*-Hybridisierung von Herzschnitten konnte ich feststellen, dass *emilin2a* im verletzten Bereich sowohl von cEC als auch von EPDCs exprimiert wird (Abbildung 4**.11 B**). Beim Vergleich der Expression von *emilin2a* in beiden Zelltypen mittels RT-qPCR zeigte sich jedoch, dass die Expression in EPDCs bei 96 hpci stärker anstieg (**Abbildung 4.11 C-E**).

Um die Rolle von *emilin2a* während der Herzregeneration in Zebrafischen zu untersuchen, erzeugte ich mit Hilfe der CRISPR-Cas9-Technologie eine Mutante des gesamten *emilin2a-Locus* (**Abbildung 4.12**). Ich verletzte *emilin2a*$^{-/-}$ Ventrikel und analysierte die koronare Revaskularisierung bei 96 hpci. *emilin2a*$^{-/-}$ Ventrikel zeigten eine signifikante Reduktion der cEC Proliferation bei 96 hpci, sowie eine reduzierte Anzahl von Koronargefäßen bei 7 dpci, während ventrikuläre Lymphgefäße fehlten (**Abbildung 4.14**). Als nächstes wollte ich testen, ob *emilin2a*$^{-/-}$ Ventrikel eine mangelhafte Herzregeneration aufweisen. Ich analysierte die KM-Proliferation und Narbenrückbildung in *emilin2a*$^{-/-}$ Ventrikeln und ihren WT-Geschwistern (**Abbildung 4.15 A,B**). Interessanterweise zeigten *emilin2a*$^{-/-}$ Ventrikel auch eine signifikante Verringerung der KM-Proliferation und eine größere Narbe bei 90 dpci (**Abbildung 4.15 E,F**). Insgesamt deuten diese Ergebnisse darauf hin, dass das EZM-Molekül Emilin2a für die koronare Revaskularisierung und die Herzregeneration im Zebrafisch erforderlich ist.

8.2.5. Emilin2a fördert die Herzregeneration

Die Erkenntnisse, dass *emilin2a* der Vegfc-Signalwirkung nachgeschaltet ist und für die koronare Revaskularisierung benötigt wird, veranlassten mich zu der Hypothese, dass eine Überexpression von *emilin2a* die reduzierte koronare Revaskularisierung aufgrund der Vegfc-Signalisierungsblockade retten kann. Um diese Möglichkeit zu testen, erzeugte ich die *Tg(hsp70l:loxP-CFP-loxP-emiln2a-p2A-mCherry)*-Linie, die in Kombination mit der *TgBAC(tcf21:CreERT2)*-Linie die räumliche und zeitliche Überexpression von *emilin2a* in EPDCs während der Herzregeneration ermöglicht (**Abbildung 4.17**). Mit der *Tg(hsp70l:sflt4)*-Linie blockierte ich die Vegfc-Signalübertragung und überexprimierte *emilin2a* in EPDCs. Tatsächlich konnte die Überexpression von *emilin2a* die Proliferation der cECs erhöhen und sie in den *Tg(hsp70l:sflt4)*-Ventrikeln wieder auf WT-Niveau bringen (**Abbildung 4.18**). Somit konnte die Überexpression von *emilin2a* in EPDCs die Vegfc-Signalblockade aufheben.

In Anbetracht dieser Ergebnisse stellte ich die Hypothese auf, dass *emilin2a* die Herzregeneration fördern kann. Um diese Hypothese zu testen, habe ich eine globale *emilin2a*-Überexpressionslinie unter einem Hitzeschock-Promotor erzeugt. Ich analysierte verschiedene Aspekte der Herzregeneration und stellte fest, dass die Überexpression von *emilin2a* zu einem signifikanten Anstieg der cEC-Proliferation bei 96 hpci und zu einer Zunahme der Koronarabdeckung bei 7 dpci führte, während die Lymphgefäße im Ventrikel fehlten (**Abbildung 4.19**). Wichtig ist, dass die Überexpression von *emilin2a* auch zu einer erhöhten KM-Proliferation bei 7 dpci und zu einer verringerten Narbenfläche bei 30 dpci führte (**Abbildung 4.20**). Insgesamt deuten diese Befunde darauf hin, dass das aus dem Epikard stammende *Emilin2a die* Herzregeneration nach dem Vegfc-Signal fördert.

8.2.6. Emilin2a fördert die epikardiale cxcl8a-Expression während der Herzregeneration

Frühere Arbeiten haben gezeigt, dass EMILIN2 die Expression des Chemokins *CXCL8* stimuliert, um die Proliferation und Migration von Endothelzellen *in vitro zu* induzieren (Andreuzzi et al., 2020; Paulitti et al., 2018). Um den Mechanismus der Förderung koronarer Revaskularisierung durch Emilin2a in Zebrafischen aufzuklären, habe ich eine RT-qPCR-Analyse an *emilin2a*$^{-/-}$ Ventrikeln bei 96 hpci durchgeführt und

eine signifikante Verringerung der *cxcl8a*-Expression beobachtet (**Abbildung 4.21 A**). In ähnlicher Weise wurde die *cxcl8a*-Expression bei der Überexpression von *emilin2a* bei 96 hpci mit der *Tg(hsp70l:emilin2a)*-Linie hochreguliert (**Abbildung 4.21 B**), was darauf hindeutet, dass Emilin2a tatsächlich die *cxcl8a*-Expression während der Herzregeneration in Zebrafischen induziert. Um zu untersuchen, welche Zelltypen *cxcl8a* während der Herzregeneration exprimieren, führte ich eine In-situ-Hybridisierung an Herzschnitten durch und stellte fest, dass *cxcl8a* im verletzten Gewebe von EPDCs exprimiert wird (Abbildung 4**.22 A**). Um die Quelle des *cxcl8a*-Signals zu bestätigen, analysierte ich die *cxcl8a*-Expression in sortierten EPDCs und cECs und stellte fest, dass EPDCs nach einer Herzverletzung *cxcl8a* exprimieren, nicht aber cECs, was die *in situ*-Ergebnisse bestätigt (**Abbildung 4.22 B-D**). Insgesamt deuten diese Daten darauf hin, dass Emilin2a die epikardiale *cxcl8a*-Expression als Folge der Vegfc-Signalisierung induziert.

8.2.7. Die Cxcl8a-Cxcr1-Signalübertragung ist für die koronare Revaskularisierung und Herzregeneration im Zebrafisch erforderlich

Das proinflammatorische Chemokin Cxcl8a wurde bereits mit der Rekrutierung von Neutrophilen und der Wundheilung in Verbindung gebracht (Fox et al., 2005; De Oliveira et al., 2016). Um zu untersuchen, ob die erhöhte *cxcl8a*-Expression während der Herzregeneration eine Rolle spielt, wurde eine *cxcl8a*-Mutante erzeugt, die auf die Dimerisierungs- und Rezeptorbindungsdomäne abzielt (**Abbildung 4.23**). Die cEC-Proliferation war in *cxcl8a*$^{-/-}$ Ventrikeln bei 96 hpci deutlich reduziert (**Abbildung 4.24**). Darüber hinaus zeigten diese Mutanten auch eine reduzierte Koronarabdeckung bei 7 dpci sowie eine vergrößerte Narbenfläche bei 90 dpci (**Abbildung 4.25**).

Angesichts der Ergebnisse, dass *cxcl8a* in EPDCs exprimiert wird und die Mutanten eine mangelhafte koronare Revaskularisierung aufweisen, schlussfolgerte ich, dass der/die von Cxcl8a aktivierte(n) Rezeptor(en) in cECs exprimiert werden. Cxcl8a kann die G-Protein-gekoppelten Rezeptoren Cxcr1 und Cxcr2 binden und aktivieren (Ha et al., 2017). Zu diesem Zweck sortierte ich cECs unter Verwendung der *Tg(-0.8flt1:RFP)*-Linie und analysierte die Expression der *cxcr1*- und *cxcr2*-Rezeptoren. *cxcr1* war in sortierten cECs nach einer Herzverletzung signifikant hochreguliert, während die Expression von *cxcr2* in cECs vor und nach der Verletzung sehr gering war (**Abbildung 4.26**).

Um zu untersuchen, ob der Rezeptor Cxcr1 bei der Herzregeneration eine Rolle spielt, habe ich Kryo-Verletzungen an *cxcr1*$^{-/-}$ Ventrikeln durchgeführt und eine signifikante Verringerung der cEC-Proliferation und der Koronarabdeckung beobachtet (**Abbildung 4.27**). Ich analysierte auch die Reaktion der Herzregeneration. Obwohl die Größe der Narbe von *cxcr1*$^{-/-}$ Ventrikeln bei 30 dpci ähnlich war wie bei WT-Geschwistern, wiesen die Mutanten bei 90 dpci eine deutlich größere Narbe auf, was darauf hindeutet, dass die Cxcr1-Signalübertragung für die Herzregeneration erforderlich ist (**Abbildung 4.28**).
Insgesamt deuten diese Ergebnisse darauf hin, dass der Cxcl8a-Cxcr1-Signalweg einen zellulären Crosstalk zwischen cECs und EPDCs reguliert, um die koronare Revaskularisierung während der Herzregeneration im Zebrafisch zu erleichtern.

8.3. Diskussion und Schlussfolgerung

Das Herz des Zebrafisches zeigt eine schnelle angiogene Reaktion, um die Regeneration des Herzens nach einer Verletzung zu unterstützen (Marín-Juez et al., 2016). In dieser Arbeit habe ich gezeigt, dass die Vegfc-Signalgebung für die koronare Revaskularisierung erforderlich ist. Ich habe *emilin2a* als neues nachgeschaltetes Ziel des Vegfc-Signals während der Herzregeneration identifiziert. Emilin2a war in der Lage, die koronare Revaskularisierung zu induzieren und die Herzregeneration im Zebrafisch zu fördern. Mechanistisch, reguliert Emilin2a downstream von Vegfc-Signalen eine Kommunikation zwischen EPDCs und Koronargefäßen über Cxcl8a-Cxcr1-Signale, um die koronare Revaskularisierung und die Herzregeneration zu fördern.

Diese Arbeit bietet einen besseren Einblick in die Mechanismen, mit denen Endothelzellen die Herzregeneration unterstützen. Die Rolle der Endothelzellen bei der Aufrechterhaltung der Entwicklung und Homöostase in verschiedenen Geweben und Organen ist gut dokumentiert (Rafii et al., 2016). Endothelzellen sezernieren verschiedene Faktoren, die auf parakrine (angiokrine) Weise wirken, um benachbarte Gewebe zu unterstützen. Hier zeige ich, dass Vegfc, das von cECs sezerniert wird, auch auf angiokrine Weise die Herzregeneration unterstützt.
Vegfc ist ein bekannter Regulator der Lymphangiogenese während der Entwicklung und Regeneration (Klaourakis et al., 2021). Hier zeige ich einen neuartigen Mechanismus, wie die Vegfc-Signalisierung die Herzregeneration auf eine

lymphatische, unabhängige Weise fördert, und lege damit eine solide Grundlage für künftige Forschung zur Untersuchung des klinischen Potenzials des Vegfc-Signalweges bei der Förderung der Kollateralbildung bei Patienten nach einem Infarkt.
In dieser Arbeit habe ich gezeigt, dass das EZM-Molekül Emilin2a die Herzregeneration fördert. Neben Emilin2a verändert der Vegfc-Signalweg die Zusammensetzung mehrerer EZM-Komponenten (**Tabelle 10.2**) und sorgt so für eine geeignete Mikroumgebung, die die Regeneration des Herzens begünstigt. Diese Arbeit unterstreicht die Notwendigkeit zu untersuchen, wie Veränderungen der EZM-Komponenten bei der Förderung der Geweberegeneration von Vorteil sein könnten (Mongiat et al., 2016).
Mechanistisch gesehen reguliert Emilin2a die zelluläre Kommunikation zwischen EPDCs und cECs über Cxcl8a-Cxcr1-Signale, um die koronare Revaskularisierung zu fördern. Frühere Studien haben gezeigt, dass die epikardial-koronare Signalübertragung für die Herzregeneration entscheidend ist (Marín-Juez et al., 2019; Zhou et al., 2011). Angesichts der Bedeutung der zellulären Kommunikation während der Herzregeneration muss noch mehr getan werden, um die molekularen Mechanismen besser zu verstehen, die die Kommunikation zwischen den verschiedenen Zelltypen im Herzen, einschließlich KMs, EPDCs, cECs sowie den verschiedenen Immunzellen, steuern, und wie diese Interaktionen die Herzregeneration regulieren.
Insgesamt liefert diese Arbeit neue mechanistische Erkenntnisse darüber, wie Vegfc-Signale verschiedene Aspekte der Herzregeneration regulieren, indem sie Matrisom-assoziierte Faktoren modulieren und so ein günstiges Milieu schaffen, das die Herzregeneration erleichtert.

9. REFERENCES

Aghajanian, H., Kimura, T., Rurik, J.G., Hancock, A.S., Leibowitz, M.S., Li, L., Scholler, J., Monslow, J., Lo, A., Han, W., et al. (2019). Targeting cardiac fibrosis with engineered T cells. Nature *573*, 430–433.

Ali, S.R., Ranjbarvaziri, S., Talkhabi, M., Zhao, P., Subat, A., Hojjat, A., Kamran, P., Müller, A.M.S., Volz, K.S., Tang, Z., et al. (2014). Developmental heterogeneity of cardiac fibroblasts does not predict pathological proliferation and activation. Circ. Res. *115*, 625–635.

Ali, S.R., Menendez-Montes, I., Warshaw, J., Xiao, F., and Sadek, H.A. (2020). Homotypic Fusion Generates Multinucleated Cardiomyocytes in the Murine Heart. Circulation *141*, 1940–1942.

Alkass, K., Panula, J., Westman, M., Wu, T. Di, Guerquin-Kern, J.L., and Bergmann, O. (2015). No Evidence for Cardiomyocyte Number Expansion in Preadolescent Mice. Cell *163*, 1026–1036.

Allanki, S., Strilic, B., Scheinberger, L., Onderwater, Y.L., Marks, A., Günther, S., Preussner, J., Kikhi, K., Looso, M., Stainier, D.Y.R., et al. (2021). Interleukin-11 signaling promotes cellular reprogramming and limits fibrotic scarring during tissue regeneration. Sci. Adv. *7*.

Andreuzzi, E., Fejza, A., Capuano, A., Poletto, E., Pivetta, E., Doliana, R., Pellicani, R., Favero, A., Maiero, S., Fornasarig, M., et al. (2020). Deregulated expression of Elastin Microfibril Interfacer 2 (EMILIN2) in gastric cancer affects tumor growth and angiogenesis. Matrix Biol. Plus *6–7*.

Astin, J.W., Haggerty, M.J.L., Okuda, K.S., Le Guen, L., Misa, J.P., Tromp, A., Hogan, B.M., Crosier, K.E., and Crosier, P.S. (2014). Vegfd can compensate for loss of Vegfc in zebrafish facial lymphatic sprouting. Dev. *141*, 2680–2690.

Astrof, S., and Hynes, R.O. (2009). Fibronectins in vascular morphogenesis. Angiogenesis *12*, 165–175.

Baehr, A., Umansky, K.B., Bassat, E., Jurisch, V., Klett, K., Bozoglu, T., Hornaschewitz, N., Solyanik, O., Kain, D., Ferraro, B., et al. (2020). Agrin promotes coordinated therapeutic processes leading to improved cardiac repair in pigs. Circulation 868–881.

de Bakker, D.E.M., Bouwman, M., Dronkers, E., Simões, F.C., Riley, P.R., Goumans, M.J., Smits, A.M., and Bakkers, J. (2021). Prrx1b restricts fibrosis and promotes Nrg1-dependent cardiomyocyte proliferation during zebrafish heart regeneration. Dev. *148*.

Baldwin, M.E., Halford, M.M., Roufail, S., Williams, R.A., Hibbs, M.L., Grail, D., Kubo, H., Stacker, S.A., and Achen, M.G. (2005). Vascular Endothelial Growth Factor D Is Dispensable for Development of the Lymphatic System. Mol. Cell. Biol. *25*, 2441–2449.

Bassat, E., Mutlak, Y.E., Genzelinakh, A., Shadrin, I.Y., Baruch Umansky, K., Yifa, O., Kain, D., Rajchman, D., Leach, J., Riabov Bassat, D., et al. (2017). The extracellular matrix protein agrin promotes heart regeneration in mice. Nature *547*, 179–184.

Baudino, T.A., Carver, W., Giles, W., and Borg, T.K. (2006). Cardiac fibroblasts: Friend or foe? Am. J. Physiol. - Hear. Circ. Physiol. *291*.

Beisaw, A., Kuenne, C., Guenther, S., Dallmann, J., Wu, C.C., Bentsen, M., Looso, M., and Stainier, D.Y.R. (2020). AP-1 Contributes to Chromatin Accessibility to Promote Sarcomere Disassembly and Cardiomyocyte Protrusion during Zebrafish Heart Regeneration. Circ. Res. *126*, 1760–1778.

Bergmann, O., Zdunek, S., Felker, A., Salehpour, M., Alkass, K., Bernard, S., Sjostrom, S.L., Szewczykowska, M., Jackowska, T., Dos Remedios, C., et al. (2015). Dynamics of Cell Generation and Turnover in the Human Heart. Cell *161*, 1566–1575.

Bertozzi, A., Wu, C.C., Nguyen, P.D., Vasudevarao, M.D., Mulaw, M.A., Koopman, C.D., de Boer, T.P., Bakkers, J., and Weidinger, G. (2021). Is zebrafish heart regeneration “complete”? Lineage-restricted cardiomyocytes proliferate to pre-injury numbers but some fail to differentiate in fibrotic hearts. Dev. Biol. *471*, 106–118.

Bevan, L., Lim, Z.W., Venkatesh, B., Riley, P.R., Martin, P., and Richardson, R.J. (2020). Specific macrophage populations promote both cardiac scar deposition and subsequent resolution in adult zebrafish. Cardiovasc. Res. *116*, 1357–1371.

Bilbija, D., Haugen, F., Sagave, J., Baysa, A., Bastani, N., Levy, F.O., Sirsjö, A., Blomhoff, R., and Valen, G. (2012). Retinoic Acid Signalling Is Activated in the Postischemic Heart and May Influence Remodelling. PLoS One *7*.

Bise, T., Sallin, P., Pfefferli, C., and Jaźwińska, A. (2020). Multiple cryoinjuries modulate the efficiency of zebrafish heart regeneration. Sci. Rep. *10*.

Bohaud, C., Johansen, M.D., Jorgensen, C., Ipseiz, N., Kremer, L., and Djouad, F. (2021). The Role of Macrophages During Zebrafish Injury and Tissue Regeneration Under Infectious and Non-Infectious Conditions. Front. Immunol. *12*.

Bolger, A.M., Lohse, M., and Usadel, B. (2014). Trimmomatic: A flexible trimmer for Illumina sequence data. Bioinformatics *30*, 2114–2120.

Bot, S., Andreuzzi, E., Capuano, A., Schiavinato, A., Colombatti, A., and Doliana, R. (2015). Multiple-interactions among EMILIN1 and EMILIN2 N- and C-terminal domains. Matrix Biol. *41*, 44–55.

Braghetta, P., Ferrari, A., De Gemmis, P., Zanetti, M., Volpin, D., Bonaldo, P., and Bressan, G.M. (2004). Overlapping, complementary and site-specific expression pattern of genes of the EMILIN/Multimerin family. Matrix Biol. *22*, 549–556.

Le Bras, B., Barallobre, M.J., Homman-Ludiye, J., Ny, A., Wyns, S., Tammela, T., Haiko, P., Karkkainen, M.J., Yuan, L., Muriel, M.P., et al. (2006). VEGF-C is a trophic factor for neural progenitors in the vertebrate embryonic brain. Nat. Neurosci. *9*, 340–348.

Bussmann, J., Bos, F.L., Urasaki, A., Kawakami, K., Duckers, H.J., and Schulte-Merker, S. (2010). Arteries provide essential guidance cues for lymphatic endothelial cells in the zebrafish trunk. Development *137*, 2653–2657.

Cao, J., and Poss, K.D. (2018). The epicardium as a hub for heart regeneration. Nat.

Rev. Cardiol. *15*, 631–647.

Cao, Y., Linden, P., Farnebo, J., Cao, R., Eriksson, A., Kumar, V., Qi, J.H., Claesson-Welsh, L., and Alitalo, K. (1998). Vascular endothelial growth factor C induces angiogenesis in vivo. Proc. Natl. Acad. Sci. U. S. A. *95*, 14389–14394.

Chablais, F., Veit, J., Rainer, G., and Jaźwińska, A. (2011). The zebrafish heart regenerates after cryoinjury-induced myocardial infarction. BMC Dev. Biol. *11*, 21.

Chen, H.I., Sharma, B., Akerberg, B.N., Numi, H.J., Kivelä, R., Saharinen, P., Aghajanian, H., McKay, A.S., Bogard, P.E., Chang, A.H., et al. (2014a). The sinus venosus contributes to coronary vasculature through VEGFC-stimulated angiogenesis. Dev. *141*, 4500–4512.

Chen, H.I., Poduri, A., Numi, H., Kivela, R., Saharinen, P., McKay, A.S., Raftrey, B., Churko, J., Tian, X., Zhou, B., et al. (2014b). VEGF-C and aortic cardiomyocytes guide coronary artery stem development. J. Clin. Invest. *124*, 4899–4914.

Chen, H.I., Poduri, A., Numi, H., Kivela, R., Saharinen, P., McKay, A.S., Raftrey, B., Churko, J., Tian, X., Zhou, B., et al. (2014c). VEGF-C and aortic cardiomyocytes guide coronary artery stem development. J. Clin. Invest. *124*, 4899–4914.

Chi, N.C., Shaw, R.M., Jungblut, B., Huisken, J., Ferrer, T., Arnaout, R., Scott, I., Beis, D., Xiao, T., Baier, H., et al. (2008). Genetic and physiologic dissection of the vertebrate cardiac conduction system. PLoS Biol. *6*, 1006–1019.

Chiu, C.H., Chou, C.W., Takada, S., and Liu, Y.W. (2012). Development and fibronectin signaling requirements of the Zebrafish interrenal vessel. PLoS One *7*.

Choi, W.Y., and Poss, K.D. (2012). Cardiac Regeneration. In Current Topics in Developmental Biology, pp. 319–344.

Chong, J.J.H., Yang, X., Don, C.W., Minami, E., Liu, Y.W., Weyers, J.J., Mahoney, W.M., Van Biber, B., Cook, S.M., Palpant, N.J., et al. (2014). Human embryonic-stem-cell-derived cardiomyocytes regenerate non-human primate hearts. Nature *510*, 273–277.

Clark-Lewis, I., Schumacher, C., Baggiolini, M., and Moser, B. (1991). Structure-Activity Relationships of Interleukin-8 Determined Using Chemically Synthesized Analogs. J. Biol. Chem. *266*, 23128–23134.

Cleutjens, J.P.M., Verluyten, M.J.A., Smits, J.F.M., and Daemen, M.J.A.P. (1995). Collagen remodeling after myocardial infarction in the rat heart. Am. J. Pathol. *147*, 325–338.

Colombatti, A., Spessotto, P., Doliana, R., Mongiat, M., Bressan, G.M., and Esposito, G. (2012). The EMILIN/multimerin family. Front. Immunol. *2*.

Curado, S., Stainier, D.Y.R., and Anderson, R.M. (2008). Nitroreductase-mediated cell/tissue ablation in zebrafish: A spatially and temporally controlled ablation method with applications in developmental and regeneration studies. Nat. Protoc. *3*, 948–954.

Das, S., Goldstone, A.B., Wang, H., Farry, J., D'Amato, G., Paulsen, M.J., Eskandari, A., Hironaka, C.E., Phansalkar, R., Sharma, B., et al. (2019). A Unique Collateral

Artery Development Program Promotes Neonatal Heart Regeneration. Cell.

Debenedittis, P., Karpurapu, A., Henry, A., Thomas, M.C., Mccord, T.J., Brezitski, K., Prasad, A., Kobayashi Phd, Y., Shah, S.H., Mhs, M.D., et al. (2021). Coupled myovascular expansion directs growth and regeneration of the neonatal mouse heart. bioRxiv 2021.01.20.425322.

Ding, B. Sen, Nolan, D.J., Guo, P., Babazadeh, A.O., Cao, Z., Rosenwaks, Z., Crystal, R.G., Simons, M., Sato, T.N., Worgall, S., et al. (2011). Endothelial-derived angiocrine signals induce and sustain regenerative lung alveolarization. Cell *147*, 539–553.

Ding, B. Sen, Cao, Z., Lis, R., Nolan, D.J., Guo, P., Simons, M., Penfold, M.E., Shido, K., Rabbany, S.Y., and Rafii, S. (2014). Divergent angiocrine signals from vascular niche balance liver regeneration and fibrosis. Nature *505*, 97–102.

Dobin, A., Davis, C.A., Schlesinger, F., Drenkow, J., Zaleski, C., Jha, S., Batut, P., Chaisson, M., and Gingeras, T.R. (2013). STAR: Ultrafast universal RNA-seq aligner. Bioinformatics *29*, 15–21.

Doliana, R., Bot, S., Bonaldo, P., and Colombatti, A. (2000). EMI, a novel cysteine-rich domain of EMILINs and other extracellular proteins, interacts with the gC1q domains and participates in multimerization. FEBS Lett. *484*, 164–168.

Doliana, R., Bot, S., Mungiguerra, G., Canton, A., Paron Cilli, S., and Colombatti, A. (2001). Isolation and Characterization of EMILIN-2, a New Component of the Growing EMILINs Family and a Member of the EMI Domain-containing Superfamily. J. Biol. Chem. *276*, 12003–12011.

Dumont, D.J., Jussila, L., Taipale, J., Lymboussaki, A., Mustonen, T., Pajusola, K., Breitman, M., and Alitalo, K. (1998). Cardiovascular failure in mouse embryos deficient in VEGF receptor-3. Science (80-.). *282*, 946–949.

El-Brolosy, M.A., Kontarakis, Z., Rossi, A., Kuenne, C., Günther, S., Fukuda, N., Kikhi, K., Boezio, G.L.M., Takacs, C.M., Lai, S.L., et al. (2019). Genetic compensation triggered by mutant mRNA degradation. Nature *568*, 193–197.

El-Sammak, H., Yang, B., Guenther, S., Chen, W., Marín-Juez, R., and Stainier, D.Y.R. (2022). A Vegfc-Emilin2a-Cxcl8a Signaling Axis Required for Zebrafish Cardiac Regeneration. Circ. Res. *130*, 1014–1029.

Fernandez, C.E., Bakovic, M., and Karra, R. (2018). Endothelial contributions to zebrafish heart regeneration. J. Cardiovasc. Dev. Dis. *5*.

Ferraro, B., Leoni, G., Hinkel, R., Ormanns, S., Paulin, N., Ortega-Gomez, A., Viola, J.R., de Jong, R., Bongiovanni, D., Bozoglu, T., et al. (2019). Pro-Angiogenic Macrophage Phenotype to Promote Myocardial Repair. J. Am. Coll. Cardiol. *73*, 2990–3002.

Fox, S.E., Lu, W., Maheshwari, A., Christensen, R.D., and Calhoun, D.A. (2005). The effects and comparative differences of neutrophil specific chemokines on neutrophil chemotaxis of the neonate. Cytokine *29*, 135–140.

Fukuda, R., Marín-Juez, R., El-Sammak, H., Beisaw, A., Ramadass, R., Kuenne, C.,

Guenther, S., Konzer, A., Bhagwat, A.M., Graumann, J., et al. (2020). Stimulation of glycolysis promotes cardiomyocyte proliferation after injury in adult zebrafish. EMBO Rep. *21*.

Gabhann, F. Mac, and Peirce, S.M. (2010). Collateral capillary arterialization following arteriolar ligation in murine skeletal muscle. Microcirculation *17*, 333–347.

Gamba, L., Amin-Javaheri, A., Kim, J., Warburton, D., and Lien, C.L. (2017). Collagenolytic activity is associated with scar resolution in zebrafish hearts after cryoinjury. J. Cardiovasc. Dev. Dis. *4*.

Gancz, D., Raftrey, B.C., Perlmoter, G., Marín-Juez, R., Semo, J., Matsuoka, R.L., Karra, R., Raviv, H., Moshe, N., Addadi, Y., et al. (2019). Distinct origins and molecular mechanisms contribute to lymphatic formation during cardiac growth and regeneration. Elife *8*.

Gauvrit, S., Villasenor, A., Strilic, B., Kitchen, P., Collins, M.M., Marín-Juez, R., Guenther, S., Maischein, H.M., Fukuda, N., Canham, M.A., et al. (2018). HHEX is a transcriptional regulator of the VEGFC/FLT4/PROX1 signaling axis during vascular development. Nat. Commun. *9*.

Gemberling, M., Karra, R., Dickson, A.L., and Poss, K.D. (2015). Nrg1 is an injury-induced cardiomyocyte mitogen for the endogenous heart regeneration program in zebrafish. Elife *2015*.

Gerri, C., Marín-Juez, R., Marass, M., Marks, A., Maischein, H.M., and Stainier, D.Y.R. (2017). Hif-1α regulates macrophage-endothelial interactions during blood vessel development in zebrafish. Nat. Commun. *8*.

Glinton, K.E., Ma, W., Lantz, C.W., Grigoryeva, L.S., DeBerge, M., Liu, X., Febbraio, M., Kahn, M., Oliver, G., and Thorp, E.B. (2022). Macrophage-produced VEGFC is induced by efferocytosis to ameliorate cardiac injury and inflammation. J. Clin. Invest.

Gong, Y., and Koh, D.R. (2010). Neutrophils promote inflammatory angiogenesis via release of preformed VEGF in an in vivo corneal model. Cell Tissue Res. *339*, 437–448.

González-Rosa, J.M., Martín, V., Peralta, M., Torres, M., and Mercader, N. (2011). Extensive scar formation and regression during heart regeneration after cryoinjury in zebrafish. Development *138*, 1663–1674.

González-Rosa, J.M., Peralta, M., and Mercader, N. (2012). Pan-epicardial lineage tracing reveals that epicardium derived cells give rise to myofibroblasts and perivascular cells during zebrafish heart regeneration. Dev. Biol. *370*, 173–186.

González-Rosa, J.M., Burns, C.E., and Burns, C.G. (2017). Zebrafish heart regeneration: 15 years of discoveries. Regeneration *4*, 105–123.

González-Rosa, J.M., Sharpe, M., Field, D., Soonpaa, M.H., Field, L.J., Burns, C.E., and Burns, C.G. (2018). Myocardial Polyploidization Creates a Barrier to Heart Regeneration in Zebrafish. Dev. Cell *44*, 433–446.e7.

Le Guen, L., Karpanen, T., Schulte, D., Harris, N.C., Koltowska, K., Roukens, G.,

Bower, N.I., van Impel, A., Stacker, S.A., Achen, M.G., et al. (2014). Ccbe1 regulates Vegfc-mediated induction of Vegfr3 signaling during embryonic lymphangiogenesis. Dev. *141*, 1239–1249.

Gunawan, F., Gentile, A., Gauvrit, S., Stainier, D.Y.R., and Bensimon-Brito, A. (2020). Nfatc1 promotes interstitial cell formation during cardiac valve development in Zebrafish. Circ. Res. 968–984.

Guo, L., Akahori, H., Harari, E., Smith, S.L., Polavarapu, R., Karmali, V., Otsuka, F., Gannon, R.L., Braumann, R.E., Dickinson, M.H., et al. (2018). CD163+ macrophages promote angiogenesis and vascular permeability accompanied by inflammation in atherosclerosis. J. Clin. Invest. *128*, 1106–1124.

Gupta, V., and Poss, K.D. (2012). Clonally dominant cardiomyocytes direct heart morphogenesis. Nature *484*, 479–484.

Ha, H., Debnath, B., and Neamati, N. (2017). Role of the CXCL8-CXCR1/2 axis in cancer and inflammatory diseases. Theranostics *7*, 1543–1588.

Habib, G.B., Heibig, J., Forman, S.A., Brown, B.G., Roberts, R., Terrin, M.L., and Bolli, R. (1991). Influence of coronary collateral vessels on myocardial infarct size in humans. Results of Phase I thrombolysis in myocardial infarction (TIMI) trial. Circulation *83*, 739–746.

Haiko, P., Makinen, T., Keskitalo, S., Taipale, J., Karkkainen, M.J., Baldwin, M.E., Stacker, S.A., Achen, M.G., and Alitalo, K. (2008). Deletion of Vascular Endothelial Growth Factor C (VEGF-C) and VEGF-D Is Not Equivalent to VEGF Receptor 3 Deletion in Mouse Embryos. Mol. Cell. Biol. *28*, 4843–4850.

Han, J., Calvo, C.F., Kang, T.H., Baker, K.L., Park, J.H., Parras, C., Levittas, M., Birba, U., Pibouin-Fragner, L., Fragner, P., et al. (2015). Vascular Endothelial Growth Factor Receptor 3 Controls Neural Stem Cell Activation in Mice and Humans. Cell Rep. *10*, 1158–1172.

Harrison, M.R., Feng, X., Mo, G., Aguayo, A., Villafuerte, J., Yoshida, T., Pearson, C.A., Schulte-Merker, S., and Ching-Ling, L. (2019). Late developing cardiac lymphatic vasculature supports adult zebrafish heart function and regeneration. Elife *8*.

Harrison, M.R.M., Bussmann, J., Huang, Y., Zhao, L., Osorio, A., Burns, C.G., Burns, C.E., Sucov, H.M., Siekmann, A.F., and Lien, C.L. (2015). Chemokine-Guided Angiogenesis Directs Coronary Vasculature Formation in Zebrafish. Dev. Cell *33*, 442–454.

He, L., Liu, Q., Hu, T., Huang, X., Zhang, H., Tian, X., Yan, Y., Wang, L., Huang, Y., Miquerol, L., et al. (2016). Genetic lineage tracing discloses arteriogenesis as the main mechanism for collateral growth in the mouse heart. Cardiovasc. Res. *109*, 419–430.

Heidemann, J., Ogawa, H., Dwinell, M.B., Rafiee, P., Maaser, C., Gockel, H.R., Otterson, M.F., Ota, D.M., Lügering, N., Domschkell, W., et al. (2003). Angiogenic effects of interleukin 8 (CXCL8) in human intestinal microvascular endothelial cells are mediated by CXCR2. J. Biol. Chem. *278*, 8508–8515.

Hesselson, D., Anderson, R.M., Beinat, M., and Stainier, D.Y.R. (2009). Distinct

populations of quiescent and proliferative pancreatic β-cells identified by HOTcre mediated labeling. Proc. Natl. Acad. Sci. U. S. A. *106*, 14896–14901.

Hogan, B.M., Herpers, R., Witte, M., Heloterä, H., Alitalo, K., Duckers, H.J., and Schulte-Merker, S. (2009a). Vegfc/Flt4 signalling is suppressed by Dll4 in developing zebrafish intersegmental arteries. Development *136*, 4001–4009.

Hogan, B.M., Bos, F.L., Bussmann, J., Witte, M., Chi, N.C., Duckers, H.J., and Schulte-Merker, S. (2009b). Ccbe1 is required for embryonic lymphangiogenesis and venous sprouting. Nat. Genet. *41*, 396–398.

Honkoop, H., de Bakker, D.E.M., Aharonov, A., Kruse, F., Shakked, A., Nguyen, P.D., de Heus, C., Garric, L., J Muraro, M., Shoffner, A., et al. (2019). Single-cell analysis uncovers that metabolic reprogramming by ErbB2 signaling is essential for cardiomyocyte proliferation in the regenerating heart. Elife *8*.

Hu, B., Lelek, S., Spanjaard, B., Guedes Simões, M., Schäfer, R., Theis, F., Panáková, D., and Philipp Junker, J. (2021). Cellular drivers of injury response and regeneration in the adult zebrafish heart. bioRxiv 2021.01.07.425670.

Hu, N., Sedmera, D., Yost, H.J., and Clark, E.B. (2000). Structure and function of the developing zebrafish heart. Anat. Rec. *260*, 148–157.

Hui, S.P., Sheng, D.Z., Sugimoto, K., Gonzalez-Rajal, A., Nakagawa, S., Hesselson, D., and Kikuchi, K. (2017). Zebrafish Regulatory T Cells Mediate Organ-Specific Regenerative Programs. Dev. Cell *43*, 659–672.e5.

Jeltsch, M., Kaipainen, A., Joukov, V., Meng, X., Lakso, M., Rauvala, H., Swartz, M., Fukumura, D., Jain, R.K., and Alitalo, K. (1997). Hyperplasia of lymphatic vessels in VEGF-C transgenic mice. Science (80-.). *276*, 1423–1425.

Jeltsch, M., Jha, S.K., Tvorogov, D., Anisimov, A., Leppänen, V.M., Holopainen, T., Kivelä, R., Ortega, S., Kärpanen, T., and Alitalo, K. (2014). CCBE1 enhances lymphangiogenesis via a disintegrin and metalloprotease with thrombospondin motifs-3-mediated vascular endothelial growth factor-C activation. Circulation *129*, 1962–1971.

Jetten, N., Verbruggen, S., Gijbels, M.J., Post, M.J., De Winther, M.P.J., and Donners, M.M.P.C. (2014). Anti-inflammatory M2, but not pro-inflammatory M1 macrophages promote angiogenesis in vivo. Angiogenesis *17*, 109–118.

Jha, S.K., Rauniyar, K., Chronowska, E., Mattonet, K., Maina, E.W., Koistinen, H., Stenman, U.H., Alitalo, K., and Jeltsch, M. (2019). KLK3/PSA and cathepsin D activate VEGF-C and VEGF-D. Elife *8*.

Joukov, V., Sorsa, T., Kumar, V., Jeltsch, M., Claesson-Welsh, L., Cao, Y., Saksela, O., Kalkkinen, N., and Alitalo, K. (1997). Proteolytic processing regulates receptor specificity and activity of VEGF-C. EMBO J. *16*, 3898–3911.

Kapuria, S., Bai, H., Fierros, J., Huang, Y., Ma, F., Yoshida, T., Aguayo, A., Kok, F., Wiens, K.M., Yip, J.K., et al. (2022). Heterogeneous *pdgfrb*+ cells regulate coronary vessel development and revascularization during heart regeneration. Development *149*.

Karaman, S., Leppänen, V.M., and Alitalo, K. (2018). Vascular endothelial growth factor signaling in development and disease. Dev. *145*.

Karkkainen, M.J., Haiko, P., Sainio, K., Partanen, J., Taipale, J., Petrova, T. V., Jeltsch, M., Jackson, D.G., Talikka, M., Rauvala, H., et al. (2004). Vascular endothelial growth factor C is required for sprouting of the first lymphatic vessels from embryonic veins. Nat. Immunol. *5*, 74–80.

Kaur, H., Takefuji, M., Ngai, C.Y., Carvalho, J., Bayer, J., Wietelmann, A., Poetsch, A., Hoelper, S., Conway, S.J., Möllmann, H., et al. (2016). Targeted Ablation of Periostin-Expressing Activated Fibroblasts Prevents Adverse Cardiac Remodeling in Mice. Circ. Res. *118*, 1906–1917.

Kettleborough, R.N.W., Busch-Nentwich, E.M., Harvey, S.A., Dooley, C.M., De Bruijn, E., Van Eeden, F., Sealy, I., White, R.J., Herd, C., Nijman, I.J., et al. (2013). A systematic genome-wide analysis of zebrafish protein-coding gene function. Nature *496*, 494–497.

Kikuchi, K., Holdway, J.E., Werdich, A.A., Anderson, R.M., Fang, Y., Egnaczyk, G.F., Evans, T., MacRae, C.A., Stainier, D.Y.R., and Poss, K.D. (2010). Primary contribution to zebrafish heart regeneration by gata4+ cardiomyocytes. Nature *464*, 601–605.

Kikuchi, K., Holdway, J.E., Major, R.J., Blum, N., Dahn, R.D., Begemann, G., and Poss, K.D. (2011a). Retinoic Acid Production by Endocardium and Epicardium Is an Injury Response Essential for Zebrafish Heart Regeneration. Dev. Cell *20*, 397–404.

Kikuchi, K., Gupta, V., Wang, J., Holdway, J.E., Wills, A.A., Fang, Y., and Poss, K.D. (2011b). Tcf21+ epicardial cells adopt non-myocardial fates during zebrafish heart development and regeneration. Development *138*, 2895–2902.

Klaourakis, K., Vieira, J.M., and Riley, P.R. (2021). The evolving cardiac lymphatic vasculature in development, repair and regeneration. Nat. Rev. Cardiol.

Klotz, L., Norman, S., Vieira, J.M., Masters, M., Rohling, M., Dubé, K.N., Bollini, S., Matsuzaki, F., Carr, C.A., and Riley, P.R. (2015). Cardiac lymphatics are heterogeneous in origin and respond to injury. Nature *522*, 62–67.

Koch, S., and Claesson-Welsh, L. (2012). Signal transduction by vascular endothelial growth factor receptors. Cold Spring Harb. Perspect. Med. *2*.

Koch, A.E., Polverini, P.J., Kunkel, S.L., Harlow, L.A., DiPietro, L.A., Elner, V.M., Elner, S.G., and Strieter, R.M. (1992). Interleukin-8 as a macrophage-derived mediator of angiogenesis. Science (80-.). *258*, 1798–1801.

Koch, S., Tugues, S., Li, X., Gualandi, L., and Claesson-Welsh, L. (2011). Signal transduction by vascular endothelial growth factor receptors. Biochem. J. *437*, 169–183.

Kocijan, T., Rehman, M., Colliva, A., Groppa, E., Leban, M., Vodret, S., Volf, N., Zucca, G., Cappelletto, A., Piperno, G.M., et al. (2021). Genetic lineage tracing reveals poor angiogenic potential of cardiac endothelial cells. Cardiovasc. Res. *117*, 256–270.

Kolaczkowska, E., and Kubes, P. (2012). Angiogenic neutrophils: A novel

subpopulation paradigm. Blood *120*, 4455–4457.

Koopmans, T., van Beijnum, H., Roovers, E.F., Tomasso, A., Malhotra, D., Boeter, J., Psathaki, O.E., Versteeg, D., van Rooij, E., and Bartscherer, K. (2021). Ischemic tolerance and cardiac repair in the spiny mouse (Acomys). Npj Regen. Med. *6*.

Koth, J., Wang, X., Killen, A.C., Stockdale, W.T., Potts, H.G., Jefferson, A., Bonkhofer, F., Riley, P.R., Patient, R.K., Göttgens, B., et al. (2020). Runx1 promotes scar deposition and inhibits myocardial proliferation and survival during zebrafish heart regeneration. Dev. *147*.

Küchler, A.M., Gjini, E., Peterson-Maduro, J., Cancilla, B., Wolburg, H., and Schulte-Merker, S. (2006). Development of the Zebrafish Lymphatic System Requires Vegfc Signaling. Curr. Biol. *16*, 1244–1248.

Künnapuu, J., Bokharaie, H., and Jeltsch, M. (2021). Proteolytic Cleavages in the VEGF Family: Generating Diversity among Angiogenic VEGFs, Essential for the Activation of Lymphangiogenic VEGFs. Biology (Basel). *10*, 167.

Lai, S.L., Marín-Juez, R., Moura, P.L., Kuenne, C., Lai, J.K.H., Tsedeke, A.T., Guenther, S., Looso, M., and Stainier, D.Y.R. (2017). Reciprocal analyses in zebrafish and medaka reveal that harnessing the immune response promotes cardiac regeneration. Elife *6*.

Lai, S.L., Marín-Juez, R., and Stainier, D.Y.R. (2019). Immune responses in cardiac repair and regeneration: a comparative point of view. Cell. Mol. Life Sci. *76*, 1365–1380.

Lepilina, A., Coon, A.N., Kikuchi, K., Holdway, J.E., Roberts, R.W., Burns, C.G., and Poss, K.D. (2006). A Dynamic Epicardial Injury Response Supports Progenitor Cell Activity during Zebrafish Heart Regeneration. Cell *127*, 607–619.

Li, A., Dubey, S., Varney, M.L., Dave, B.J., and Singh, R.K. (2003). IL-8 Directly Enhanced Endothelial Cell Survival, Proliferation, and Matrix Metalloproteinases Production and Regulated Angiogenesis. J. Immunol. *170*, 3369–3376.

Li, F., Wang, X., Capasso, J.M., and Gerdes, A.M. (1996). Rapid transition of cardiac myocytes from hyperplasia to hypertrophy during postnatal development. J. Mol. Cell. Cardiol. *28*, 1737–1746.

Liao, Y., Smyth, G.K., and Shi, W. (2014). FeatureCounts: An efficient general purpose program for assigning sequence reads to genomic features. Bioinformatics *30*, 923–930.

Lien, C.L., Schebesta, M., Makino, S., Weber, G.J., and Keating, M.T. (2006). Gene expression analysis of zebrafish heart regeneration. PLoS Biol. *4*, 1386–1396.

Livak, K.J., and Schmittgen, T.D. (2001). Analysis of relative gene expression data using real-time quantitative PCR and the 2-ΔΔCT method. Methods *25*, 402–408.

Love, M.I., Huber, W., and Anders, S. (2014). Moderated estimation of fold change and dispersion for RNA-seq data with DESeq2. Genome Biol. *15*.

Lowe, V., Wisniewski, L., Sayers, J., Evans, I., Frankel, P., Mercader-Huber, N.,

Zachary, I.C., and Pellet-Many, C. (2019). Neuropilin 1 mediates epicardial activation and revascularization in the regenerating zebrafish heart. Dev. *146*.

Lupu, I.E., De Val, S., and Smart, N. (2020). Coronary vessel formation in development and disease: mechanisms and insights for therapy. Nat. Rev. Cardiol. *17*, 790–806.

Marastoni, S., Andreuzzi, E., Paulitti, A., Colladel, R., Pellicani, R., Todaro, F., Schiavinato, A., Bonaldo, P., Colombatti, A., and Mongiat, M. (2014). EMILIN2 down-modulates the Wnt signalling pathway and suppresses breast cancer cell growth and migration. J. Pathol. *232*, 391–404.

Marín-Juez, R., Marass, M., Gauvrit, S., Rossi, A., Lai, S.-L., Materna, S.C., Black, B.L., and Stainier, D.Y.R. (2016). Fast revascularization of the injured area is essential to support zebrafish heart regeneration. Proc. Natl. Acad. Sci. U. S. A. *113*, 11237–11242.

Marín-Juez, R., El-Sammak, H., Helker, C.S.M., Kamezaki, A., Mullapuli, S.T., Bibli, S.I., Foglia, M.J., Fleming, I., Poss, K.D., and Stainier, D.Y.R. (2019). Coronary Revascularization During Heart Regeneration Is Regulated by Epicardial and Endocardial Cues and Forms a Scaffold for Cardiomyocyte Repopulation. Dev. Cell *51*, 503–515.e4.

Marques, I.J., Lupi, E., and Mercader, N. (2019). Model systems for regeneration: Zebrafish. Dev. *146*.

Martin-Puig, S., Wang, Z., and Chien, K.R. (2008). Lives of a Heart Cell: Tracing the Origins of Cardiac Progenitors. Cell Stem Cell *2*, 320–331.

Matsuo, Y., Ochi, N., Sawai, H., Yasuda, A., Takahashi, H., Funahashi, H., Takeyama, H., Tong, Z., and Guha, S. (2009). CXCL8/IL-8 and CXCL12/SDF-lα co-operatively promote invasiveness and angiogenesis in pancreatic cancer. Int. J. Cancer *124*, 853–861.

Matsuoka, R.L., Marass, M., Avdesh, A., Helker, C.S.M., Maischein, H.M., Grosse, A.S., Kaur, H., Lawson, N.D., Herzog, W., and Stainier, D.Y.R. (2016). Radial glia regulate vascular patterning around the developing spinal cord. Elife *5*.

MAURO, A. (1961). Satellite cell of skeletal muscle fibers. J. Biophys. Biochem. Cytol. *9*, 493–495.

Mehta, A.S., and Singh, A. (2019). Insights into regeneration tool box: An animal model approach. Dev. Biol. *453*, 111–129.

Meyers, J.R. (2018). Zebrafish: Development of a Vertebrate Model Organism. Curr. Protoc. Essent. Lab. Tech. *16*.

Milanetto, M., Tiso, N., Braghetta, P., Volpin, D., Argenton, F., and Bonaldo, P. (2008). Emilin genes are duplicated and dynamically expressed during zebrafish embryonic development. Dev. Dyn. *237*, 222–232.

Mongiat, M., Marastoni, S., Ligresti, G., Lorenzon, E., Schiappacassi, M., Perris, R., Frustaci, S., and Colombatti, A. (2010). The extracellular matrix glycoprotein elastin

microfibril interface located protein 2: A dual role in the tumor microenvironment. Neoplasia *12*, 294–304.

Mongiat, M., Andreuzzi, E., Tarticchio, G., and Paulitti, A. (2016). Extracellular matrix, a hard player in angiogenesis. Int. J. Mol. Sci. *17*.

Moore-Morris, T., Guimarães-Camboa, N., Banerjee, I., Zambon, A.C., Kisseleva, T., Velayoudon, A., Stallcup, W.B., Gu, Y., Dalton, N.D., Cedenilla, M., et al. (2014). Resident fibroblast lineages mediate pressure overload-induced cardiac fibrosis. J. Clin. Invest. *124*, 2921–2934.

Münch, J., Grivas, D., González-Rajal, Á., Torregrosa-Carrión, R., and de la Pompa, J.L. (2017). Notch signalling restricts inflammation and Serpine1 expression in the dynamic endocardium of the regenerating zebrafish heart. Dev. *144*, 1425–1440.

Murphy, P.M., and Tiffany, H.L. (1991). Cloning of complementary DNA encoding a functional human interleukin-8 receptor. Science (80-.). *253*, 1280–1283.

Nicenboim, J., Malkinson, G., Lupo, T., Asaf, L., Sela, Y., Mayseless, O., Gibbs-Bar, L., Senderovich, N., Hashimshony, T., Shin, M., et al. (2015). Lymphatic vessels arise from specialized angioblasts within a venous niche. Nature *522*, 56–61.

Norris, R.A., Borg, T.K., Butcher, J.T., Baudino, T.A., Banerjee, I., and Markwald, R.R. (2008). Neonatal and adult cardiovascular pathophysiological remodeling and repair: Developmental role of periostin. In Annals of the New York Academy of Sciences, pp. 30–40.

Ogle, B.M., Bursac, N., Domian, I., Huang, N.F., Menasché, P., Murry, C.E., Pruitt, B., Radisic, M., Wu, J.C., Wu, S.M., et al. (2016). Distilling complexity to advance cardiac tissue engineering. Sci. Transl. Med. *8*.

Oh, S.J., Jeltsch, M.M., Birkenhäger, R., McCarthy, J.E.G., Weich, H.A., Christ, B., Alitalo, K., and Wilting, J. (1997). VEGF and VEGF-C: Specific induction of angiogenesis and lymphangiogenesis in the differentiated avian chorioallantoic membrane. Dev. Biol. *188*, 96–109.

Okuda, K.S., Astin, J.W., Misa, J.P., Flores, M. V., Crosier, K.E., and Crosier, P.S. (2012). Lyve1 expression reveals novel lymphatic vessels and new mechanisms for lymphatic vessel development in zebrafish. Dev. *139*, 2381–2391.

De Oliveira, S., Rosowski, E.E., and Huttenlocher, A. (2016). Neutrophil migration in infection and wound repair: Going forward in reverse. Nat. Rev. Immunol. *16*, 378–391.

Olsson, A.K., Dimberg, A., Kreuger, J., and Claesson-Welsh, L. (2006). VEGF receptor signalling - In control of vascular function. Nat. Rev. Mol. Cell Biol. *7*, 359–371.

Pätilä, T., Ikonen, T., Rutanen, J., Ahonen, A., Lommi, J., Lappalainen, K., Krogerus, L., Ihlberg, L., Partanen, T.A., Lähteenoja, L., et al. (2006). Vascular endothelial growth factor C-induced collateral formation in a model of myocardial ischemia. J. Hear. Lung Transplant. *25*, 206–213.

Paulitti, A., Andreuzzi, E., Bizzotto, D., Pellicani, R., Tarticchio, G., Marastoni, S., Pastrello, C., Jurisica, I., Ligresti, G., Bucciotti, F., et al. (2018). The ablation of the matricellular protein EMILIN2 causes defective vascularization due to impaired EGFR-dependent IL-8 production affecting tumor growth. Oncogene *37*, 3399–3414.

Pfeffer, M.A., and Braunwald, E. (1990). Ventricular remodeling after myocardial infarction: Experimental observations and clinical implications. Circulation *81*, 1161–1172.

Porrello, E.R., Mahmoud, A.I., Simpson, E., Hill, J.A., Richardson, J.A., Olson, E.N., and Sadek, H.A. (2011). Transient regenerative potential of the neonatal mouse heart. Science (80-.). *331*, 1078–1080.

Poss, K.D., Wilson, L.G., and Keating, M.T. (2002). Heart regeneration in zebrafish. Science (80-.). *298*, 2188–2190.

Powell, D., Tauzin, S., Hind, L.E., Deng, Q., Beebe, D.J., and Huttenlocher, A. (2017). Chemokine Signaling and the Regulation of Bidirectional Leukocyte Migration in Interstitial Tissues. Cell Rep. *19*, 1572–1585.

Puente, B.N., Kimura, W., Muralidhar, S.A., Moon, J., Amatruda, J.F., Phelps, K.L., Grinsfelder, D., Rothermel, B.A., Chen, R., Garcia, J.A., et al. (2014). The oxygen-rich postnatal environment induces cardiomyocyte cell-cycle arrest through DNA damage response. Cell *157*, 565–579.

Qi, J., Rittershaus, A., Priya, R., Mansingh, S., Stainier, D.Y., and Helker, C.S. (2022). Apelin signaling dependent endocardial protrusions promote cardiac trabeculation in zebrafish. Elife *11*.

Quaife-Ryan, G.A., Sim, C.B., Ziemann, M., Kaspi, A., Rafehi, H., Ramialison, M., El-Osta, A., Hudson, J.E., and Porrello, E.R. (2017). Multicellular transcriptional analysis of mammalian heart regeneration. Circulation *136*, 1123–1139.

Quijada, P., Trembley, M.A., and Small, E.M. (2020). The Role of the Epicardium during Heart Development and Repair. Circ. Res. 377–394.

Rafii, S., Butler, J.M., and Ding, B. Sen (2016). Angiocrine functions of organ-specific endothelial cells. Nature *529*, 316–325.

Räsänen, M., Sultan, I., Paech, J., Hemanthakumar, K.A., Yu, W., He, L., Tang, J., Sun, Y., Hlushchuk, R., Huan, X., et al. (2021). VEGF-B Promotes Endocardium-Derived Coronary Vessel Development and Cardiac Regeneration. Circulation 65–77.

Rasouli, S.J., and Stainier, D.Y.R. (2017). Regulation of cardiomyocyte behavior in zebrafish trabeculation by Neuregulin 2a signaling. Nat. Commun. *8*.

Rhee, S., Paik, D.T., Yang, J.Y., Nagelberg, D., Williams, I., Tian, L., Roth, R., Chandy, M., Ban, J., Belbachir, N., et al. (2021). Endocardial/endothelial angiocrines regulate cardiomyocyte development and maturation and induce features of ventricular non-compaction. Eur. Heart J. *42*, 4264–4276.

Rienks, M., Papageorgiou, A.-P., Frangogiannis, N.G., and Heymans, S. (2014). Myocardial Extracellular Matrix. Circ. Res. *114*, 872–888.

Robich, M.P., Chu, L.M., Oyamada, S., Sodha, N.R., and Sellke, F.W. (2011). Myocardial therapeutic angiogenesis: A review of the state of development and future obstacles. Expert Rev. Cardiovasc. Ther. *9*, 1469–1479.

Rossi, A., Kontarakis, Z., Gerri, C., Nolte, H., Hölper, S., Krüger, M., and Stainier, D.Y.R. (2015). Genetic compensation induced by deleterious mutations but not gene knockdowns. Nature *524*, 230–233.

Rossi, A., Gauvrit, S., Marass, M., Pan, L., Moens, C.B., and Stainier, D.Y.R. (2016). Regulation of Vegf signaling by natural and synthetic ligands. Blood *128*, 2359–2366.

S.T., D., L., R., A., G.-P., J., S., A., R., R.P., G., and K., R. (2010). Monomeric and dimeric CXCL8 are both essential for in vivo neutrophil recruitment. PLoS One *5*, e11754.

Sabia, P.J., Powers, E.R., Ragosta, M., Sarembock, I.J., Burwell, L.R., and Kaul, S. (1992). An Association between Collateral Blood Flow and Myocardial Viability in Patients with Recent Myocardial Infarction. N. Engl. J. Med. *327*, 1825–1831.

Sánchez-Iranzo, H., Galardi-Castilla, M., Sanz-Morejón, A., González-Rosa, J.M., Costa, R., Ernst, A., de Aja, J.S., Langa, X., and Mercader, N. (2018). Transient fibrosis resolves via fibroblast inactivation in the regenerating zebrafish heart. Proc. Natl. Acad. Sci. U. S. A. *115*, 4188–4193.

Sanz-Morejón, A., and Mercader, N. (2020). Recent insights into zebrafish cardiac regeneration. Curr. Opin. Genet. Dev. *64*, 37–43.

Schnabel, K., Wu, C.C., Kurth, T., and Weidinger, G. (2011). Regeneration of cryoinjury induced necrotic heart lesions in zebrafish is associated with epicardial activation and cardiomyocyte proliferation. PLoS One *6*.

Secker, G.A., and Harvey, N.L. (2015). VEGFR signaling during lymphatic vascular development: From progenitor cells to functional vessels. Dev. Dyn. *244*, 323–331.

Seiler, C., Stoller, M., Pitt, B., and Meier, P. (2013). The human coronary collateral circulation: Development and clinical importance. Eur. Heart J. *34*, 2674–2682.

Shi, J., and Wei, P.K. (2016). Interleukin-8: A potent promoter of angiogenesis in gastric cancer. Oncol. Lett. *11*, 1043–1050.

Simões, F.C., Cahill, T.J., Kenyon, A., Gavriouchkina, D., Vieira, J.M., Sun, X., Pezzolla, D., Ravaud, C., Masmanian, E., Weinberger, M., et al. (2020). Macrophages directly contribute collagen to scar formation during zebrafish heart regeneration and mouse heart repair. Nat. Commun. *11*.

Soonpaa, M.H., Kim, K.K., Pajak, L., Franklin, M., and Field, L.J. (1996). Cardiomyocyte DNA synthesis and binucleation during murine development. Am. J. Physiol. - Hear. Circ. Physiol. *271*.

Srivastava, D., and DeWitt, N. (2016). In Vivo Cellular Reprogramming: The Next Generation. Cell *166*, 1386–1396.

Stacker, S.A., Stenvers, K., Caesar, C., Vitali, A., Domagala, T., Nice, E., Roufail, S., Simpson, R.J., Moritz, R., Karpanen, T., et al. (1999). Biosynthesis of vascular

endothelial growth factor-D involves proteolytic processing which generates non-covalent homodimers. J. Biol. Chem. *274*, 32127–32136.

Stoll, S.J., Bartsch, S., Augustin, H.G., and Kroll, J. (2011). The transcription factor HOXC9 regulates endothelial cell quiescence and vascular morphogenesis in zebrafish via inhibition of interleukin 8. Circ. Res. *108*, 1367–1377.

Stoyek, M.R., Croll, R.P., and Smith, F.M. (2015). Intrinsic and extrinsic innervation of the heart in zebrafish (Danio rerio). J. Comp. Neurol. *523*, 1683–1700.

Strieter, R.M., Kunkel, S.L., Elner, V.M., Martonyi, C.L., Koch, A.E., Polverini, P.J., and Elner, S.G. (1992). Interleukin-8: A corneal factor that induces neovascularization. Am. J. Pathol. *141*, 1279–1284.

Talman, V., and Ruskoaho, H. (2016). Cardiac fibrosis in myocardial infarction—from repair and remodeling to regeneration. Cell Tissue Res. *365*, 563–581.

Tazzyman, S., Lewis, C.E., and Murdoch, C. (2009). Neutrophils: Key mediators of tumour angiogenesis. Int. J. Exp. Pathol. *90*, 222–231.

Tian, X., and Zhou, B. (2022). Coronary vessel formation in development and regeneration: origins and mechanisms. J. Mol. Cell. Cardiol. *167*, 67–82.

Tombor, L.S., John, D., Glaser, S.F., Luxán, G., Forte, E., Furtado, M., Rosenthal, N., Baumgarten, N., Schulz, M.H., Wittig, J., et al. (2021). Single cell sequencing reveals endothelial plasticity with transient mesenchymal activation after myocardial infarction. Nat. Commun. *12*.

Travers, J.G., Kamal, F.A., Robbins, J., Yutzey, K.E., and Blaxall, B.C. (2016). Cardiac fibrosis: The fibroblast awakens. Circ. Res. *118*, 1021–1040.

Tsedeke, A.T., Allanki, S., Gentile, A., Jimenez-Amilburu, V., Rasouli, S.J., Guenther, S., Lai, S.L., Stainier, D.Y.R., and Marín-Juez, R. (2021). Cardiomyocyte heterogeneity during zebrafish development and regeneration. Dev. Biol. *476*, 259–271.

Tzahor, E., and Poss, K.D. (2017). Cardiac regeneration strategies: Staying young at heart. Science (80-.). *356*, 1035–1039.

Vieira, J.M., Norman, S., Del Campo, C.V., Cahill, T.J., Barnette, D.N., Gunadasa-Rohling, M., Johnson, L.A., Greaves, D.R., Carr, C.A., Jackson, D.G., et al. (2018). The cardiac lymphatic system stimulates resolution of inflammation following myocardial infarction. J. Clin. Invest. *128*, 3402–3412.

Villefranc, J.A., Nicoli, S., Bentley, K., Jeltsch, M., Zarkada, G., Moore, J.C., Gerhardt, H., Alitalo, K., and Lawson, N.D. (2013). A truncation allele in vascular endothelial growth factor c reveals distinct modes of signaling during lymphatic and vascular development. Development *140*, 1497–1506.

Virag, J.A.I., Rolle, M.L., Reece, J., Hardouin, S., Feigl, E.O., and Murry, C.E. (2007). Fibroblast growth factor-2 regulates myocardial infarct repair: Effects on cell proliferation, scar contraction, and ventricular function. Am. J. Pathol. *171*, 1431–1440.

Vivien, C.J., Pichol-Thievend, C., Sim, C.B., Smith, J.B., Bower, N.I., Hogan, B.M.,

Hudson, J.E., Francois, M., and Porrello, E.R. (2019). Vegfc/d-dependent regulation of the lymphatic vasculature during cardiac regeneration is influenced by injury context. Npj Regen. Med. *4*.

Wang, J., Panáková, D., Kikuchi, K., Holdway, J.E., Gemberling, M., Burris, J.S., Singh, S.P., Dickson, A.L., Lin, Y.F., Khaled Sabeh, M., et al. (2011). The regenerative capacity of zebrafish reverses cardiac failure caused by genetic cardiomyocyte depletion. Development *138*, 3421–3430.

Wang, J., Karra, R., Dickson, A.L., and Poss, K.D. (2013). Fibronectin is deposited by injury-activated epicardial cells and is necessary for zebrafish heart regeneration. Dev. Biol. *382*, 427–435.

Wang, J., Cao, J., Dickson, A.L., and Poss, K.D. (2015). Epicardial regeneration is guided by cardiac outflow tract and Hedgehog signalling. Nature *522*, 226–230.

White, J.R., Lee, J.M., Young, P.R., Hertzberg, R.P., Jurewicz, A.J., Chaikin, M.A., Widdowson, K., Foley, J.J., Martin, L.D., Griswold, D.E., et al. (1998). Identification of a potent, selective non-peptide CXCR2 antagonist that inhibits interleukin-8-induced neutrophil migration. J. Biol. Chem. *273*, 10095–10098.

WHO (2020). The top 10 causes of death - Factsheet. WHO Reports 1–9.

Wu, B., Zhang, Z., Lui, W., Chen, X., Wang, Y., Chamberlain, A.A., Moreno-Rodriguez, R.A., Markwald, R.R., O'Rourke, B.P., Sharp, D.J., et al. (2012). Endocardial cells form the coronary arteries by angiogenesis through myocardial-endocardial VEGF signaling. Cell *151*, 1083–1096.

Wu, C.C., Jeratsch, S., Graumann, J., and Stainier, D.Y.R. (2020). Modulation of Mammalian Cardiomyocyte Cytokinesis by the Extracellular Matrix. Circ. Res. *127*, 896–907.

Zeisberg, E.M., Tarnavski, O., Zeisberg, M., Dorfman, A.L., McMullen, J.R., Gustafsson, E., Chandraker, A., Yuan, X., Pu, W.T., Roberts, A.B., et al. (2007). Endothelial-to-mesenchymal transition contributes to cardiac fibrosis. Nat. Med. *13*, 952–961.

Zhou, B., Honor, L.B., He, H., Qing, M., Oh, J.H., Butterfield, C., Lin, R.Z., Melero-Martin, J.M., Dolmatova, E., Duffy, H.S., et al. (2011). Adult mouse epicardium modulates myocardial injury by secreting paracrine factors. J. Clin. Invest. *121*, 1894–1904.

Zhou, X., Rowe, R.G., Hiraoka, N., George, J.P., Wirtz, D., Mosher, D.F., Virtanen, I., Chernousov, M.A., and Weiss, S.J. (2008). Fibronectin fibrillogenesis regulates three-dimensional neovessel formation. Genes Dev. *22*, 1231–1243.

10. APPENDIX

10.1. List of abbreviations

Abbreviation	Description
µg	microgram
µl	microliter
µm	micrometer
µM	micromolar
4-OHT	4-Hydroxytamoxifen
AFOG	Acid Fuchsin Orange G
AP	Alkaline Phosphatase
BFP	Blue fluorescent protein
bp	basepair
BSA	Bovine serum albumin
CA	constitutively active
$CaCl_2$	Calcium Chloride
CAD	Coronary artery disease
cDNA	Complementary DNA
CDS	Coding sequence
cEC	Coronary Endothelial Cell
Clo-Lipo	Clodronate Liposomes
CM	Cardiomyocyte
cm	centimeter
Cre	cyclic recombinase
CRISPR	Clustered Regularly Interspaced Short Palindromic Repeats

CVD	Cardiovascular diseases
cxcl12	C-X-C motif chemokine ligand 12
cxcl8	C-X-C motif chemokine ligand 8
cxcr1	C-X-C motif Chemokine Receptor 1
cxcr2	C-X-C motif Chemokine Receptor 2
cxcr4	C-X-C motif Chemokine Receptor 4
cyp26a1	cytochrome p450 26a1
DAPI	4',6-diamidino-2-phenylindole
ddH2O	double distilled water
DEPC	Diethyl pyrocarbonate
DIG	Digoxygenin
DMSO	Dimethyl sulfoxide
DN	Dominant negative
DNA	Deoxyribonucleic acid
DNase	Deoxyribonuclease
dNTP	Nucleoside triphosphate
dpa	Days post amputation
dpci	Days post cryoinjury
dpf	Days post fertilization
dpMI	days post myocardial infarction
DSHB	Developmental Studies Hybridoma Bank
EC	Endothelial cell
E.coli	Escherichia coli
ECM	Extracellular matrix

EDTA	Ethylenediaminetetraacetic acid
EdU	5-ethynyl-2′-deoxyuridine
EGF	Epidermal growth factor
EGFP	Enhanced Green Fluorescent Protein
EGM	Endothelial growth medium
embCMHC	embryonic Cardiac Myosin Heavy Chain
EMT	Epithelial-to-mesenchymal transition
EndoMT	Endothelial-to-mesenchymal transition
EPDCs	Epicardial derived cells
Et	Enhancer trap
FC	Fold change
FGF	Fibroblast growth factor
g	gram
gata4	GATA binding protein 4
GFP	Green Fluorescent Protein
H&E	Hematoxyline and eosin
H_2O_2	Hydrogen peroxide
HCl	Hydrochloric acid
hif1	hypoxia inducible factor
hpa	Hours post amputation
hpci	Hours post cryoinjury
HRMA	High Resolution Melt Analysis
hrs	hours
HUVECs	Human umbilical vein endothelial cells

IGF	Insulin-like growth factor
IHC	Immunohistochemistry
ISH	In situ hybridization
jak	janus kinase
kb	kilobase
KCl	Potassium Chloride
L	Liter
LB	Lysogeny broth
lit	Liter
LOF	Loss of function
lox	Lysyl Oxidase
LoxP	locus of X-over P1
LSM	Laser scanning microscope
LV	left ventricle
m	meter
M	molar
MEF2C	Myocyte Enhancer Factor 2C
Mek-Erk	Mitogen-activated protein kinase kinase – extracellular signal–regulated kinase
$MgCl_2$	Magnesium Chloride
$MgSO_4$	Magnesium sulphate
MHC	Myosin heavy chain
MI	Myocardial infarction
mins	minutes
miRNA	micro RNA

MLCK	Myosin Light Chain Kinase
mm	millimeter
MMP	Matrix metalloproteinase
mRNA	messenger RNA
myl7	myosin light chain 7
Na_2HPO_4	Disodium phosphate
NaCl	Sodium chloride
NaOH	Sodium hydroxide
NF-κB	Nuclear factor kappa light chain enhancer of activated B cells
ng	nanogram
nm	nanometer
nrg	neuregulin
OCT	Optimal cutting temperature
OE	overexpression
O/N	overnight
PBS	Phosphate buffered saline
PCNA	Proliferating cell nuclear antigen
PCR	Polymerase chain reaction
PFA	Paraformaldehyde
pg	picogram
pH	negative log of hydrogen ion concentration
Pi3k-Akt	Phosphatidylinositol 3-kinase – protein kinase B
postnb	periostin b
RA	Retinoic acid

raldh2	retinaldehyde dehydrogenase 2
RFP	Red fluorescent protein
rh	recombinant human
rm	recombinant mouse
RNA	Ribonucleic acid
RNase	Ribonuclease
rpl13a	60s ribosomal protein L13a
RPM	rotations per minute
RT	room temperature
RT-qPCR	Real-time quantitative PCR
RV	right ventricle
s	second
S.D.	Standard deviation
S.E.M.	Standard error of mean
siRNA	Small interfering RNA
SSC	Saline sodium citrate
tbx18	T-box transcription factor 18
tcf21	transcription factor 21
TGF-β	Transforming growth factor beta
Tricaine	Ethyl-m-aminobenzoate methanesulfonate
tRNA	transfer RNA
U	unit
UV	Ultra violet
V	volt

vegfa	Vascular endothelial growth factor A
vegfb	Vascular endothelial growth factor B
vegfc	Vascular endothelial growth factor C
vegfd	Vascular endothelial growth factor D
vegfr1	Vascular endothelial growth factor receptor 1
vegfr2	Vascular endothelial growth factor receptor 2
vegfr3	Vascular endothelial growth factor receptor 3
WNT	Wingless-related integration site
WT	Wild type
wt1b	Wilm's tumour 1b
ZIRC	Zebrafish International Resource Center

10.2. List of genes differentially expressed in *Tg(hsp70l:sflt4)* at 24 hpci.

Table 10.1. List of genes significantly differentially expressed in *Tg(hsp70l:sflt4)* at 24 hpci.

Ensembl gene ID	Ensembl gene	log2 Fold Change TG/WT
ENSDARG00000103716	*si:busm1-194e12.11*	7.63
ENSDARG00000021265	*mybpc2b*	7.21
ENSDARG00000070579	*ggact.3*	6.54
ENSDARG00000104635	*CU929676.1*	6.47
ENSDARG00000111788	*BX511067.1*	5.79
ENSDARG00000053502	*cryaa*	5.76
ENSDARG00000096690	*CR376838.1*	5.47
ENSDARG00000013856	*amy2a*	5.34
ENSDARG00000060034	*tmem151ba*	5.18

ENSDARG00000078994	*muc2.2*	5.04
ENSDARG00000103260	*si:ch211-57b15.1*	5.00
ENSDARG00000043798	*ms4a17a.1*	4.91
ENSDARG00000100991	*chrna3*	4.75
ENSDARG00000039747	*BX914200.1*	4.65
ENSDARG00000098216	*si:ch211-215e19.3*	4.57
ENSDARG00000095179	*si:ch211-235f1.3*	4.48
ENSDARG00000092770	*si:ch211-253p18.2*	4.48
ENSDARG00000057173	*ifit8*	4.36
ENSDARG00000096949	*si:dkey-197j19.5*	4.31
ENSDARG00000053563	*ms4a17a.12*	4.31
ENSDARG00000100721	*TRIM35*	4.28
ENSDARG00000079657	*si:dkey-53k12.1*	4.25
ENSDARG00000015854	*chata*	4.10
ENSDARG00000100449	*BX322631.1*	3.77
ENSDARG00000075352	*brinp3b*	3.59
ENSDARG00000098131	*BX511136.1*	3.52
ENSDARG00000105118	*zgc:171566*	3.40
ENSDARG00000101535	*col10a1b*	3.28
ENSDARG00000019763	*acp5a*	2.99
ENSDARG00000116524	*zgc:103700*	2.88
ENSDARG00000097596	*tac3b*	2.73
ENSDARG00000098803	*cyp2aa4*	2.48
ENSDARG00000043396	*fndc4a*	2.41
ENSDARG00000026165	*col11a1a*	2.31
ENSDARG00000003994	*syt9a*	2.31
ENSDARG00000075963	*mhc1uba*	2.29
ENSDARG00000002509	*zgc:153911*	2.23
ENSDARG00000090901	*si:ch211-256e16.11*	2.21
ENSDARG00000105162	*CR293509.1*	2.16
ENSDARG00000110878	*si:dkey-28k24.2*	2.16
ENSDARG00000093198	*c3a.4*	2.11

ENSDARG00000010729	*CABZ01073795.1*	2.11
ENSDARG00000042332	*plin2*	2.11
ENSDARG00000105033	*BX897691.1*	2.10
ENSDARG00000100520	*si:dkey-25o1.7*	1.96
ENSDARG00000076090	*jakmip1*	1.92
ENSDARG00000075785	*HERC5*	1.85
ENSDARG00000008732	*zgc:66479*	1.84
ENSDARG00000076182	*stat1b*	1.83
ENSDARG00000038587	*CU929150.1*	1.82
ENSDARG00000105355	*zgc:165555*	1.80
ENSDARG00000105258	*cep72*	1.77
ENSDARG00000075757	*gig2e*	1.75
ENSDARG00000089463	*dhx58*	1.75
ENSDARG00000100313	*pip5k1cb*	1.67
ENSDARG00000096562	*wu:fj29h11*	1.61
ENSDARG00000115425	*CABZ01038524.1*	1.56
ENSDARG00000021688	*mxa*	1.56
ENSDARG00000069563	*zgc:153151*	1.56
ENSDARG00000096906	*si:dkey-7i4.24*	1.55
ENSDARG00000103760	*cfhl2*	1.53
ENSDARG00000071586	*tgfbi*	1.52
ENSDARG00000095298	*ftr73*	1.51
ENSDARG00000041257	*smtnl1*	1.50
ENSDARG00000035101	*dicp2.1*	1.50
ENSDARG00000088908	*CU570691.1*	1.48
ENSDARG00000040528	*lgals3bpb*	1.48
ENSDARG00000053204	*snx22*	1.45
ENSDARG00000055133	*cenpf*	1.44
ENSDARG00000032820	*rxfp2a*	1.43
ENSDARG00000093623	*CR392341.1*	1.42
ENSDARG00000093044	*si:ch211-161h7.5*	1.42
ENSDARG00000055377	*gnb5b*	1.41

ENSDARG00000079327	*hmcn2*	1.41
ENSDARG00000086703	*si:dkey-126g1.7*	1.38
ENSDARG00000025903	*lgals9l1*	1.35
ENSDARG00000033355	*zgc:101699*	1.33
ENSDARG00000024365	*crlf1a*	1.33
ENSDARG00000100442	*cfh*	1.29
ENSDARG00000024877	*ptgr1*	1.29
ENSDARG00000075263	*ankrd1a*	1.29
ENSDARG00000068275	*ptx3a*	1.28
ENSDARG00000076140	*clcf1*	1.28
ENSDARG00000078468	*fap*	1.27
ENSDARG00000103466	*ccl35.1*	1.26
ENSDARG00000060094	*ptgis*	1.26
ENSDARG00000089362	*grn1*	1.25
ENSDARG00000093098	*ccl34b.8*	1.25
ENSDARG00000071095	*abi3bpb*	1.19
ENSDARG00000036104	*MYO1G*	1.18
ENSDARG00000099546	*kynu*	1.18
ENSDARG00000086337	*si:dkey-102g19.3*	1.17
ENSDARG00000038583	*abraa*	1.16
ENSDARG00000040076	*pycard*	1.15
ENSDARG00000014215	*cdh13*	1.15
ENSDARG00000037539	*tnnc1b*	1.15
ENSDARG00000013022	*si:ch211-59h6.1*	1.13
ENSDARG00000027345	*mpzl2b*	1.11
ENSDARG00000018809	*abhd3*	1.09
ENSDARG00000058348	*scinlb*	1.08
ENSDARG00000052567	*tmem35*	1.05
ENSDARG00000035907	*fam49al*	1.04
ENSDARG00000026766	*bcl2l10*	1.04
ENSDARG00000071658	*ywhag2*	1.02
ENSDARG00000026417	*ccr12b.2*	1.01

ENSDARG00000058731	*slc2a6*	1.01
ENSDARG00000035018	*thy1*	1.00
ENSDARG00000056026	*tprg1*	0.99
ENSDARG00000089079	*si:ch211-214b16.3*	0.99
ENSDARG00000099874	*agap2*	0.99
ENSDARG00000002986	*gda*	0.99
ENSDARG00000016691	*cd9b*	0.98
ENSDARG00000052783	*cdc42ep3*	0.98
ENSDARG00000019307	*dusp5*	0.97
ENSDARG00000089667	*MFAP4*	0.96
ENSDARG00000030743	*sptlc3*	0.94
ENSDARG00000057323	*e2f8*	0.93
ENSDARG00000099969	*zgc:152863*	0.93
ENSDARG00000099674	*dicp3.3*	0.92
ENSDARG00000042983	*has1*	0.91
ENSDARG00000038095	*socs1a*	0.91
ENSDARG00000031506	*flvcr2b*	0.89
ENSDARG00000100461	*CABZ01078737.1*	0.88
ENSDARG00000019815	*fn1a*	0.86
ENSDARG00000039579	*cfd*	0.85
ENSDARG00000017504	*si:ch211-1o7.3*	0.83
ENSDARG00000074818	*si:cabz01036022.1*	0.83
ENSDARG00000094451	*cfp*	0.83
ENSDARG00000077975	*si:ch73-343l4.8*	0.83
ENSDARG00000042496	*parp12a*	0.82
ENSDARG00000000002	*ccdc80*	0.82
ENSDARG00000075818	*dok2*	0.82
ENSDARG00000076312	*myot*	0.81
ENSDARG00000102798	*mcm2*	0.80
ENSDARG00000067751	*si:rp71-68n21.9*	0.80
ENSDARG00000019507	*mcm5*	0.79
ENSDARG00000098774	*si:zfos-741a10.3*	0.79

ENSDARG00000006468	*grap2a*	0.79
ENSDARG00000031044	*lipg*	0.78
ENSDARG00000053568	*pstpip1b*	0.77
ENSDARG00000054610	*coro1a*	0.76
ENSDARG00000037654	*pmm2*	0.75
ENSDARG00000101169	*grap2b*	0.74
ENSDARG00000116660	*si:ch211-9d9.8*	0.73
ENSDARG00000092115	*eif4a1a*	0.72
ENSDARG00000016939	*itgb2*	0.70
ENSDARG00000078734	*myo1f*	0.70
ENSDARG00000044318	*itgb7*	0.68
ENSDARG00000017128	*myofl*	0.64
ENSDARG00000005789	*enpp1*	0.62
ENSDARG00000104801	*tubb6*	0.61
ENSDARG00000074667	*akt1s1*	-0.62
ENSDARG00000054597	*cnot6l*	-0.63
ENSDARG00000076241	*txlnbb*	-0.65
ENSDARG00000021140	*pabpc1b*	-0.68
ENSDARG00000076850	*si:ch211-157b11.14*	-0.69
ENSDARG00000043313	*ank2b*	-0.71
ENSDARG00000075881	*si:ch211-39k3.2*	-0.72
ENSDARG00000079578	*rbpms2b*	-0.74
ENSDARG00000075608	*mical2a*	-0.74
ENSDARG00000044295	*pip5k1ba*	-0.75
ENSDARG00000062262	*ednrab*	-0.76
ENSDARG00000009142	*ppp1r13bb*	-0.76
ENSDARG00000059259	*pabpc4*	-0.77
ENSDARG00000006031	*abat*	-0.78
ENSDARG00000041665	*mkrn1*	-0.78
ENSDARG00000086342	*zgc:101566*	-0.78
ENSDARG00000043497	*scrn2*	-0.79
ENSDARG00000055792	*foxo4*	-0.80

ENSDARG00000093549	*selenop*	-0.82
ENSDARG00000035256	*eef2l2*	-0.82
ENSDARG00000040002	*pnpla7b*	-0.83
ENSDARG00000020239	*lpin1*	-0.84
ENSDARG00000099974	*ldb3b*	-0.84
ENSDARG00000076547	*si:ch211-221f10.2*	-0.85
ENSDARG00000017246	*prx*	-0.85
ENSDARG00000018985	*gatsl2*	-0.85
ENSDARG00000033609	*map1lc3a*	-0.85
ENSDARG00000008447	*fkbp4*	-0.86
ENSDARG00000036695	*calcoco1a*	-0.87
ENSDARG00000030656	*sept3*	-0.88
ENSDARG00000013921	*frya*	-0.88
ENSDARG00000059815	*oaz2b*	-0.89
ENSDARG00000060796	*slc20a2*	-0.89
ENSDARG00000008030	*myl9b*	-0.90
ENSDARG00000074507	*rmdn1*	-0.90
ENSDARG00000040971	*zgc:92606*	-0.90
ENSDARG00000060316	*cish*	-0.91
ENSDARG00000025855	*camk2n1a*	-0.92
ENSDARG00000062359	*scn3b*	-0.92
ENSDARG00000054916	*eif4ebp3*	-0.93
ENSDARG00000003165	*nr2f6b*	-0.93
ENSDARG00000114870	*CABZ01078594.1*	-0.94
ENSDARG00000008275	*klhl24b*	-0.97
ENSDARG00000100782	*F7*	-0.97
ENSDARG00000052690	*arrdc3a*	-0.97
ENSDARG00000025436	*msrb1a*	-0.98
ENSDARG00000013317	*pygmb*	-0.99
ENSDARG00000045634	*lmod2a*	-1.02
ENSDARG00000102572	*si:ch211-260e23.9*	-1.04
ENSDARG00000045485	*rassf8b*	-1.04

ENSDARG00000041607	*eif4ebp3l*	-1.06
ENSDARG00000082789	*NC_002333.18*	-1.08
ENSDARG00000061736	*ank3b*	-1.08
ENSDARG00000076386	*epdl1*	-1.08
ENSDARG00000079078	*si:ch211-5k11.8*	-1.10
ENSDARG00000012694	*c3a.1*	-1.11
ENSDARG00000001733	*gulp1a*	-1.12
ENSDARG00000111701	*LT631684.2*	-1.12
ENSDARG00000100352	*aglb*	-1.14
ENSDARG00000057687	*sbk3*	-1.15
ENSDARG00000035942	*hrh3*	-1.16
ENSDARG00000063375	*pter*	-1.16
ENSDARG00000057652	*dbpb*	-1.19
ENSDARG00000051879	*abcc8*	-1.20
ENSDARG00000079307	*si:dkey-205h13.1*	-1.22
ENSDARG00000028027	*trim63a*	-1.23
ENSDARG00000070873	*ccl25b*	-1.23
ENSDARG00000057419	*slc44a5b*	-1.24
ENSDARG00000053820	*pcmtd2*	-1.25
ENSDARG00000103834	*rbm14b*	-1.26
ENSDARG00000029105	*ftr51*	-1.28
ENSDARG00000093019	*si:dkey-83k24.5*	-1.28
ENSDARG00000020693	*sesn1*	-1.29
ENSDARG00000092889	*zgc:194246*	-1.29
ENSDARG00000075172	*fbxo25*	-1.30
ENSDARG00000106669	*CABZ01068358.1*	-1.31
ENSDARG00000099511	*CABZ01034698.2*	-1.31
ENSDARG00000070597	*prelp*	-1.31
ENSDARG00000033170	*sult2st1*	-1.33
ENSDARG00000092240	*si:ch211-243a20.3*	-1.35
ENSDARG00000074387	*alkal1*	-1.35
ENSDARG00000061416	*c2cd4a*	-1.35

ENSDARG00000069473	*frem1a*	-1.36
ENSDARG00000090930	*si:ch211-120g10.1*	-1.40
ENSDARG00000004115	*mgat4b*	-1.41
ENSDARG00000051914	*slc14a2*	-1.41
ENSDARG00000012381	*hsc70*	-1.42
ENSDARG00000022437	*cd81b*	-1.42
ENSDARG00000086512	*prodhb*	-1.43
ENSDARG00000006526	*fn1b*	-1.44
ENSDARG00000037099	*irs2a*	-1.45
ENSDARG00000022832	*bnip4*	-1.45
ENSDARG00000088567	*VPS72*	-1.46
ENSDARG00000097553	*BX908750.1*	-1.46
ENSDARG00000093052	*c6*	-1.50
ENSDARG00000095901	*col18a1b*	-1.51
ENSDARG00000031745	*si:busm1-266f07.2*	-1.51
ENSDARG00000089586	*ncam3*	-1.52
ENSDARG00000090468	*ppp1r3aa*	-1.56
ENSDARG00000058943	*cdcp1a*	-1.58
ENSDARG00000095295	*si:rp71-36a1.1*	-1.59
ENSDARG00000101199	*rbp4*	-1.60
ENSDARG00000052895	*htra3a*	-1.61
ENSDARG00000042988	*slc24a2*	-1.63
ENSDARG00000091009	*si:ch211-28p3.4*	-1.63
ENSDARG00000025595	*agmo*	-1.70
ENSDARG00000079347	*zgc:194659*	-1.72
ENSDARG00000010878	*cdkn1ca*	-1.72
ENSDARG00000077775	*baalca*	-1.76
ENSDARG00000079645	*sc:d217*	-1.77
ENSDARG00000057417	*nudt13*	-1.78
ENSDARG00000096898	*CR925728.1*	-1.79
ENSDARG00000103833	*si:dkey-77g12.1*	-1.84
ENSDARG00000087303	*cebpd*	-1.85

ENSDARG00000091974	*CR356233.1*	-1.90
ENSDARG00000057000	*camkvl*	-1.90
ENSDARG00000023228	*vsnl1a*	-1.93
ENSDARG00000069590	*tmem150c*	-1.96
ENSDARG00000044685	*nr0b2a*	-1.97
ENSDARG00000008333	*znfl2a*	-1.98
ENSDARG00000028804	*ankrd9*	-2.05
ENSDARG00000098348	*znf326*	-2.09
ENSDARG00000093303	*ifitm1*	-2.14
ENSDARG00000077115	*si:ch73-44m9.1*	-2.14
ENSDARG00000078258	*CABZ01049847.1*	-2.18
ENSDARG00000037618	*ddit4*	-2.25
ENSDARG00000061196	*emilin2a*	-2.26
ENSDARG00000019686	*fgl2b*	-2.31
ENSDARG00000075833	*lyve1a*	-2.45
ENSDARG00000070116	*nit1*	-2.46
ENSDARG00000092920	*si:ch211-106h4.12*	-2.53
ENSDARG00000075727	*map1lc3cl*	-2.56
ENSDARG00000104752	*COLEC10*	-2.65
ENSDARG00000039726	*zgc:123321*	-2.73
ENSDARG00000023448	*galnt14*	-2.75
ENSDARG00000099023	*CABZ01034698.1*	-2.79
ENSDARG00000057975	*plcd4a*	-2.92
ENSDARG00000012311	*myoz2a*	-2.95
ENSDARG00000034757	*zdhhc2*	-3.10
ENSDARG00000054510	*adrb2b*	-3.22
ENSDARG00000068966	*si:ch211-261n11.7*	-3.41
ENSDARG00000110460	*si:ch211-156l18.4*	-3.44
ENSDARG00000038666	*igfbp1b*	-3.79
ENSDARG00000079532	*zgc:194242*	-3.88
ENSDARG00000104656	*si:dkeyp-97a10.3*	-4.73
ENSDARG00000096577	*adgre9*	-4.78

ENSDARG00000096579	*si:dkey-9c18.3*	-4.95
ENSDARG00000091757	*adgrf6*	-5.00
ENSDARG00000092381	*si:dkey-23c22.9*	-6.19
ENSDARG00000079105	*mhc2dab*	-6.82

10.3. List of genes encoding for ECM proteins differentially expressed in *Tg(hsp70l:sflt4)* at 24 hpci.

Table 10.2. List of ECM genes significantly differentially expressed in *Tg(hsp70l:sflt4)* at 24 hpci.

List of ECM genes downregulated in *Tg(hsp70l:sflt4)*	List of ECM genes upregulated in *Tg(hsp70l:sflt4)*
ccl25b	*abi3bpb*
prelp	*fn1a*
frem1a	*hmcn2*
fn1b	*tgfbi*
htra3a	*col10a1b*
emilin2a	*col11a1a*
fgl2b	*lgals9l1*
igfbp1b	*muc2.2*
	brinp3b
	clcf1
	crlf1a